Intensity-Modulated Proton Therapy for Locally Advanced Cervical Cancer

IMRT and IMPT of cervical cancer and effect of reduced margins

Arpit

Group of Biophysics and Medical Physics, Department of Physics

UNIVERSITETET I OSLO

August 2015

2015

IMRT and IMPT of cervical cancer and effect of reduced margins

http://www.duo.uio.no/

Print: Reprosentralen, Universitetet i Oslo

Preface

This thesis is a part of my Masters degree in Biophysics and Medical Physics at University of Oslo. The thesis work has been carried out in the Department of Medical Physics at Norwegian Radium Hospital and Ulleval Hospital from August 2014 till August 2015.

First and the foremost, I must acknowledge and thank The Almighty God for His blessing. I would like to take this opportunity to express my heartfelt gratitude and sincere thanks to my supervisors Prof. Taran Hellebust Paulsen and Prof. Eirik Malinen for guiding me through this thesis and providing valuable help in understanding the essentials of clinical implications of radiation therapy in cervical cancer. A special thanks to Marius Røthe Arnesen, who led me through the world of treatment planning. Thanks to Bernt Louni Rekstad for his support in treatment planning. Thanks to my family for moral support, advice and encouragement.

All Birds find shelter during a rain.

But Eagle avoids rain by flying above the Clouds.

Problems are common, but attitude makes the difference

Dr. A.P.J. Abdul Kalam

Abstract

Background and Purpose: The objective of the study was to compare intensity modulated radiotherapy (IMRT) and intensity modulated proton therapy (IMPT) for locally advanced cervical cancer in terms of dose-volume parameters, dose coverage, homogeneity and conformity. Furthermore, to study the effect of reduced margins.

Study design: External beam radiotherapy planning was carried out for 10 patients with locally advanced cervical cancer, out of which 5 recieved treatment for para-aortic lymph node involvement in addition to pelvic irradiation. Dose prescription for the PTV was 50.4Gy in 28 fractions with a dose coverage criteria set to $D_{98\%} \geq 95\%$. Two sets of treatment plans were prepared for both modalities based on different CTV-PTV margins: clinical margin (7 mm L-R, 10 mm S-I, 15 mm A-P) and reduced margin (7 mm isotropic). The IMRT and IMPT plans were generated using the Eclipse treatment planning system (Varian Medical Systems, Palo Alto, CA). Dose-volume histograms (DVHs) were analyzed for the PTV and various organs at risk (OARs; rectum, bladder, bowel, sigmoid, left, right kidney, medulla, cauda equina and pelvic bone). Student's t-test was used for all statistical comparison.

Results: The prescription was well achieved with all IMRT and IMPT plans covering 98% of the PTV with the 95% isodose. The ratio between IMRT and IMPT was calculated. IMPT demonstrated the potential in sparing doses to OARs, where significant differences were seen compared to IMRT for many dose-volume parameters (table 5). Concerning the reduced margins, increased differences between IMPT and IMRT were seen in the rectum, bladder for all parameters and for the low, medium dose region of bowel. For OARs sigmoid and high dose range of bowel however, less changes in the IMRT to IMPT dose-ratio was found when reducing CTV-PTV margins. Moreover, the same effect was seen for the medium, high dose regions of pelvic bone. Importantly, a decent dosimetric gain was also apparent in low dose to outer body. A clinically non-significant dosimetric variation was seen for medulla and cauda equina. The dosimetric gain was however reduced for kidneys (table 6).

Lastly, a considerably large reduction in high dose to rectum and bladder was seen for IMRT, utilizing smaller margins as compared to clinical margins whereas, a decent dosimetric gain was also clearly seen for the sigmoid and bowel, at high dose level (table 8).

Conclusions: IMPT has considerable potential to spare the OARs, while maintaining excellent planning target coverage, for patients with cervical cancer. Advanced image guided strategies and adaptive radiotherapy approaches could open this therapeutic window further.

List of abbreviations

EBRT	External Beam Radiatherapy
GU	Gastro-Urinary
GI	Gastro-Intestional
HT	Hematologic Toxicity
IMRT	Intensity Modulated Radiotherapy
LN	Lymph Nodes
OARs	Organs at risk
IMPT	Intensity Modulated Proton Therapy
SSPT	Spot Scanning Proton Therapy
MFO	Multi Field Optimization
SFO	Single Field Optimization
SFUD	Single Field Uniform Dose
CT	Computed Tomography
DNA	Deoxyribonucleic Acid
HPV	Human Papillomavirus
FIGO	International Federation of Gynecological and Obstetrics
HU	Hounsfield Unit
MRI	Magnetic Resonance Imaging
ICRU	International Commission on Radiation Units and Measurements
GTV	Gross Tumour Volume
CTV	Clinical Target Volume
PTV	Planning Target volume
IM	Internal Margins
SM	Set-up Margins

DVH	Dose Volume Histogram
QUANTEC	Quantitative Analysis of Normal Tissue Effects in the Clinic
DHI	Dose Homogenity Index
DCI	Dose Conformity Index
IGRT	Image Guided Radiotherapy
MLCs	Multileaf Collimators
RT	Radiation Therapy
IMBs	Intensity Modulated Beams
SOBP	Spread Out Bragg Peak
TCP	Tumour Complication Probability
NTCP	Normal Tissue Complication Probability
RF	Radio Frequency
TPS	Treatment Planning System
DET	Distal Edge Tracking
VOI	Volume of Interest
RBE	Relative Biological Effectiveness
LET	Linear Energy Transfer
IAEA	International Atomic Energy Agency
CGE	Cobalt Gray Equivalent
A-P	Anterior-Posterior
S-I	Superior-Inferior
L-R	Left-Right
CBCT	Cone Beam Computed Tomography

List of tables

Table of Content

1 Introduction

Locally advanced cervical cancer is a gynecological cancer which often has a tendency to metastasize, primarily through the pelvic lymph nodes and then to the para-aortic LN. Locally advanced cervical cancer patients are generally given whole pelvic radiation therapy to limit local metastasis in the pelvic area while para-aortic radiotherapy is given to sterilize distant metastasis (1, 2). Radiation therapy can be administered externally or internally to the affected area. External radiotherapy (EBRT) involves the irradiation of tumour from external source whereas internal radiotherapy involves the placement of radioactive source in or in the vicinity of the tumour area. The latter technique is known as 'brachytherapy'. For cervical cancer brachytherapy is used in combination with EBRT to deliver a local boost dose to the tumour. This combined radiotherapy is then delivered with concurrent chemotherapy. Such protocol is considered as a primary standard protocol for locally advanced cervical cancer patients (3, 4) (2).

Conventionally EBRT is delivered, with high energy photon beams using a four-field box technique to achieve local tumour control. However, due to the large field size in the radiation portal, rather large volumes of the bowel and rectum have to be included to adequately treat the lymph nodes. It is well known that radiotherapy in pelvic area is often associated to many complications in normal pelvic organs. Several studies have confirmed the incidences of both acute and late gastrointestinal (GI) and genitourinary (GU) toxicities (5, 6) (7). Few studies have shown the incidences of acute hematological (HT) toxicities following pelvic chemo-radiation (4, 5). These substantial risks of acute and late complications have driven the need to develop intensity-modulated radiation therapy (IMRT). It has been considered as a potential replacement of traditional four-field box technique. IMRT allows the delivery of highly conformal dose due to steeper dose gradient to the complex and irregular shape and size of the target volume in cervical cancer. IMRT has shown the potential to reduce the harmful dose to the healthy surrounding structures without compromising adequate dose to the tumour volume (8, 9). Various studies on IMRT to pelvic gynecological malignancies have shown the significant reduction in the incidence of acute GI toxicities (10, 11) (12). Various studies have also shown the decrease in the incidence of HT toxicities (13, 14). For para-aortic LN irradiation, extended field IMRT for cervical cancer has shown the reduction in acute and late side-effects (15, 16). Furthermore, IMRT potentially allows dose escalation. However, there exists a downside to IMRT in its potential to increase the risks of radiation

induced secondary cancers mainly due to two reasons: larger total body dose and higher integral dose as larger volume of normal tissues receive low dose (17).

In the hope of further reducing the radiation induced toxicities in normal organs and avoid the chances of having secondary cancer, protons are considered as an attractive replacement to IMRT in delivering highly conformal dose to the target coverage and increasing organs at risk (OARs) sparing to much further extent (18). The fundamental reasons underlining the benefits of protons is due to their physical characteristics like low entrance dose, flat and uniform spread-out Bragg peak (SOBP), finite range of particles and sharp distal dose fall-off (19). Few studies have looked into the use of proton therapy in cervical cancer patients and have concluded the excellent dosimetric advantages in sparing dose to OARs (20, 21). In proton therapy, dose can be delivered using passive scattering techniques and active spot scanning techniques. Active spot scanning is also known as intensity modulated proton therapy (IMPT). It is this technique which reduces the chances of radiation induced secondary cancer because of no production of neutrons and hence, less scattered dose to patients (17).

Accuracy is a prerequisite to deliver high quality radiotherapy. Factors like range and, energy uncertainties affect delivery of radiation therapy and should be taken into account during the treatment planning procedures. Considering the fact that pelvic organs are naturally prone to positional and volumetric changes over time (22), such variations should be accounted for. Also, various studies have demonstrated the existence of correlation between bladder and rectum filling on uterus and cervix motion, respectively (23). As a result, it changes the shape and position of cervix-uterus target volume. Figure 1 shows the variable bladder filling in a cervical cancer patient. The use of a drinking protocol during the treatment course to reproduce bladder filling will minimize the impact of bladder filling on cervix-uterus motion (24, 25). Therefore, depending upon the pre-treatment established co-relation between bladder filling and inter-fractional cervix-uterus motion suitable margins should be added to adequately cover the target volume in cervix-uterus tumour. It has been agreed through various studies that the impact of bladder variation on cervix-uterus movement is patient-specific (26, 27), thus varies from patient to patient. Figure 2 shows the inter-patient variation in cervix-uterus motion during treatment course. Moreover, cervix-uterus tumour is known to regress during the course of treatment as shown in few studies (28). All the reasons mentioned above provides evidence against the usage of clinical recommended population-based margins as they unnecessarily includes normal tissues under high dose irradiation for patients with

smaller target motion. Therefore, large inter-patient variability in cervix-uterus motion limits the benefit of highly conformal treatment techniques (29). This calls for the employment of patient-specific total margins around tumour volume to support personalized treatment strategies or adaptive radiotherapy (30).

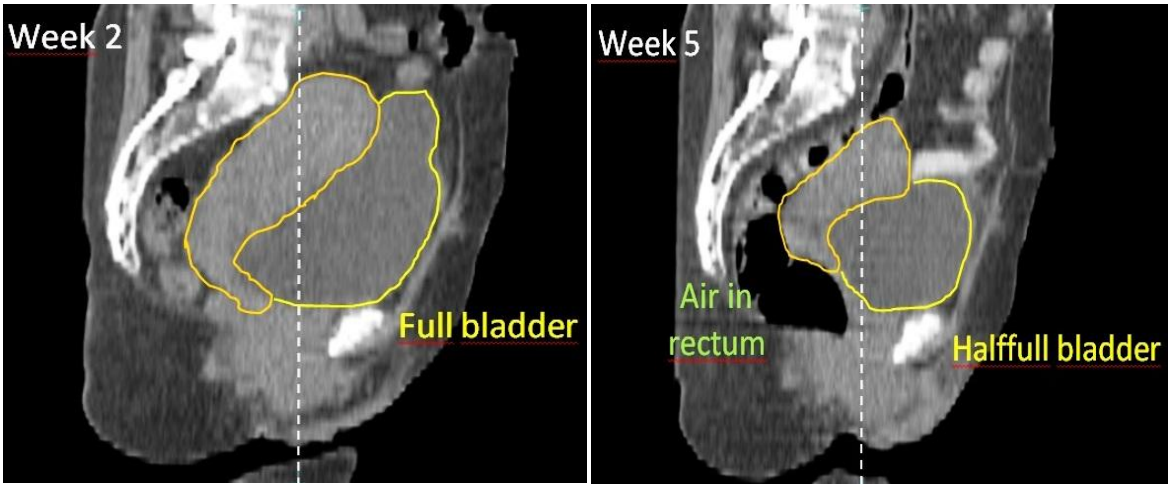

Figure 1 Sagittal view of variable bladder and rectum filling CT-scans in week 2 and week 5 during treatment course, respectively for cervix-uterus cancer patient. The influence of variable bladder and rectum filling can be seen in the change of cervix-uterus position. The above shown images are taken from (31)

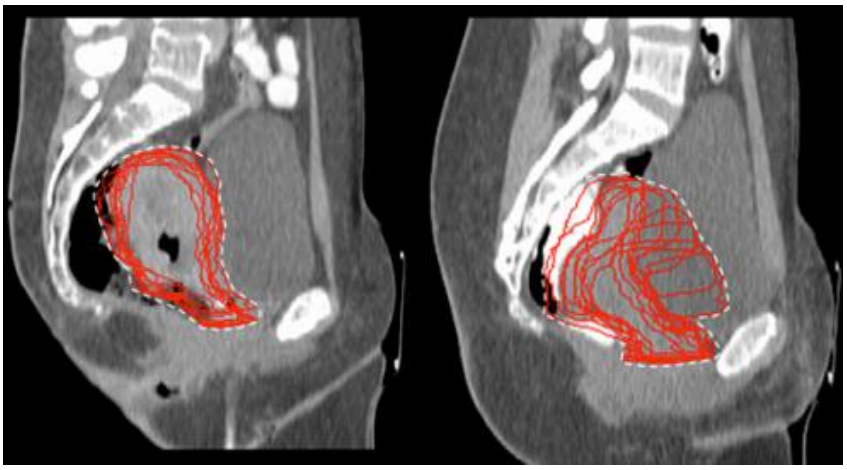

Figure 2 Sagittal cuts of the CT-scans showing inter-patient variability in cervix-uterus motion for two cervical cancer patients during the entire treatment course. Image is taken from (32)

This thesis

The primary aim of this study is to evaluate dosimetric benefits between IMRT and IMPT for locally advanced cervical cancer. The secondary aim is to investigate the effects of a reduced margin and its dosimetric impact on IMRT and IMPT.

More explicitly, the following research questions are addressed in this thesis:

1. Does IMPT reduce dose to normal organs at risk for cervical cancer patients comparative to IMRT using clinical margins?

2. How does a reduced margin influence this result?

3. Does smaller margin benefits in sparing normal organs at risk for IMRT as compare to clinical margins?

2 Background

2.1 Cancer

Human body is made up of many types of cells. These cells grow and divide in a controlled way to replace the old and damaged cells after they die to keep the body healthy. When genetic material of the cells “DNA” undergoes change, this can cause mutation. Such mutation can leads to abnormal and uncontrolled multiplication of the affected cells results in the mass of the tissue known as tumour. Cancer is the class of diseases characterized by uncontrolled growth and division of abnormal cells.

There are over 100 different types of cancers (33) and each is named after the type of cell it is initially originated from. Cancer types are grouped in two broader categories: Malignant and benign tumours. Malignant tumours are invasive and can manage to move to the other part of the body through blood vessels and lymphatic system. This activity is termed as “distant metastasis”. Moreover, these cells manage to grow and divide, forming new blood vessels to feed itself in the process called “angiogenesis”. Hence, malignant tumours are more dangerous and difficult to treat as they exhibit distant metastasis. Unlike malignant tumours, benign tumours are not invasive. They stay at one spot and demonstrate limited growth and consequently, less harmful and can easily be removed depending upon site (e.g. Brain).

Carcinogens are substances directly responsible for the DNA damage and promoting cancer. These substances can be tobacco, arsenics, ionizing radiation like x-rays and gamma rays, etc. They interact with our body and form free radicals which in turn try to steal the electrons from the DNA molecule of the normal cells causing damage to the cells and hence affect their ability to function normally (34).

The extent and localization of the spread of the disease can be assessed by utilizing medical imaging techniques. Doctors may also do endoscopy to look inside the body for the abnormalities. However, concerning the characterization of the disease, biopsy is the gold standard to verify the presence of cancer. The possible ways to cure cancer are chemotherapy, radiation therapy and undergoing surgical procedure. The choice of the treatment procedure is done in view of the type and position of the tumour, over and above, the age of the patient and the grade of the disease (33, 34).

2.2 Cervical cancer

Cervical Cancer is the second most common cancer in women worldwide, with an estimated 530000 new cases every year. Out of the total number of cases, more than 270000 women die every year from cervical cancer (World Health Organization, 2013). In Norway, the number of new cases reported in 2013 was 282 (35).

Cervical cancer is the abnormal growth in the epithelial lining of the cervix. The greatest risk factor behind the development of more than 99% of the cervical cancer is Human Papillomavirus (HPV), followed by smoking and weak immune system. There are more than 100 types of HPV. Most of the HPV types are low-risk types and do not cause cancer. However, high-risk HPV types may cause cervical cell abnormalities. About 70% of the cervical cancer can be attributed to HPV type 16 and 18 which are considered as High-risk HPV types. HPV infection can be caused by the sexual intercourse or by having multiple partners, however not all the HPV infected women develop cancer. Most of the HPV infections are eliminated by the host's immune system without intervention. On the contrary, some women have persistent infection. These viruses have high risk of transforming normal cells into abnormal, which may further then develop to cervical carcinoma (36).

According to FIGO (International Federation of Gynecology and Obstetrics), cervical cancer is classified into various stages depending upon the extent of invasiveness in other part of the body (table 1). Staging is based on clinical examination rather than surgical procedures or imaging (37).

Figure 3-10 shown below illustrates the various stages of cervical cancer extending from stage I to stage IV (38). Stage I cervical cancer is usually treated with surgery. But, in case of IB2 and IIA stage, combined chemotherapy and radiation therapy may be used. Stage IIB and III (A and B) are usually treated with combined chemotherapy and radiation therapy. In Stage IV, surgery, chemotherapy, radiation therapy or a combination of these treatments are usually chosen to control the symptoms of the disease.

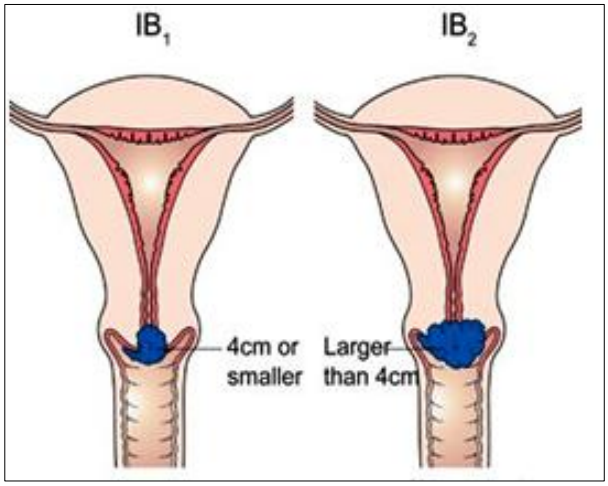

Figure 3: Stage IA1 and IA2

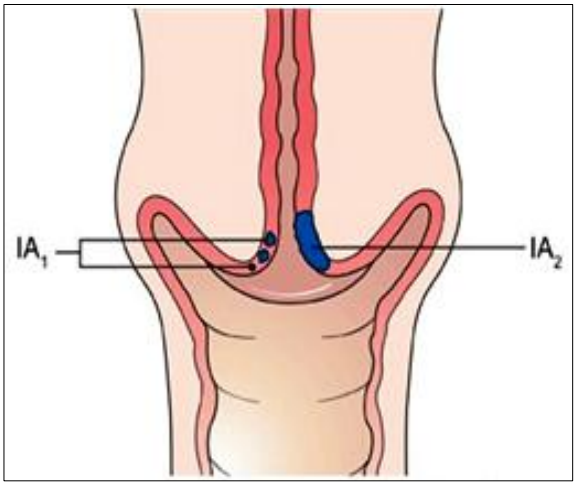

Figure 4: Stage IB1 and IB2

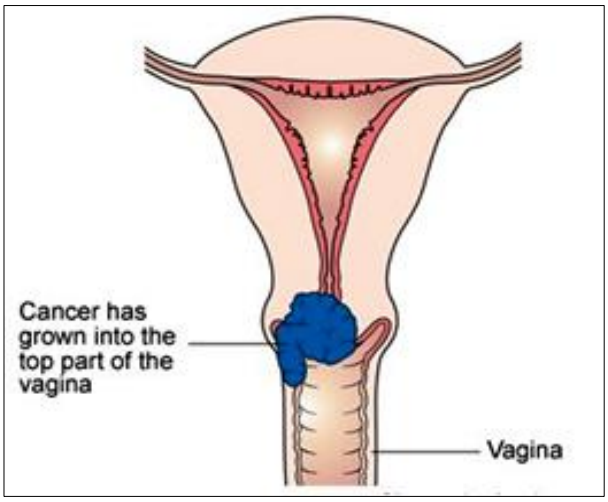

Figure 5: Stage IIA

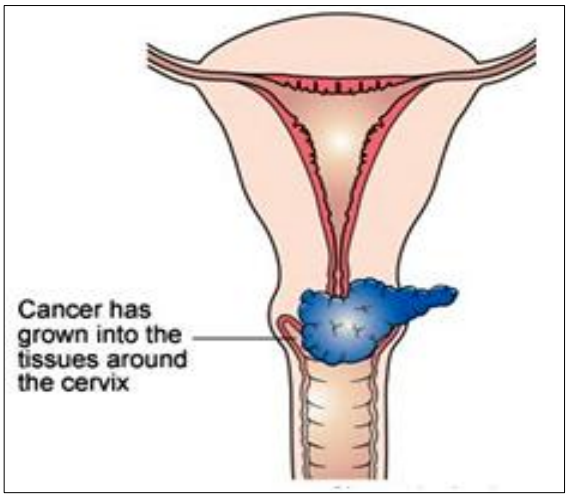

Figure 6: Stage IIB

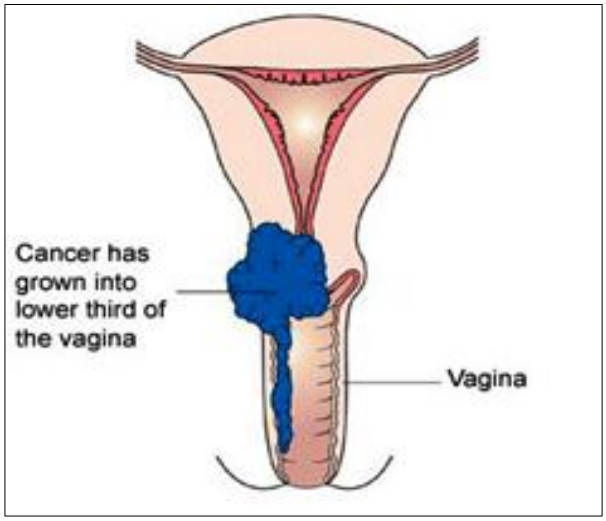

Figure 7: Stage IIIA

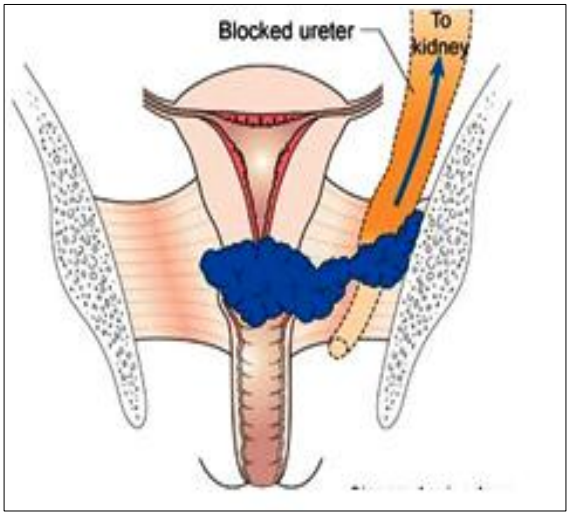

Figure 8: Stage IIIB

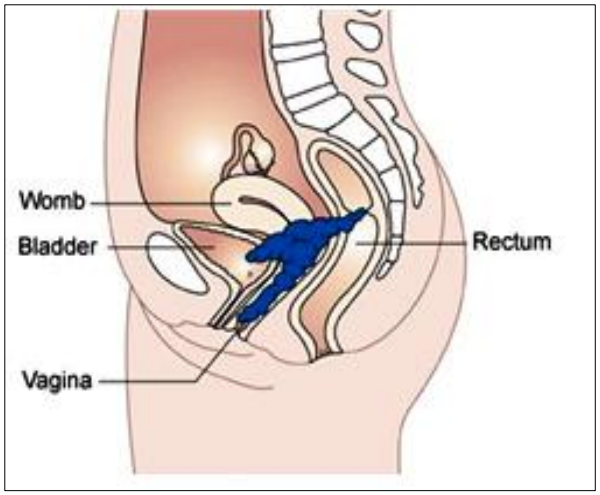

Figure 9: Stage IVA

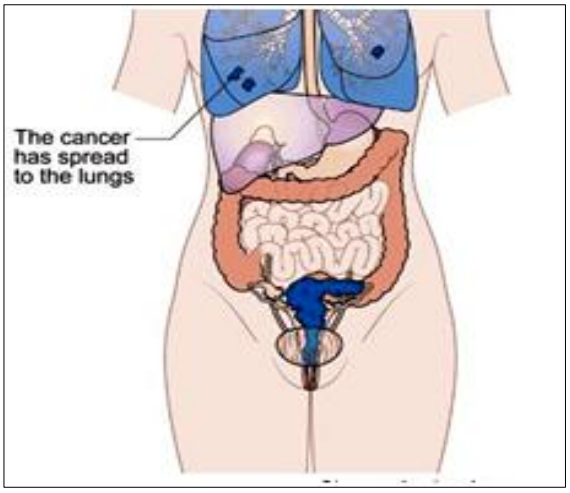

Figure 10: Stage IVB

Table 1 Description of the cervical cancer staging as per FIGO (37).

Stage	Description
0	Carcinoma in situ, i.e. the carcinoma is situated in the original position.
I	The carcinoma is strictly confined to the cervix (extension to the uterine corpus should be disregarded).
IA	Invasive cancer is identified only microscopically. (All gross lesions even with superficial invasion are stage IIB cancers.)
IA1	Measured invasion of stroma ≤3mm in depth and ≤7mm width.
IA2	Measured invasion of stroma >3mm and <5mm in depth and ≤7mm width.
IB	Clinical lesions confined to the cervix, or preclinical lesions greater than stage IA.
IB1	Clinical lesions no greater than 4 cm in size.
IB2	Clinical lesions >4 cm in size.
II	The carcinoma extends beyond the uterus, but has not extended onto the pelvic wall or to the lower third of vagina.
IIA	Involvement of up to the upper 2/3 of the vagina. No obvious parametrial involvement.
IIA.1	Clinically visible lesion ≤4cm
IIA.2	Clinically visible lesion >4cm
IIB	Obvious parametrial involvement but not onto the pelvic sidewall.
III	The carcinoma has extended onto the pelvic sidewall. On rectal examination, there is no cancer-free space between the tumour and pelvic sidewall. The tumour involves the lower third of the vagina. All cases of hydronephrosis or non-functioning kidney should be included unless they are known to be due to other causes.
IIIA	Involvement of the lower vagina but no extension onto pelvic sidewall.
IIIB	Extension onto the pelvic sidewall, or hydronephrosis/non-functioning kidney.
IV	The carcinoma has extended beyond the true pelvis or has clinically involved the mucosa of the bladder and/or rectum.
IVA	Spread to adjacent pelvic organs
IVB	Spread to distant organs.

2.3 Computed tomography

Computed tomography provides variety of purposes in various medical disciplines such as diagnosis of the cancer and guidance in the intervention procedures (figure 11a). Historically, computed tomography has gone through a tremendous and rapid development within the context of evolution of the CT. However, the basic principle of the working and construction of the CT scanners has remained same throughout the innovation and advancement.

Computed tomography uses x-ray beams generated from x-ray tube and an array of detectors (figure 11b). The narrow pencil beams of x-rays sweep across the subject in a transverse direction and together, the tube-detector assembly is continuously rotated around the subject. This translational-rotational motion of the scan allows the measurement of x-ray transmission along the subject. Each rotation generates a large series of 2D radiographic projections (slices). An image reconstruction algorithm essentially transforms these multiple 2D images into the 3D volumetric image of the subject.

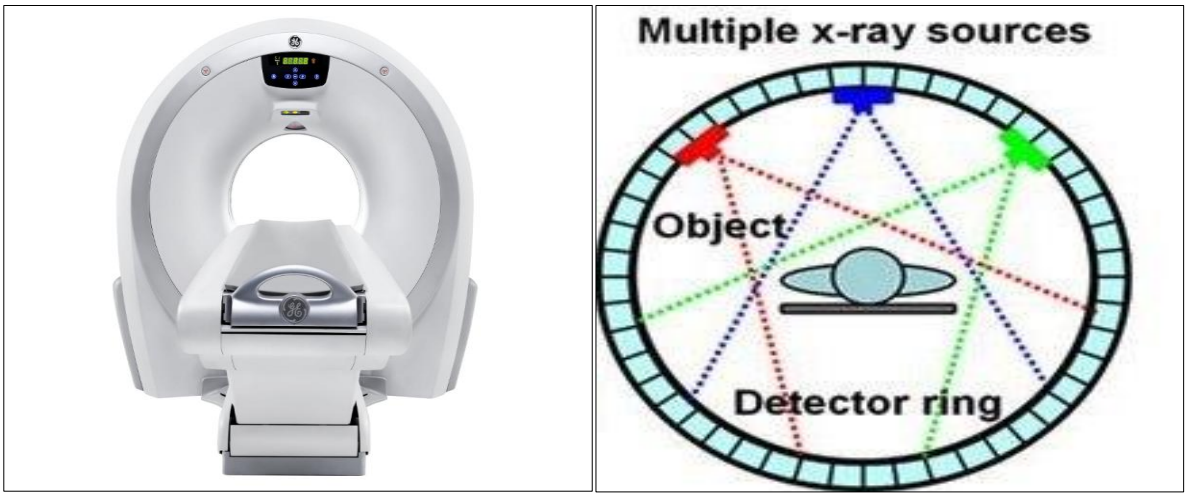

Figure 11a: Image of Computed Tomography from GE healthcare. 11b: Geometry of fan beam x-rays with an array of detectors rotating simultaneously.

Computed tomography imaging is based upon the attenuation characteristics of the different structure and tissues in the body. Each slice is divided into a matrix of three dimensional volume (tissue) elements known as "Voxels". Each voxel of the tissue has designated attenuation coefficient (μ). X and Y dimension of each voxel lies in the same plane of the slice whereas the Z-dimension of the voxel corresponds to the slice thickness. Under the image reconstruction process, the attenuation measured along the path of x-ray through the voxels is calculated. Therefore, the resultant attenuation along the path of x-ray is the sum of attenuation values in each of the voxel. The x-ray attenuation measured at any position of the detector can be summarized by the following expression of exponential attenuation law:

$$\mathbf{I_1 = I_0\, e^{-\mu x}} \qquad (1)$$

Where in equation (1), I_1 is intensity of the x-rays emitted out from x thickness of tissue and I_0 is the initial intensity of x-rays without x thickness of tissue. μ is the attenuation coefficient of tissue thickness.

Back to the earlier days of CT, efforts were made to replace the attenuation values with another quantity. Hence, the new concept of CT number has been introduced. Thereafter, the diagnostic information on the CT image is visualized by the contrast difference. Contrast difference is the CT number calculated from attenuation value of each voxel of tissues in the reconstruction matrix. The measurement unit for CT number is Hounsfield units (HU). Water is used as a reference medium since its attenuation coefficient is zero. The following expression is used for the calculation of CT number:

$$\textbf{CT number (HU)} = [1000 \times (\mu_{voxel} - \mu_{water})]/ \mu_{water} \quad (2)$$

In equation (2), μ_{voxel} is the voxel attenuation coefficient and μ_{water} is attenuation coefficient of water.

Evidently, much smaller contrast differences have been seen for computed tomography compared to conventional x-ray radiography. As a result, CT has revealed subtle differences between different tissues. The range of the CT number varies between -1000 for air and +1000 for bone. Water has CT number of approximately 0 but not exactly 0 due quantum noise in image (39, 40) .

The possibility of tumour spread locally and distantly is higher in the advanced stages of cervical cancer. Therefore, it requires cross-sectional imaging to be performed. The diagnosis of the advanced cervical cancer is done with MRI. MRI provides superior soft tissue contrast resolution. It has shown significant results in the assessment of the size of the tumour, the depth of cervical invasion and distant metastasis. Therefore, cervical cancer is better diagnosed on MR imaging (41). Despite all the advantages of the MRI, CT is a preferable choice for treatment planning since it provides tissue density information needed for calculation of the absorbed dose. Undisputedly, CT plays a primary role in RT treatment planning (42).

2.4 External beam radiotherapy

Radiotherapy can be delivered as an external or internal radiotherapy. In external beam radiotherapy (EBRT) an external source of radiation is used and directs the radiation at the tumour from outside the body. The important steps in radiotherapy are as follows: Imaging and tumour localization, target volume and organ delineation, treatment planning, patient positioning and treatment verification, and treatment delivery (43).

2.4.1 Tumour localization and imaging

Tumour localization in radiotherapy is a whole process from primary, actual tumour localization during treatment planning, guiding treatment delivery through patient set-up. Patient set-up depends upon the reproducibility of the patient position and immobilization devices (44). The success of radiotherapy depends upon ensuring that a tumour and its subclinical extension are irradiated efficiently with the tumouricidal dose. For that reason, the tumour should be localized properly, delineated precisely and accurately to increase the survival rate and minimize the normal tissue damage. The geometric shape, size and location of the tumour are defined with clinical examination (inspection, palpation, and endoscopy) and optimal imaging methods available for a particular tumour site. However, the radiation dose needed to eradicate the tumour is limited by the surrounding normal organs because of their organ-dependant radio sensitivity. The normal organ radiation tolerance should always be kept in mind while treatment planning otherwise it would cause fatal complications to the normal tissues (45). Based on diagnostic imaging, it is radiation oncologist responsibility to contour accurately the target volume and the organs at risk to be spared (46).

The choice of imaging modality depends upon the location of the tumour site and to the adjacent sensitive organs. CT and MRI both have become main stage imaging modalities for providing high spatial resolution. Both modalities provide superior anatomical geometric data of the tumour and anatomical structures to define GTV in 3D radiotherapy treatment planning (45). CT imaging is more attractive option for tumour localization. With advances in CT, 4D CT imaging provides trajectory information of normal organs while treating moving tumour. Serial imaging can also be considered to visualize and quantify the uncertainty due to change in tumour size and tissue densities. Thus, serial imaging forms the basis for adaptive radiotherapy. Even if the tumour is accurately and precisely contoured, uncertainty does exist

due to patient set-up error, organ and target motion due to various physiological processes. Therefore, tumour localization plays a crucial role in correcting patient position at treatment site. In room cone beam computed tomography imaging (CBCT) can be used for patient positioning verification during or before treatment delivery. Hence, tumour localization is considered as a range of processes utilized to minimize geometric uncertainties during treatment planning and field checking to the treatment itself (47).

2.4.2 Treatment planning

Treatment planning is one of the pivotal tasks in radiotherapy. It determines the best appropriate way of delivering dose to patient. It deals with several major steps, that includes reproducing patient positioning and immobilization at treatment time, accurate delineation of target volumes and critical structures, selection of appropriate beam arrangement and configuration, computation of dose to be delivered, evaluation of resulting dose distribution and transfer of information from treatment planning system to treatment delivery system (47). X-ray CT images forms the basis for treatment planning, but, in case of soft tissue contouring MR images can also be acquired as an adjuvant to CT for accurate judgment of target and normal tissue delineation. Dose computation algorithms perform complex calculation of dose to be delivered. Therefore, model based algorithms has become an integral feature of radiotherapy treatment planning systems. Utilizing the fact that each voxel represents a CT number and one to one relation between CT number and electron density, voxels in the CT image set forms the most applicable representation of patient for dose calculation algorithms (47).

Introduction of 3D treatment planning has given more degree of freedom to radiation therapy treatment planning. Consequently, faster and precise evaluation tools are essentially required to simply this process. Isodose curves are one of those essential treatment evaluation tools. Isodose information is displayed on 3D treatment plan. Isodose curves can be defined as a surface or line of equal doses overlaid on a patient's planning image. Isodose curves can be displayed in both absolute and relative dose. The corresponding isodose curves can also be seen in color wash display, which may be easier to understand than the standard isodose curves (48). An illustration of 3D dose display is visualized in figure 12, where different color in the image indicates a particular dose level in relative dose (where the dose is expressed as a

percentage of reference doses). However, the 3D dose distribution shown below corresponds to IMRT and hence, it will be discussed later in detail in section 2.4.4

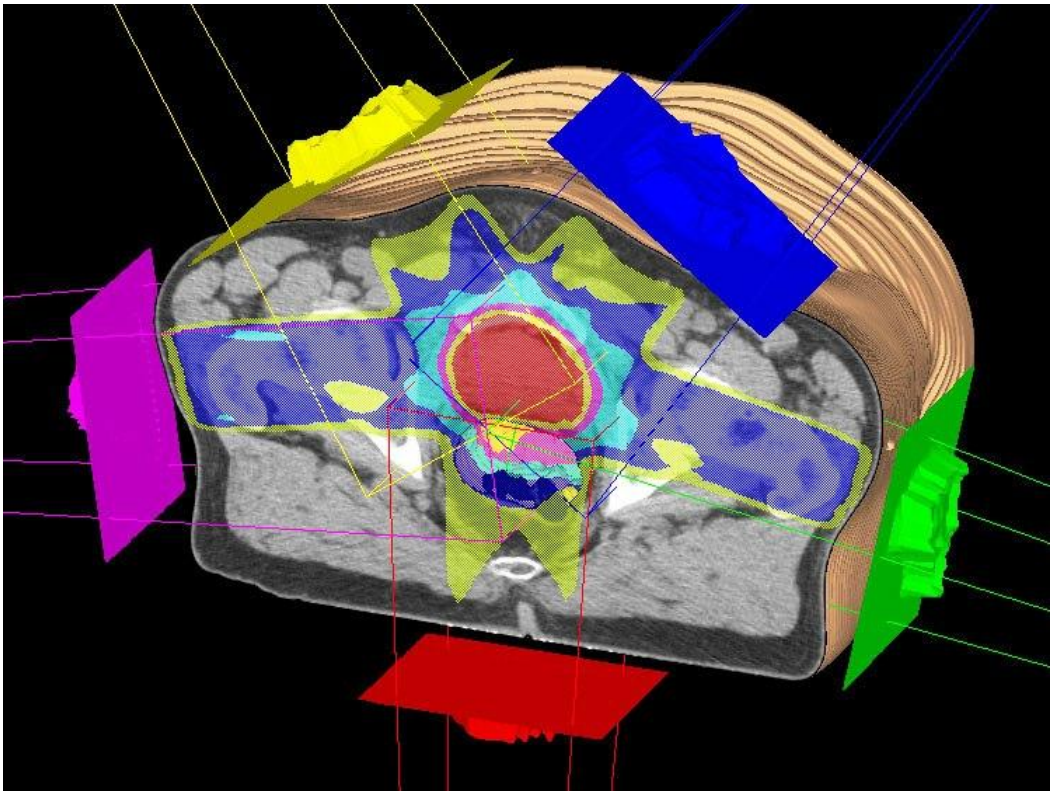

Figure 12: 3D isodose display in color wash mode for corresponding isodose curves in IMRT treatment plan. Red, yellow, pink, sky blue, blue, light green indicates 100%, 95%, 90%, 80%, 70% and 60%, respectively. Image source: Philips healthcare

- **Volumes in treatment planning**

ICRU has attempted to address the issue of geometrical variation in report 50 and 62. ICRU has standardized the concepts of prescribing, recording and reporting doses. For that reason, ICRU has recommended to define the whole target volume in different sub-volumes. GTV is the gross or visible malignant growth. The delineation of resultant GTV is done by outlining the area of tumour in each slice and multiplies it by its thickness. GTV has highest tumour cell density and hence, an adequate dose must be delivered in order to obtain local tumour control. With the progression of treatment time, GTV can change its shape and size due to tumour regression, growth or therapeutic intervention. In case of post-operative treatment of cervical cancer prior to radiotherapy then no GTV_{tumour} and CTV_{tumour} can be defined due to

the changes caused by surgery itself (49). Contrast enhancement, oedema and hyper or hypo density of the tissue are the another factors that may result in inaccurate delineation of the GTV (50). CTV is the expansion of the GTV with an appropriate margin to cover the subclinical extent of the microscopic disease. PTV is the geometrical volume defined during treatment planning. It is the volume used in recording and reporting of dose. It encompasses CTV with an adequate margin to account for patient set-up uncertainties and organ motion. Therefore, it is the patient positioning error and the organ motion which causes the geometrical misses in the radiotherapy (47). The concept of PTV was implemented to help in the selection of beam sizes and alignments to ensure that an adequate radiation dose must be delivered in all parts of CTV. It is considered as 3D envelope in which the GTV and CTV reside and move within this volume but not through it. The margins for different types of variations and uncertainties to CTV are internal margin (IM) and set-up margin (SM). IM accounts for internal physiological movements in organ relative to internal reference point whereas SM relates to compensate for error in patient positioning and alignment of therapeutic beams (51, 52).

Treated volume: It is the tissue volume enclosed by an isodose surface that is selected and specified by radiation oncologist as being appropriate to achieve tumour eradication. Generally, it is the volume enclosed by 95% isodose surface(52).

Irradiated volume: It is the volume that receives dose considered significant in relation to normal tissue tolerance. Usually, this volume is enclosed by 50% isodose level (52).

Organs at Risk: OARs are the normal anatomical structures located close to the target volume or a part of them is in overlap with that target volume. Normal tissues and organs are radiosensitive so they significantly influence the process of treatment planning and prescribed dose. OARs have significant dose tolerance level which affects the dose-volume constraints in optimization. Considering the radiosensitive nature of the OARs, it is desirable to delineate the critical structures accurately and dose distribution to these regions is visualized by isodose curves or dose-volume histogram (DVH). Moreover, the physiological movement of the organs at risk causes geometrical uncertainties; therefore a margin is added to compensate errors and uncertainties.

One of the most significant tasks in the treatment planning is defining the tolerance dose limit for organs at risk. Based upon the tolerance dose and radio sensitivity, the critical structures

behave differently. Organs at risk are classified in three distinct categories: serial, parallel and serial- parallel. Serial organ is a continuous unit and most radiosensitive structure so even if the small part of the organ is exposed to dose higher than the acceptable dose limit of the organ will cause complete damage of the organ; therefore, even a point dose is significant. The spinal cord is the examples of this group. Parallel organ consist of several functional units and if one part is damaged, the rest of the organ makes up for the loss. The dose to a given volume or mean dose is considered more important for this class of organs. Kidneys are the example for the same (50-52).

- **Dose-volume analysis**

Dose-Volume Histograms are the mathematical tool of the 3D treatment planning system, which summarizes the entire treatment plan into 2D graph. The x-axis and y-axis of the graph represents dose and volume receiving dose, respectively. Dose and volume can be expressed in both absolute and relative values. DVH doesn't show any spatial distribution of doses. It is an excellent tool to evaluate and compare different optimal isodose distribution of treatment plans using dose-volume parameters, isodose curves, colored display of isodose distributions in treatment volume, dose homogeneity index and dose conformity index. The required dose-volume parameters are same between IMRT and IMPT treatment plans. Some useful dose-volume parameters are shown below in figure 13.

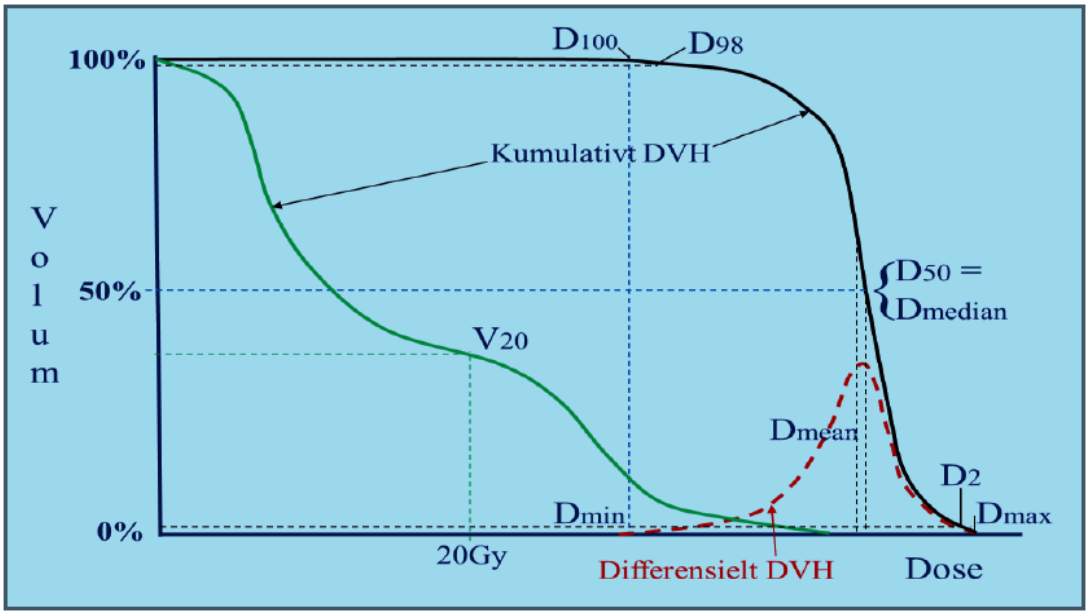

Figure 13: Schematic representation of the dose-volume histogram (DVH). Image source (53)

As per Norwegian radiation protection authority report in volume and dose in external radiotherapy by Levernes S, definitions of some of the most relevant dose-volume histogram parameters are given below:

$D_{98\%}$ - Dose $_{near\text{-}minimum}$, i.e. it is the minimum dose to a specified volume of interest. At least 98% of the volume is receiving high dose and only 2% volume is receiving low dose. $D_{98\%}$ of target volume should be equal to or greater than 95% of the prescribed dose. $D_{98\%}$ is much useful and robust in comparison to D_{min} ($D_{0\%}$). $D_{98\%}$ is dose specified to a certain volume, in contrast to D_{min} ($D_{0\%}$) which is dose to a point or one voxel. For that reason, $D_{98\%}$ is less sensitive to any uncertainty in patient movement, dose matrix location (grid size, grid placement and steep dose gradient) and resolution. Generally, $D_{98\%}$ is estimated for target volume to evaluate target coverage.

$D_{2\%}$ - Dose $_{near\text{-}maximum}$, i.e. it is the maximum dose to a specified volume of interest. It implies that only 2% of volume receives higher dose. $D_{2\%}$ is clinically much useful than D_{max} ($D_{100\%}$). The reason is same as explained above for $D_{98\%}$. ICRU recommends the use of D_{2cc} instead of $D_{2\%}$ in case of larger volumes of organs at risk. Reasonably, D_{2cc} represents a constant volume rather than $D_{2\%}$ which varies with size of volume of interest.

$D_{50\%}$ - Dose $_{median}$, i.e. dose received by 50% of the volume. This corresponds to $D_{50\%}$ on the DVH. $D_{50\%}$ indicates equal volumes receives higher and lower dose. This dose parameter is suitable for reporting dose in target volume. It is also used to normalize 100% dose in target mean.

D_{2cc} - Clinical maximum dose, i.e. it is the maximum dose in 2cc of the whole body. This dose value is suitable to estimate hot spot areas. ICRU recommends that dose to 2cc of the volume should not exceed 107% of the prescribed dose.

V_{45cc}, i.e. it is volume receiving 45Gy. This dose parameter is estimated particularly for bowel as per the recommendation from QUANTEC.

V_{10Gy}, **V_{30Gy}** and **V_{45Gy}**, i.e. volume of the organs at risk receiving at least 10, 30 and 45Gy respectively. The above defined volume parameters are generally used to estimate the volumes of the organs at risk receiving a particular dose level (53).

Dose homogeneity index and dose conformity index are the two objective tools to assess the quality of the treatment plans. Varieties of formulae are available in literature for dose homogeneity index and dose conformity index. The one used in this study are described below:

Dose homogeneity index (DHI): $(D_{2\%}-D_{98\%})/D_{mean.}$ It tells about how homogenous the dose distribution is in the target volume. A value of DHI=0 indicates that $D_{2\%}$ and $D_{98\%}$ is equal and hence, high dose homogeneity in target volume (20, 53).

Dose conformity index (DCI): V_{95}/V_{PTV}. It is the ratio of the PTV receiving 95% of the prescribed dose and total PTV volume. A value of DCI=1 indicates high conformity around target volume (52).

2.4.3 Patient positioning and treatment verification

The primary goal of conformal radiotherapy is to deliver focal radiation dose to a defined target volume while limiting concomitant radiation dose to the normal tissues around the target. It is important to consider the factors affecting the geometrical accuracy of the radiation treatment delivery. The uncertainties in the patient positioning and organ motion are the two prime factors responsible for inaccuracies in precision radiotherapy. Therefore, rational strategies have to be adopted to overcome the significant geometrical uncertainties and achieving maximum tumour control (47).

In order to understand the various source of error and a way to deal, the errors are further categorized in two components: systematic and random error. The systematic component of any error is a deviation that occurs in the same direction and, it is of similar magnitude for each fraction of radiotherapy. Systematic error occurs particularly at the localization, treatment planning and delivery phases. Random component of any error is a deviation that varies unpredictably in any direction and, it is of different magnitude for each fraction of radiotherapy. Random errors are limited to organ motion, patient movement and inconsistent repositioning in daily treatment fraction delivery. Therefore, the uses of immobilization device are more likely to affect the random error. It may also be possible to use imaging strategies for patient position correction (54).

A variety of immobilization devices are available to aid patient positioning. The sole intent of utilizing these devices is to limit the patient movement and keep the patient at a fixed and well-defined position during localization or treatment. These devices should be rigid and comfortable at the same time so that it allows the fast and accurate patient set-up. They should ensure the reproducibility of the patient position for each treatment field. This ensures the use of minimum CTV-PTV margins in order to reduce random set-up errors. Thus, the amount of normal critical tissues and related radiation induced toxicity can be reduced with an adequate dose to CTV. Some of the efficient immobilization devices used readily in radiotherapy is alpha cradle, vacuum loc bags, knee and arm support (47).

As quoted in second paragraph, imaging strategies can also be efficiently utilized to minimize the random errors in patient positioning. This technique of treatment verification in patient positioning to maintain geometrical accuracy is known as “Image-guided radiotherapy”. IGRT is a broader term which makes use of imaging to outline target volumes at the time of localization and patient positioning for treatment verification. The choice of imaging modality depends upon the anatomical site. The images acquired can be kV imaging or MV imaging. Some of the well-adopted imaging strategies are online and offline treatment verification, also, inter-fractional and intra-fractional treatment verification. In online treatment verification, the images are acquired in the treatment room immediately prior to each treatment fraction and corrections in patient positioning are made before the treatment delivery. The time required in analyzing for set-up accuracy and taking decision either to act or not to act should be as low as possible. Beyond a certain time limit, the position of the patient may no longer represent true position because of the variation in patient and organ motion occurred during that time. In offline treatment verification, the images are acquired in the treatment room immediately prior to each treatment fraction but no action for set-up correction is taken until the delivery of next treatment fraction. Inter-fraction verification indicates the set-up accuracy between different treatment fractions whereas intra-fraction verification deals with the set-up accuracy during each treatment fraction. Since intra-fraction organ and patient motion are unavoidable during the treatment delivery. Therefore, real-time treatment verification strategies are adopted to quantify the geometrical inaccuracy. A comparison is made between a reference image and the images acquired during treatment delivery. The underline concept is based on the detection of the displacement between the acquired images and reference image over an acceptable tolerance level. One such real time system uses the co-relation between external skin markers and internal anatomy. If in case the

external marker drifts beyond the reference pre-determined tolerance level then the treatment can be stopped/gated manually or automatically (54).

2.4.4 Intensity modulated radiotherapy

Intensity modulated radiotherapy is an advanced radiotherapy technique used to minimize the amount of normal tissue being irradiated in the treatment field. One feasible approach to achieve this objective is to use intensity modulated beams across the treatment field whose sum will produce relatively uniform high dose within the complex target volume while avoiding dose to the neighboring organs at risk. IMRT uses non-uniform radiation beam intensities that can be designed using multi leaf collimators (MLCs) which can deliver spatially modulated dose distribution in each radiation beam. Typically, the combination of the multiple intensity modulated radiation fields from different directions will produce custom tailored radiation dose to the tumour volume and minimizing dose to the normal critical structures (55). The effective use of the inverse planning optimization algorithm enables the RT planner to find the best beam parameters (beam weights) based upon delineation, desired dose objectives and weighting factors associated with target volume and critical structures to calculate an optimum planned dose distribution. Thus, IMRT requires the precise identification of the exact location and shape of the tumour volume.

Technically, the geometrical arrangement of the target region and the surrounding normal tissues demands the precise selection of the beam angles and beam directions at which the radiation is delivered to the tumour. Each radiation beam is delivered to the target in multiple segments or subfields varying in shape, size and intensity. The number of segments required increases with the complexity of the geometrical arrangement of a clinical case to achieve an optimal dose plan. Multiple fixed gantry angles ensure less integral dose compared to rotational deliveries such as VMAT and tomotherapy (47).

- **Linear accelerators**

For the treatment of cervical cancer, several high energy photon beams are applied to deliver high dose to centrally located primary tumour without giving too high dose to normal critical structures in the pelvic region. The most widely used sources of external beam radiotherapy

are high energy photons which are generated using linear accelerators, known as linac (figure 14a). Commercially available medical accelerators produce high energy photons. They have the energy typically in the range of 4-15Mev. The principle of a linac is as follows: electrons are produced from electron gun filament and accelerated to high velocity by applying high electric potential across the waveguide. The electron beam is guided throughout the waveguide using beam focusing and beam steering magnets. After taking exit from secondary part of the waveguide, these accelerated electron beam bends by the application of three bending magnets so as to direct the electron beam to hit the target. Then photons are produced in rapid deceleration of the electron beam undergoing columbic interaction in the target material (generally tungsten). This phenomenon of x-ray production is known as "Bremsstrahlung radiation" (figure 14b). The x-ray spectrum produced will be polyenergetic where the maximum energy in the spectrum will be defined by the maximum electric potential applied. The average x-ray energy is generally 1/3 of the maximum energy. The shape and the intensity of the x-ray spectrum are modified by multi-leaf collimators, wedges and field blocks.

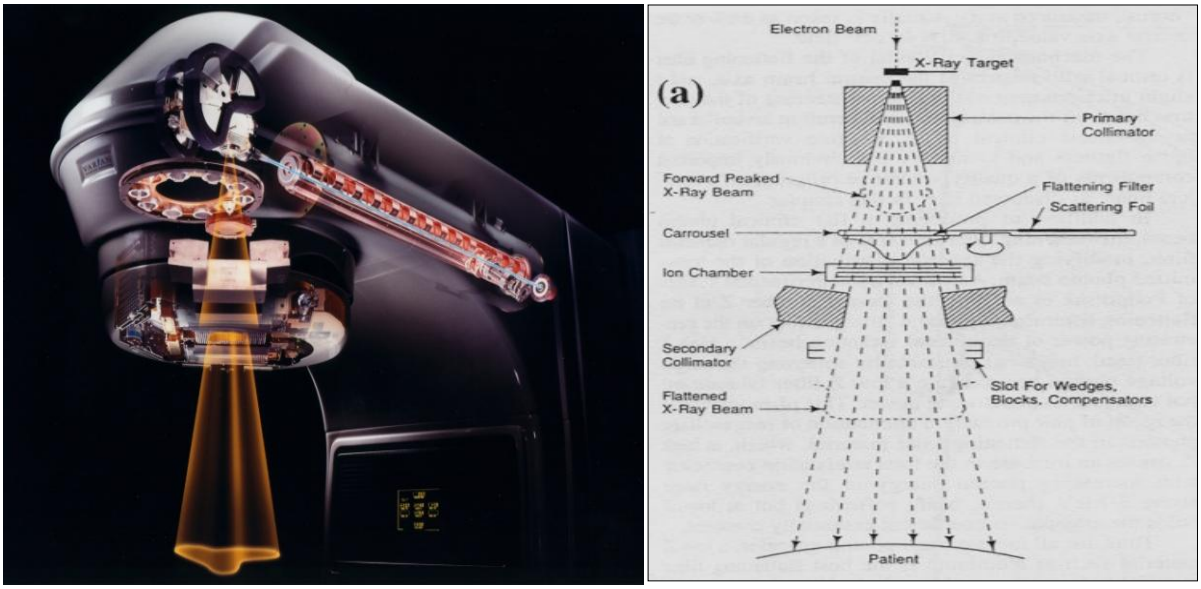

Figure 14a: Representation of linear accelerator. Image on the left shows the clinical linear accelerator with its components. Figure 14b: Image on the right illustrates the production and delivery of photon beams with their corresponding components in the head assembly. Image 14a source: varian.com

- **Intensity modulation and beam shaping devices**

The intensity of the beam generated by linear accelerator is modulated by multi leaf collimators (MLCs). Multi leaf collimators are located in the head assembly of the linear accelerator. MLCs are used to modify and collimate the x-ray beam intensity. MLCs are dynamically controlled leaves move in the opposing pair and flexibly shape the treatment field into any irregular shape to conform the dose to the tumour and hence blocking dose to the adjacent normal tissues. Figure 15a: shows the multi-leaf collimator assembly. They are leaves of tungsten usually having thickness range of 0.5 to 1cm (width defined at isocentre distance). MLC thickness and design varies with different vendors. Figure 15b: visualize the concept of irregular beam shaping using multi-leaf collimator assembly. Collimator assembly is integrated with digitally controlled leaves that move with rapid leaf speed for effective modulation. MLCs are combined with the collimator jaws in the collimator assembly. Each MLC design has its own characteristic resulting in lead transmission, interleaf leakage and end leaf leakage (56).

Similar intensity modulation could be created by physical modulators ***compensators*** but it is an unpractical alternative as construction and placement of compensators for each radiation beam is time consuming and tedious. Therefore, it is efficient to employ automated controlled dynamic driven leaf collimators in irregularly shaping the radiation field from the beam eye view perspective. Therefore, MLCs perform an important role in conformal therapy (56).

- **IMRT leaf delivery sequence**

The shape of intensity modulated profile delivered by any leaf sequence is determined by the position of the leaf end set at each control point of the sequence. There are multiple sequences possible to deliver a desired intensity modulated beam. The series of leaf sequences are formed with associated beam weight for each leaf positions. Multiple static fields are subdivided into small segments. In each static treatment field, leaves take step to from segment while the radiation is off and start irradiation after the leaves are properly positioned. This type of dose delivery is commonly known as step and shoot (or segmental MLC). When leaves at one side move to the other side at variable speed while the radiation is constantly delivered at constant dose rate. This type of dose delivery is known as sliding window (dynamic MLC) technique (56).

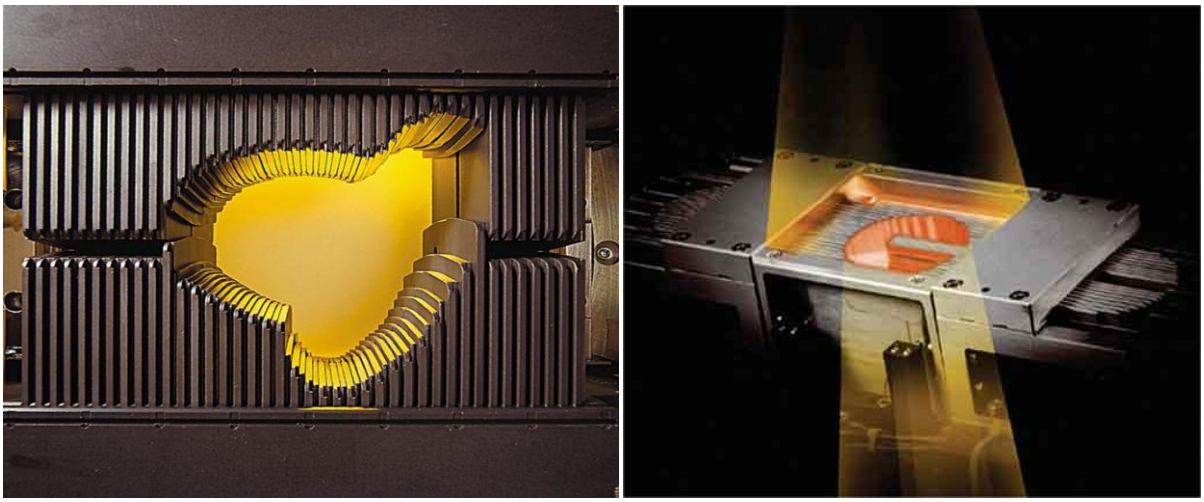

Figure 15a: Multi-leaf collimator assembly and 15b: shaping of the leaves to produce conformity of the radiation field to tumour shape. Image source: varian.com

- **Dose planning**

Dose planning for photon beam takes into consideration its physical and dosimetric characteristics. It is important to understand the depth dose deposition pattern of photon beams to shape the dose around target volume. Photon deposit maximum energy close to the skin surface after build up region and thereafter, the energy deposition decreases exponentially with depth in tissue. Skin surface dose increases with the increase in beam energy due to larger build up region. A typical percentage depth dose distribution of photon beam at central axis of its path length in patient has been shown in figure 16 (57).

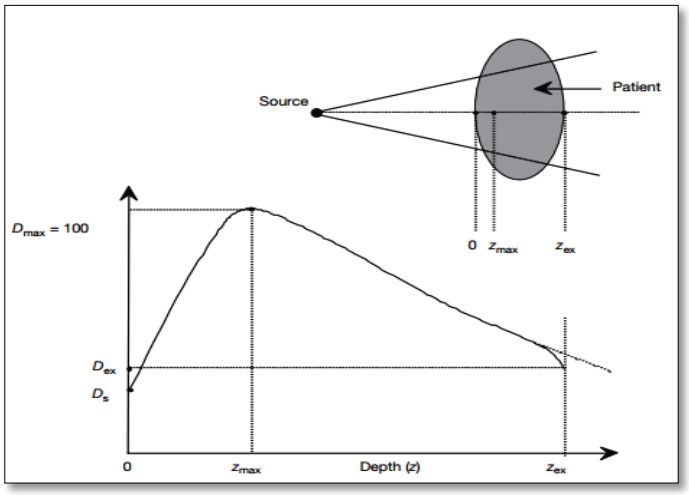

Figure 16: A typical depth dose distribution of photon beam at central axis of its pathlength. D_s is the skin surface dose at Z=0, D_{max} is the maximum dose often normalized to 100% dose at a depth of Z_{max} and D_{ex} is the exit dose at a depth distance of Z_{ex}. The distance between Z=0(D_s) and Z_{max} (D_{max}) is known as build up region. Image source (57)

The complex shape of tumor demands precise dose delivery to target volume. Therefore, multiple intensity modulated fields from different projections are required to shape concavities around tumor and minimizing the volume of normal tissue from irradiation. Illustration of multiple intensity modulated beams is shown in figure 12. Therefore, choices of beam properties (beam weight) are made through inverse planning optimization during treatment planning process (57).

- **Inverse planning**

IMRT treatment planning involves inverse planning where the target volume and critical structures are clearly defined and dose objectives to obtain optimum planned dose distribution are specified (56). Dose conformity to the target volume is often a clinical requirement but it is difficult to accomplish in clinic due to the presence of critical structures in the vicinity of target volume. Furthermore, if the critical structures are located in the concavity of the tumour volume then it is hard to keep the dose off this region. This may incur unavoidable complications and indisputably limiting the dose to be delivered. The above addressed issues limits successful radiotherapy. However, the employment of multiple intensity-modulated beams (IMBs) have shown its potential in shaping dose around the target volume precisely and quite satisfactorily fulfilled the clinical requirements of conformal radiotherapy. Figure 17 shows the advantage of the IMBs to shape the beam profile of the individual field shape and consequently, the collaboration of the multiple beams delivers high dose conformity to the concave target shape. Generally, the more complex the geometrical arrangement, the larger the number of fields segment required to achieve the optimal plan (47).

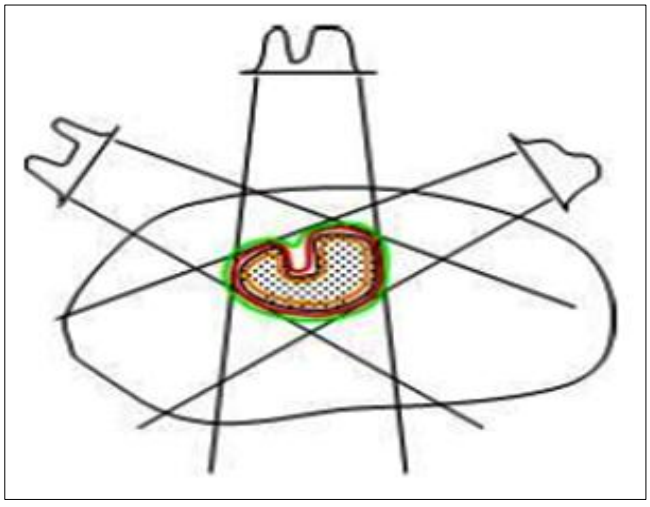

Figure 17: Demonstrates the potential of Intensity modulated radiation therapy in shaping the beam profile of the individual fields to conform high dose to concave region of the target shape. Image source (56)

Inverse planning is called inverse in the sense that the dose is specified to the point in the target volume and a mathematical algorithm works backward to compute the optimal dose distribution and the corresponding beam weights that match the prescription as close as possible (58). The general goal of the inverse treatment planning is to obtain low dose to the volume outside target and high dose inside. Success of the optimization algorithm depends upon how accurately and closely the solution satisfies the specified dose volume objectives. Since the process is iterative and interactive the RT planner slides the volume value to the lowest achievable while not compromising the target coverage. The problem arises if the given dose volume constraints are vague, that causes non-optimal results and often no solution.

- **Optimization algorithm**

The mathematical optimization algorithm uses physical (dose, volume) parameters to find out best possible treatment plan. Ideally, dose is calculated from each voxel on the 3D image. The dose calculation is based on beamlets associated with each treatment beam. Each beamlet is subdivided into small intensity elements called “bixel”. The 2D elements on the dose matrix represent bixel weights. The beam intensity map is directly proportional to matrix of bixel weights. The dose calculation estimates the dose delivered by each beam equivalent to the values stored in each beam’s bixel matrix. Once the dose is calculated for each beam, the voxels on the 3D image contain the calculated dose values. The fundamental role of the optimization algorithm is to select those bixel weights that deliver the most favorable dose distribution. The parameter used to do assessment is the cost function or the objective function (47). Figure 18 is an example of the beam intensity map.

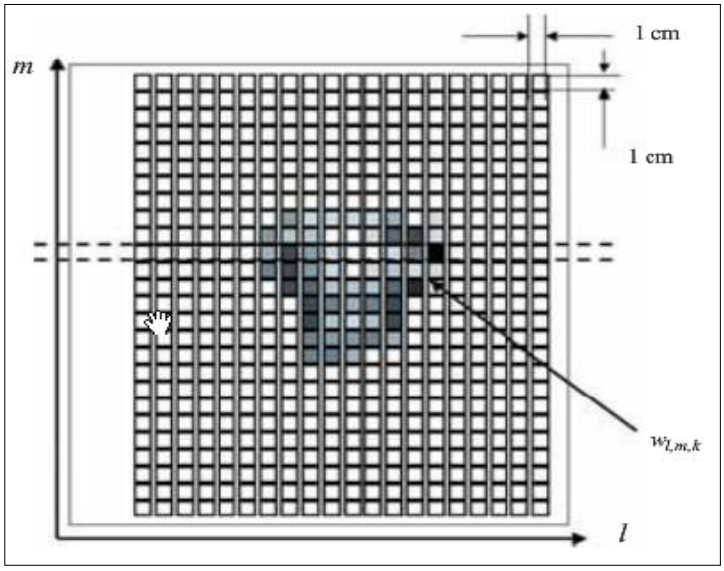

Figure 18: Exemplifies the beam intensity map. Each square represents a bixel. The rows and column are labelled with an index l and m respectively. Each square represents a bixel with a beam weight of $W_{l,m,k}$. Bixels blocked by MLC leaves are displayed white and shades of gray indicates beam intensity levels. Black corresponds to highest intensity level. Image source: (47)

The cost function is a measure of fit between a calculated dose distribution and some ideal, user specified dose distribution. The optimization of the bixel weights employ numerical method to find a set of beam-weights that corresponds to minimum of cost function. Fast simulated annealing is one of the numerical iterative methods to find the cost function minimum. In each iteration, grains of the beam weights randomly selected from Cauchy distribution perturbs the set of beam weights causes the individual beam weights to either increase or decrease. The resulting cost function is compared with the running cost function value (lowest cost function value from previous iteration). If the new cost function value is lower than the running value, then the running value is set to new value and the new beam weights are stored in the dose matrix. The process keeps on repeating until the best set of beam weights are found corresponding to the minimum of the cost function (58).

The minimum of the cost function defines the close of the computed dose distribution to the prescribed dose distribution. The overall cost function ($Ctotal$) has been subdivided into component terms: $Cptv, Coar, Cbody$. The dose is calculated in each of the clinical region. Following are the mathematical representation of the clinical dose in each region.

$$Cptv = \sum_i in\ ptv(Di - 100)^2 \quad (3)$$

$$Coar = \sum_i in\ oar(Di) \quad (4)$$

$$Cbody = \sum_i in\ body(Di) \quad (5)$$

$$Ctotal(n) = Wptv \times \frac{Cptv(n)}{Cptvst(1)} + \sum_{j=1}^{m}(Woarj \times \frac{Coarj(n)}{Coarst(1)}) + Wbody \times Cbody(n)/ Cbodyst(1)$$

..... (6)

Di: Dose to the ith volume element, the number 100 represents the desire 100% uniform dose to the PTV. Wptv, Woar and Wbody are the weighting factor used to stress the relative importance of the PTV, OARs and Body respectively. n is the iteration number, subscript ST denotes the starting value of the term (i.e. at n=1), m is the number of OARs.

In nutshell, minimizing the overall cost function $Ctotal$ is based upon attaining a uniform homogenous dose in the planning target volume (PTV) and minimizing integral dose to the OARs and body (58).

2.4.5 Proton therapy

Proton, being a charge particle shows different dosimetric characteristics than photons. Photon, after a small build up looses energy exponentially with tissue penetration depth thereby low dose to the target volume and high dose proximally (figure 16). In contrast, protons loose energy in interaction with orbital electrons or nuclear interactions as they traverse through the tissue. Decrease in their velocity causes increase in interaction time which in turn results in maximum energy deposition near the end of range of proton beam known as ‘Bragg peak’. The individual pristine Bragg peaks of successively lower energies and intensities are superimposed to yield a spread out Bragg peak (SOBP). The individual proton beams from different directions are positioned in target area and combined together to yield a distinct localized high-dose concentration. This creates a highly conformal dose

distribution with accurately covering the tumour volume while sparing healthy tissues in comparison to the photon therapy (59). Figure 19a illustrates the dose distribution curve of protons and the concept of spread out Bragg peak (SOBP). Figure 19b shows the difference in dose distribution by photons and protons.

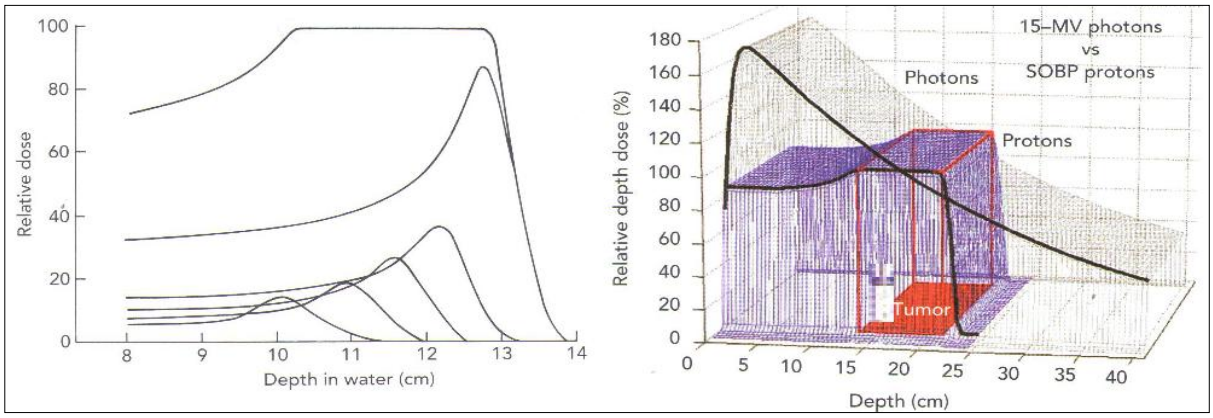

Figure 19a): on the left illustrates a clinical spread out Bragg peak as a superimposition of the multiple individual pristine Bragg peaks of different energy and intensity. 19b): Comparison of the depth dose deposition pattern of SOBP protons and 15MV photons with respect to tumour volume. Image source: (60)

The rationale for the clinical use of the proton beams is the feasibility of delivering higher doses to the tumour, leading to an increased tumour control probability (TCP). It can also be used to lower the dose to OARs and hence, potentially lowering normal tissue complication probability (NTCP) (61). Due to its potential in steep dose gradient comparative to the photons, results in highly conformal high-dose region while substantially sparing irradiation in the volume of normal tissues. Therefore, proton therapy is well suited for irregular lesions near sensitive structures. Protons deliver less integral dose to the critical structures by the factor of two compared to the intensity modulated photon plans (62).

- **Proton beam production**

Proton originates from ion source where hydrogen atom is separated in electron and proton. Protons are injected into cyclotron or synchrotron where they are accelerated. Figure 20 depicts the pictorial description of the principle in cyclotron. Cyclotron consists of dipole magnets placed parallel to each other with a gap in between. The dipole magnets produce

uniform magnetic field and electric field is produced across the gap by an oscillating voltage. The protons are injected in the magnetic field and follow semicircular path until they reach the gap where they are accelerated for another half of a semi-circular path. In the meantime, polarities of the dipole magnets are reversed thereby accelerating the protons with high speed. The size of the magnets and the strength of the magnetic field decide the maximum energy produced by a cyclotron. The maximum proton beam energy is directly proportional to the maximum range in the tissue. For example, proton beam energy of 230Mev is equivalent to 32cm range in tissue (59).

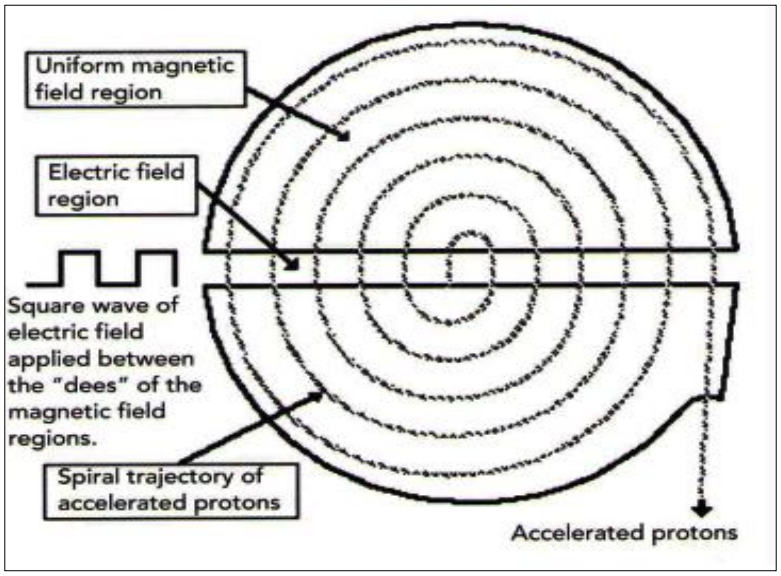

Figure 20:Pictorial description of the beam, electric and magnetic fields in a cyclotron. Electric field accelerates the protons every time they cross the gap. Magnetic field limits the beam in the Dee volume until the beam reaches to maximum energy and extracted from the edge of cyclotron. Image source: (60)

Cyclotrons can be either isochronous or synchrocyclotron. In isochronous cyclotron, all the protons have same orbital period regardless of the radius and speed of particles. As a result, RF power operates at a single frequency and hence, a continuous wave is produced. Isochronous are well suited for beam scanning technique (it will be described later) because beam can be turned on and off quickly with short response time during beam current modification. Since the isochronous cyclotron extracts the fixed proton beam energy, an energy selection system needs to be placed in the beam line. It consists of carbon wedge degrader of variable thickness to move in and out of the proton beam. As a result, increases emittance, energy spread and reduces efficiency. Moreover, the use of degradation material in beam path leads to secondary radiation and, hence, more shielding is required. In

synchrocyclotron, the driving RF electric field is not kept constant so as to compensate for the increasing velocity of particles (59).

Synchrotron, it is a circular accelerator ring enclosed in electromagnetic resonating cavities which accelerates the particles. As the particle energy increases with each turn, the magnetic field strength needs to be changed to synchronize the particle energy with magnetic field strength. This approach allows the ability of the synchrotron to produce pulsed beam of variable energies (59).

The major advantage of synchrotron is its ability to produce proton beam of variable energies. Consequently, no use of energy degrader system that will avoid secondary radiation. Overall, synchrotron is a more flexible solution over cyclotron in the generation of proton beams (59).

- **Beam delivery techniques**

Passive beam scattering:

Passive beam scattering uses arrangements of scatterers and degraders to spread out the beam to cover the treatment field and extend in depth of the PTV. The spreading of the beam occurs in the section of the beam line called “nozzle”, to achieve adequate conformation of the dose to the PTV (60). A single scatterer lead slab (High Z material) broadens the beam sufficiently for the coverage of the small fields. For larger fields, a second scatterer is needed to ensure a uniform, flat lateral dose profile (63, 64). In case of deep seated targets, range modulators in addition to scatterers are used to spread out the Bragg peak in depth. Range modulator is basically a propeller based object of successive layers of varying thickness. Each layer pulls back the Bragg peak of the each pristine proton beam proportional to the water equivalent thickness of the layer to form the flat characteristic spread out Bragg peak (SOBP). In case the distal part of the target is shallower than the range of the beam, constant thickness range shifter can be employed to achieve a global adjustment of the SOBP depth to match the depth of target volume. This setup is placed upstream near the nozzle entrance and contributes for upstream modulation, whereas traditionally the range modulators were used close to the patient called downstream modulation, so that the scattering in the modulator itself can be ignored but it causes the edges of the dose distribution less sharp (60).

Alternatively, range modulation is accomplished by inserting the individual constant thickness degraders and scatterers into the beam in a programmed way. The plastic degrader and lead scatterer combination is most often used since low Z-material (Plastic) and high Z material (lead) can stop the protons more efficiently with correspondingly minimum scattering at each depth. The SOBP is created step-wise in a process called lamination. Because of the switch over time between degraders, lamination delivers the proton beam sequentially as a function of range and this increases sensitivity to organ motion in the depth dimension, not in lateral dimension as it is produced by scattering over the entire treatment field. The number of modulator required to cover all clinical requirements can be efficiently reduced by varying the beam current during the modulation cycle. Beam current modulation from zero to full beam current provides the full dynamic control of the creation of the SOBP depth dose profile independent of the particular range modulator (60). Figure 21 demonstrate the double scattering nozzle with sequentially placed beam modifying components.

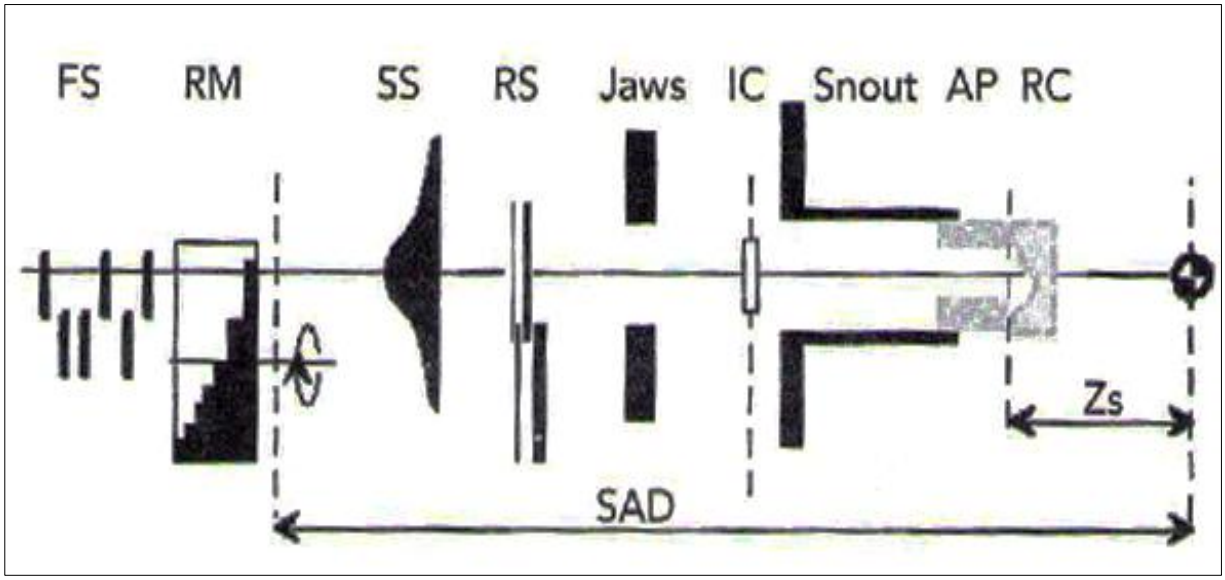

Figure 21: Illustrates double-scattering nozzle with relevant beam modifying components. FS= First scatterer of lead foil, RM=range modulator, SS=second scatterer, RS=range shifter, Jaws, IC=ionization chamber, Snout, AP= aperture, RC= range compensator. Image source: (60)

Double scattering uses second scatterer to reduce energy loss and produce uniform, lateral dose profile thus making the large fields practical. It can be seen in figure 22. The upstream range modulator S1 serves both as range sifter and primary scatterer to produce a non-uniform

Gaussian on the secondary scatterer S2, modified to produce a flat or nearly flat dose distribution at the patient. The second scatterer typically consists of the two materials, that is high Z material to maximize the scattering and minimize the range loss whereas a low Z material to minimize the scattering and maximize the range loss. In order to flatten the beam profile the protons at the field centre must be scattered more than the protons further outside the field centre thus resulting in the optimized profile of useful radius R (60).

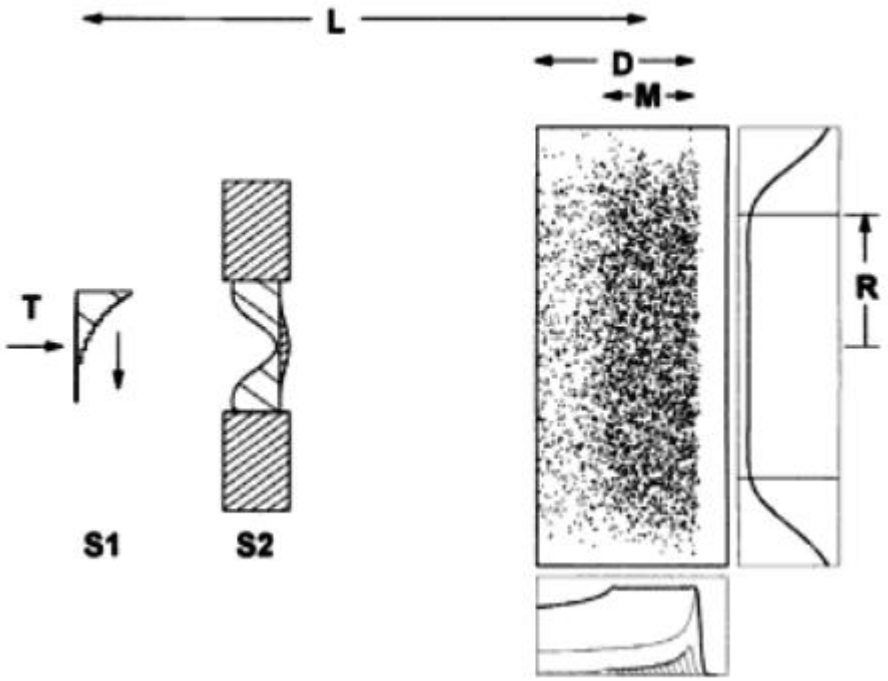

Figure 22: Double scattering with upstream range modulator. Image source: (60)

The major disadvantage of the dual scattering is an increased sensitivity to beam steering. The mechanical or beam steering magnet error can easily cause the beam to tilt off centre as little as millimeter on the secondary scatterer which correspondingly tilt the flat dose distribution at the patient (60).

Aperture: It is a patient specific hardware device made up of brass with a hole inside to fit the outer projection of the target beam's eye view. It is used for the lateral dose conformation to the target and in addition eliminates the proton heading outside the PTV (60).

Range compensator: It is complex shaped plastic block which is used to tailor the dose in depth by shifting the proton range depending upon the PTV shape to achieve the distal dose conformation (60).

Lateral and Distal dose fall off:

Practically, it is important to have a good nozzle design. Primary and secondary scatterer or range modulators should be placed far upstream from the patient to produce the sharp dose distribution. Further, scattering occurs in the patient resulting in unavoidable poor dose gradient for the deep seated tumour, no matter how good the nozzle design is.

Moreover, air gap is another significant factor deciding the dose gradient for the target volume. For illustration, large air gap between the final aperture and patient spoils the lateral dose fall off. Unlike lateral dose fall off, the distal dose fall off is determined by the shape of the Bragg peak. Both aperture and compensator are mounted on the retractable snout on the treatment head. The retractable snout ensures that the air gap between the beam shaping devices and patient should be kept as low as possible to reduce the effects of scattering in air, which causes softening of the beam penumbra (60).

Beam scanning techniques:

One peculiar characteristic of the protons is its charge which enables magnetic deflection of a narrow pencil beams. Proton beam can be scanned in the lateral direction (x-y) through magnetic deflection across the target volume and modulation in depth (z) can be achieved by dynamically varying energy of the protons (60).

In principle, the individual narrow pencil beam is scanned across the target volume layer by layer at various depths. One can initiate with the deepest layer with highest energy and scan in zigzag fashion. With the change in energy, the next layer is repainted and so forth until the whole target volume has been scanned. For each layer intensity needs to be modulated as the distal part of SOBP delivers more doses depending upon the shape of the distal surface than to the proximal layer in order to generate the uniform target dose and conformity. Each layer may be repainted multiple times in order to avoid delivery error and uncertainties (60). Individual pencil beams are sequentially deposited onto the patient under computer control

and range of the beams can be adjusted as a function of beam position in both X-Y and Z direction called variable range modulation (65).

Spot scanning proton therapy (SSPT) is the fast, dynamic scanning of a proton pencil beam over a target volume to provide better conformal coverage. SSPT can be delivered, either by using multifield optimization (MFO) or single field optimization (SFO). In MFO, all spots from all fields are optimized simultaneously. In SFO, each field is optimized individually to deliver the prescribed dose to the target volume while respecting tolerance of the normal structures. SFO, is also known as single-field uniform dose (SFUD). MFO has so far only been introduced in combination with IMPT. It is important to note that in IMPT, it is the modulation of particle number rather than beam intensity(66). In MFO-IMPT, non-uniform dose distributions are delivered from each treatment field at a given direction, with large dose gradients. The desired uniform dose in the target volume is achieved by summing the dose contributions from all the fields. MFO-IMPT is sensitive to range and set-up uncertainties. On the other hand, SFO has more robustness but constant and limited modulation unable it to achieve OARs sparing (59, 67).

Intensity Modulation proton therapy (IMPT) can only be done by pencil beam scanning. IMPT is analogy to intensity modulated radiation therapy. Various modes of the beam scanning techniques have been devised as follows:

Discrete Spot scanning: It is a specific mode of beam scanning where a beam is moved to the static position without delivering the dose and the dose is delivered once the correct position has been achieved. It is similar to step & shoot approach of the IMRT, it keeps the constant magnetic settings when targeting at the static spot (68). Then the beam is switched off and the magnet settings are changed to target the next spot and so forth. Of note is the fact that intensity modulation is produced by causing the variation in the irradiation time per spot, not the variation in beam intensity. The scanning is done in longitudinal dimension only and the other dimensions are being achieved by couch movement.

Dynamic spot scanning: Here the beam scanning is done continuously across the target volume. The intensity modulation is achieved through the modulation of the beam current or by modulating speed of the scan, or both. It has several advantages over discrete spot scanning as it results in faster delivery and shorter beam-on time. Therefore, it is less sensitive to organ motion and more efficient in avoiding range uncertainties.

Wobbling: It is the application of relatively broad beam (diameter in the order of 5cm) scanning across the target volume. It results in broad penumbra. The easy achievement of larger field sizes than attained from passive scattering accounts for its advantage.

One advantage of the MFO-IMPT is that the modulation width of the SOBP in each pencil beam axis can be varied along the length of the target. Therefore, region of 100% dose in the Bragg peak is strictly confined within the target and reduces skin dose. It delivers 3D conformal dose distribution in lateral, proximal and distal dimensions. In contrast, the beam scattering employs constant modulation width and is equal to the maximum length of the target along each broad beam axis resulting in some unnecessary amount of dose spilling proximal to the target volume, especially at places where the target shrinks. Another advantage of the MFO-IMPT technique is the minimum neutron dose deposition due to the absence of primary and secondary scatterers as well as the reduction of the field specific hardware. Furthermore, the MFO-IMPT approach do not use field or patient specific devices, collimators and compensators, therefore sequential fields are delivered without entering into the treatment room. Thus, reduces treatment time and increases patient throughput. The biggest advantage of the MFO-IMPT is the utilization of full flexibility and variability of the spot scanning technique and hence, it is potentially capable in increasing OARs sparing (60). Accounting for its disadvantages, MFO-IMPT approach has higher sensitivity to organ motion comparative to passive scattering (69, 70). Another disadvantage is the technical complication to generate very narrow pencil beams (59).

IMPT has dosimetric advantages over IMRT: It is possible to construct steeper dose gradient with scanned proton beams. For that obvious reason it is feasible to shape 3D conformal dose distributions with convexities and holes and can avoid those pencil beams which point at sensitive structure or pass through complex density heterogeneities (60).

- **Target volumes in proton therapy**

The concept of target volumes is similar to both photons and protons except little dissimilarity in PTV owes to range uncertainties for protons. Particularly for protons, the concept of PTV margin depends primarily upon their physical properties as opposed to geometrical properties of the field for photons, where physical properties signify range uncertainty due to distal dose

fall-off and geometrical properties indicate beam position, respectively (71). The PTV is used primarily to determine lateral beam margins as well as distal margins (margins in depth) to account for range uncertainties. Correspondingly, for photons PTV is just used to determine the lateral beam margins. Protons in principle need a separate PTV with different lateral and distal margins for each beam orientation. It is therefore unpractical to use different PTV for each beam employed and incorporating computer beam-design algorithm for separate lateral and distal margins. As a result, for protons the PTV will be defined relative to the CTV for lateral uncertainties alone and adjustment will be made in the computer beam algorithm in case of differences between margins needed to account for uncertainties along the beam direction (i.e. range uncertainties) and PTV (i.e. based on lateral uncertainties) (72).

- **Patient positioning and immobilization**

Generally, most part of the patient positioning and immobilization in IMRT applies equally well to the proton therapy. Unlike in IMRT, online patient position verification and correction protocol extends to not only verify after initial patient set-up but also before each field within the treatment fraction. Moreover, the use of latest image information for intra-fractional verification guarantees the best tumour coverage and the efficient sparing of the normal tissues. However, there are few issues significantly specific to proton therapy. One of the major differences relates to the physical properties of the protons. Since, proton has no build up effect on skin so this allows the use of immobilization device in contact with the skin. Other relates to the range of the proton particles. Proton ranges are adversely affected by the sharp dose fall off at distal end due to the variation in radiological depth of the SOBP. Furthermore, immobilization devices do have influence on lateral dose gradient. Lateral dose penumbra can be influenced by both increase in distance from beam source to patient, and an increase in aperture to patient distance. Therefore, the radiological and geometrical thickness of the immobilization devices should be kept to minimum to have maximum dose conformity around target area and minimum risk to organs at risk laterally to beam direction. Treatment couch also causes increase in distance between beam limiting device and the target; thereby increase in lateral dose fall. All these factors affecting distal and lateral dose conformation should be taken into consideration during treatment planning. Whereas, in case of scanning beams the knowledge of tumour motion and immobilization is even more important because of interference effects between scanned proton beam and moving tumour. Therefore, it is

important to ensure the correct position of the tumour and critical structures as planned to avoid the geometrical misalignments (71).

- **Inverse planning**

An appropriate inverse treatment planning system (TPS) is strictly necessary to take full benefit of scanning techniques. Inverse planning determines the best fluences of individual beams to achieve optimal dose conformation around target volume (73). The resultant optimized plan in IMPT is a set of particle fluence distribution, generally known as "fluence or intensity map". Fluence map gives the position of the beam spots with respective intensities. Unlike in IMRT, IMPT utilizes different and separate fluence map for each of the pencil beam from the same direction in the field. Therefore, for a constant energy setting it is possible to deliver fluence maps sequentially from layer to layer (60).

The only major difference outlining IMPT is that both energy and intensity of the each pencil beam should be varied (74). Thus, increases the number of degree of freedom drastically. As a result, better dose conformation potential can be achieved with IMPT but the computational time and delivery complexity also increases. The dose calculations can be simplified if the appropriate intensity modulation technique is pre-selected. One method is distal edge tracking (DET) originally explained by Deasy et al, 1997 (75). The Pristine Bragg peaks of the individual pencil beams are placed on the distal surface of the target volume with optimized intensity modulation thereby creates a highly non-uniform dose per field. Thus, a desired dose distribution is obtained by combining all the treatment fields from different directions. DET creates steep dose gradient as it shapes the dose distribution with distal fall-off of the Bragg peak (distal fall-off of the Bragg peak is sharper than lateral fall-off). For that reason, it is difficult to achieve uniform dose in the target volume. DET produces lowest possible integral dose because each constituent pencil beam delivers maximum dose at distal edge with minimum dose to the critical normal structures. However, this technique is also sensitive to range uncertainties. Simpler technique is the 2.5D technique where a spread out Bragg peak distribution of the individual pencil beam can be applied to create SOBP modulation. Multiple pencil beams of variable modulation width (different energy for each pencil beam) are individually shape to the proximal and distal edge of the target volume such that the dose is constant along the depth of target volume. The most generally used IMPT technique is 3D-

modulation; it places the pristine Bragg peaks of the individual pencil beams throughout the target volume with optimized intensity modulation (60). Figure 23 shows the different approaches for intensity modulation.

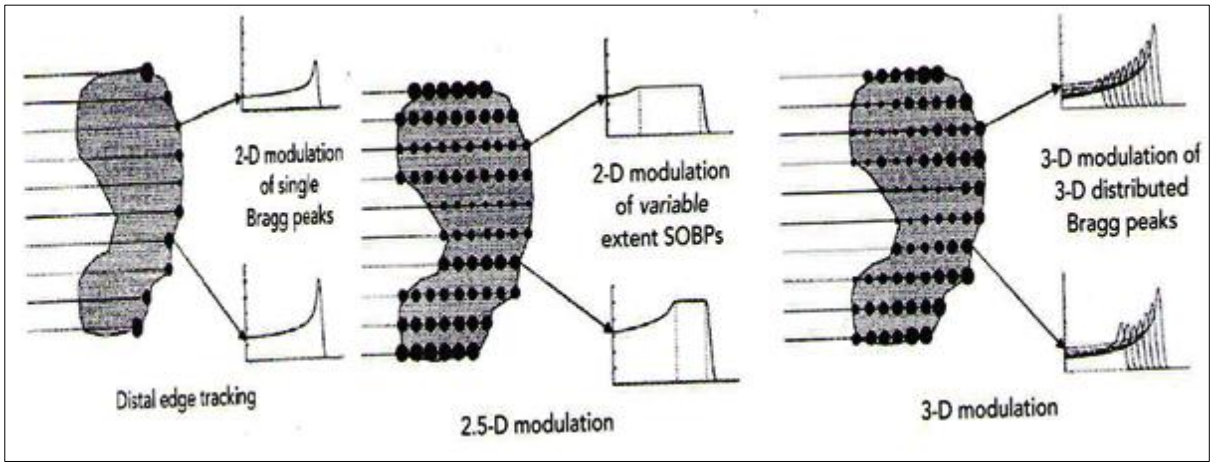

Figure 23: Three different approaches to intensity modulated proton therapy. The solid circle on the target volume represents position of individual Bragg peak. The diameter of the solid circles indicates the relative intensities. Image source: (60)

In 3D modulation, treatment fields can be delivered either by layer scanning or by depth scanning. Layer scanning can be accomplished by irradiating consecutive layers of equal radiological thickness. Constant proton energy should be kept per layer as well as modulation of the intensity in the transverse plane. The same process is repeated for next consecutive layer and so on with different proton energy settings. Alternatively, depth scanning can also be used. For each pencil beam position, a number of depth positions are consecutively scanned with highest energy setting for the most distal layer and decreasing the energy for successive layers (60). A basic illustration of the dynamic delivery in the IMPT is shown in the figure 24

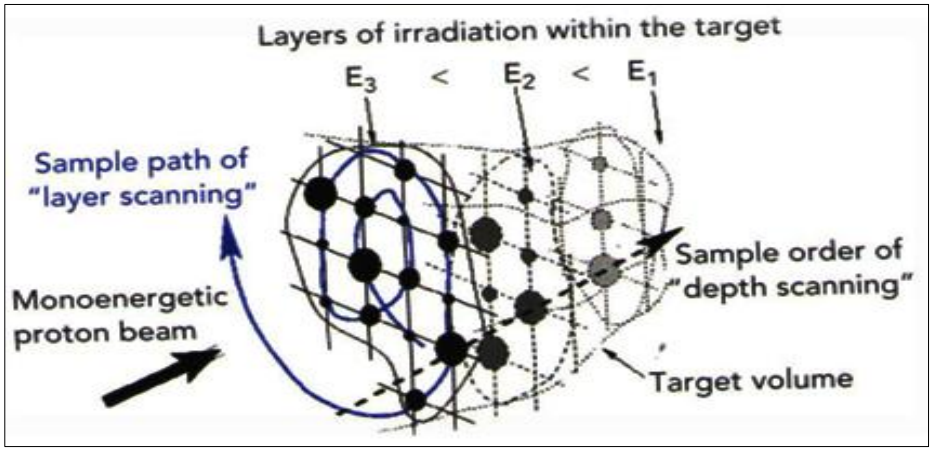

Figure 24: The target is sliced in multiple layers. Each layer has a constant radiological depth indicate by energies E1, E2 and E3. The target is irradiated in successive layer. Each layer contains a set of pristine Bragg peaks of varying intensity to produce desired dose variation within a layer. Image source: (60)

- **Optimization algorithm**

Conformity, selectivity and gradient index are the three major entities of the objective function. For the purpose of assigning dose-volume objectives to the volume of interest (VOI). The 3D patient image is grouped into 3D volume elements called "Voxels". Volume of interest (VOI) consists of voxels as a function of which target volume and critical structures are defined. The fluence map provides information about the beam spots with their respective intensities. The term optimization in IMPT treatment planning typically signifies the search for a set of beam spot weights that minimizes the objective function. The dose-volume constraints for OARs are specified in such a way that no voxel in the OARs should receive that exceeds the maximum tolerance dose limit. Similarly, for target volumes, no voxel should receive dose short of prescription dose. Since it is not practically possible to satisfy all the constraints simultaneously, hence weighting or penalty factors are also defined for the target volumes and OARs. Consequently, the optimized treatment plan represents a compromise solution in which the actual and prescribed dose matches as close as possible (60).

The generalized form of the optimized dose function can be expressed as follows:

Objective function= $\sum_n^N Wn \sum_i^{In} F(di - Dn)$ (7)

In equation 7, N is the total number of constraints, I*n* is the total number of voxels in a volume n and F is the constraint specific objective function (OF) which expresses the difference between actual dose distribution (d*i)* and prescription dose (D*n*) (60).

2.5 Radiobiology

Relative biological effectiveness (RBE) is an indicator of the biological effectiveness of the radiation dose. As per definition, RBE of protons states that dose of the reference radiation (i.e. X-rays) at 250KVp divided by dose of test radiation required to produce the same effect (76). Protons are biologically more effective than photons. Basically, it means that protons require lower doses to produce the same biological effect as compared to photons. The effect ionizing radiation have in a specific biological material is LET dependent, and also influenced by factors such as the dose and the individual energy of the irradiating beam particles amongst, other. One way to increase the differential radiobiological effect can be modifying the radiation quality parameter, i.e. LET.

Linear energy transfer (LET) has been viewed as a qualitative indicator of the biological effects of different kinds of radiation (77). It depends upon nature and initial beam energy of the particles. As the charge and energy of the particle changes along particle's path, LET also changes. It is a parameter associated with the change in RBE. The change in the RBE occurs with the change in the energy deposition density or LET along the particle's path. The LET at which the maximum RBE occurs is particle specific. The RBE increases continuously along the SOBP and significantly at the declining edge of most distal part of the Bragg peak resulting in the extension of the biological effectiveness of RBE corrected dose by 1-2 mm (78). The maximum LET is 100kev/µm at Bragg peak for protons (77). Beyond that LET range, RBE decreases due to over killing effect (dose deposited is more than dose required to kill the cells). It is well known that the RBE is not a fixed value, but varies over the physical depth dose curve, and also varies with tissue type and with the fraction size. Clinically, a generic RBE of 1.1 is applied independent of physical (beam energy, position in SOBP, dose/fraction, depth of penetration) and biological (irradiated cell or tissue, biological endpoint) parameters as recommended in ICRU report 78 (72). This value is applied to all the

tissues types that fall in direct beam path (78). Generic RBE is just a rough approximation and it is applied to neglect RBE variations along the SOBP.

Absorbed dose is a physical quantity in radiation therapy. It is an important predictor of clinical outcome but it doesn't hold a unique correlation to biological effect. Several factors like dose/fraction, overall treatment time, dose rate, dose homogeneity as well as radiation quality (RBE) influences the clinical outcome. Absorbed dose (D) is defined as the amount of energy absorbed per unit mass of the matter irradiated. The dose is expressed in Gy (Joule/kg). The same amount of physically deposited dose from different types of radiation does not necessarily produce an equal biologic effect in the irradiated tissue. RBE is applied to relate proton dose to photon dose. Therefore, to determine what dose of proton is equal in producing the same identical biological effect as a certain dose from photons, the RBE weighted dose is defined:

D_{RBE}=D X 1.1, D_{IsoE} = D_{RBE} = D X 1.1, keeping all other irradiation conditions identical (dose/fraction, treatment time, etc) .....Where, D_{RBE} is RBE corrected dose in cobalt-gray equivalent. (8)

In equation 8, the D_{RBE} is the RBE-weighted dose and the D is the physical proton dose in Gy. Since, the unit for RBE corrected dose and absorbed dose is same (Gy), therefore, to avoid confusion cobalt-gray equivalent (CGE) is used as a unit for RBE corrected dose in protons (79).

The RBE of the SOBP abutting critical normal structures contributes dose at the distal end are of principal concern. This clinical consequence compel the treatment planners in not utilizing one of the dosimetric advantage of the protons, namely sharp dose fall-off for single field plans (59).

2.6 Recommended dose-volume constraints for limiting OARs toxicity

2.6.1 Rectum

The most frequent endpoint used to quantify the dose-volume tolerance for radiation induced late effects in rectum is grade≥2, i.e. late rectal toxicity. The volume of rectum receiving dose

≥60Gy is constantly associated with risk of grade≥2 or rectal bleeding. Generally, high doses are predominantly related to risk of toxicity. Volume receiving dose ≤45Gy are not significantly linked to rectal toxicity (80).

For whole organ volume segmentation, V_{50Gy}<50% (81)

2.6.2 Bladder

There exist difficulties in keeping reproducible shape and volume of bladder throughout the treatment course due to highly distensible nature, variation in its volume with filling, post void residual volume, breathing and positioning. Therefore, partial irradiation of bladder doesn't guarantee the true treated volume of bladder during the course of treatment. Hence, reliable dose volume constraints cannot be defined unless the whole pelvic is irradiated.

Treatment of locally advanced cervix cancer with EBRT alone usually requires higher dose (>60Gy) which often results in incidence of late complications (82). Therefore, EBRT is combined with brachytherapy. EBRT component of treatment limits the dose to 40-50Gy, and rarely outcome severe late effects. However, intra-cavity brachytherapy increases the total dose to 70-90Gy, and even higher, to a small volume. Upper dose limit of bladder tolerance has yet not been defined. Further study considering the non static nature of bladder and long term clinical follow-up is required to produce actual dose-volume tolerance limits for bladder (83).

2.6.3 Bowel

For whole-organ irradiation, $TD_{5/5}$ [1]and $TD_{50/5}$[2] estimated for small-bowel toxicities were 40Gy and 55Gy respectively. Whereas for partial organ irradiation (1/3 small-bowel irradiation), $TD_{5/5}$ and $TD_{50/5}$ estimated were 50Gy and 60Gy. These RT dose limits are related to acute and late toxicity risk (84).

Concurrent chemotherapy in addition to radiotherapy is related to RT-induced acute toxicities in small-bowel, and previous abdominal surgery has been linked to higher risk of RT-induced late injuries. According to published date in the QUANTEC review for small bowel, maximum dose is likely related to late toxicity and volume threshold parameters (V_D) are

[1] TD5/5 is the estimated doses with a 5% risk at 5 years
[2] TD50/5 is the etimated doses with a 50% risk at 5 years

related to acute toxicity. It is important to mention that the results for volume threshold-based risks are dependent upon methodology of contouring small bowel. Roeske et al. outlined the entire peritoneal cavity (excluding bladder and rectum) as small bowel (11). Such volume is associated with dose 45Gy. Therefore, V_{45Gy} should be minimized and kept less than 195cc to reduce acute and chronic late toxicities (84). However, according to dose planning in cervix cancer at Oslo University Hospital, V_{45Gy}<195cc may be difficult to achieve and recommended to use V_{45Gy}<300cc (85). Note that this limit is only valid for pelvic irradiation. Treatment plans with para-aortic irradiation in addition to pelvic irradiation are well accepted with V_{45} to 450-600cc.

2.6.4 Pelvic bone

The mean dose to pelvic bone is significantly related to the hip and sacral pain for patients with pelvic radiotherapy. It was recommended to reduce the D_{mean}<37.5Gy during treatment to lower the chances of long-lasting pain (86).

2.6.5 Kidneys

The kidneys are dose-limiting organs in radiotherapy of gynecological cancer when the para-aortic region is included. Several dose/volume parameters are estimated to evaluate the risk of RT-induced renal injury. Risk of kidney injury depends upon the bilateral kidney RT or partial volume RT. Kidneys are parallel organ so even if a part of kidney is irradiated, it will not cause renal toxicity. For bilateral kidney irradiation, the mean kidney dose ($D_{50\%}$) should be <15-18Gy and <28Gy for $TD_{5/5}$ and $TD_{50/5}$, respectively. Several other dose volume constraints for combined kidneys are given below:

V_{12}<55%

V_{20}<32%

V_{23}<30%

V_{28}<20% (87)

2.6.6 Spinal cord

With the conventional scheme of 1.8-2Gy per fraction for full cord cross-section, the estimated risk of myelopathy is 0.2 at maximum dose (D_{max}) of 50Gy (88) (81).

2.6.7 Cauda equina

The maximum dose to cauda equina should not exceed 60Gy, (D_{max}<60Gy) (85).

2.7 Clinical margins for cervical cancer

This chapter is taken from a review study done by Jadon et al (22).

In the treatment of cervical cancer, the pelvic organs at risk inherently tend to show positional and volumetric variation over time. As an effect, any variation in bladder and rectum filling can cause change in the cervix-uterus position and shape. Therefore, margins are required to ensure CTV coverage and, thus results in unnecessary inclusion of the OARs into high dose region. Owning to the steep dose gradients around the PTV produced in the conformal therapy, cervix-uterus motion can cause geometrical uncertainties. Thus, cervix-uterus movement reduces the potential and benefits of conformal radiotherapy in cervical cancer. To tackle the issue of cervix-uterus motion, it is important to establish accurate and precise strategies. First and foremost step in the implementation of the radiotherapy is the accurate delineation of the CTV on the planning CT scan and determining the margins around to form PTV. Based upon the knowledge of the extent and pattern of the cervix-uterus motion and influences of bladder, rectum filling, CTV-PTV should be kept large enough to minimize organ motion and patient set-up uncertainties respectively. R. Jadon et al has reviewed organ motion and IGRT strategies in EBRT for cervical cancer. The study had investigated the issue of inter-fractional, intra-fractional organ motion and influence of rectal, bladder filling during treatment in cervical cancer. It was indicated that the effect of intra-fraction motion is less distinct than inter-fraction motion but the internal margin should be selected such that it accounts for both. It was confirmed that bladder filling has more impact on uterine motion whereas rectum filling is more responsible for cervix motion. They reported displacement of up to 15mm in uterus compared to up to 6mm in cervix. The examination reported a maximum of 48mm, 32mm uterine motion relative to 19mm and 12mm cervical motion in A-P and S-I direction respectively. This validates the fact that uterine is more mobile than

cervix. Potential solutions include an isotropic margins of 15.3-21mm and anisotropic margins of up to 32mm in A-P, 20mm in S-I and 17.5mm in L-R. This validates that the mean CTV-PTV margin of 15mm is not sufficient in encompassing the CTV successfully. However, a study by Tyagi et al has investigated that with the use of 15mm CTV-PTV margins there exists only a minimal miss of 4cc in CTV, with maximum missing in uterine fundus (89). It is important to notify that the presence of microscopic disease in uterine fundus is a topic of current research debate and hence, the use of 15mm margins is well accepted clinically.

Two studies investigated set-up margin using daily CBCT to create PTV for designing IMRT/IGRT protocol. These significant set-up margins add up with internal margins to create CTV-PTV margins. However, it is recommended to follow institution-specific set-up margins as they are determined on specific patient positioning, immobilization, treatment verification and imaging protocols. Even though, treatment in prone position has shown the significant sparing of the small bowel but it is also coupled with a larger set-up error. The use of Generous CTV-PTV margins will diminish the benefit of sparing small bowel.

Alternative Strategies were considered effective to deal with complex issue of organ motion. Strategies include offline and online imaging. However, according to UK national guidance, both offline and online imaging are found incompetent in improving treatment accuracy, given the unpredictable, complex nature of uterine and patient specific organ motions. Therefore, personalized adaptive IGRT strategies are probably the most promising option to manage the observed motion. Based upon the analysis of pre-treatment correlation between the bladder filling and displacement pattern of the cervix-uterus, a library of treatment plans with incremental CTV-PTV margins are created. Using the daily in-room CBCT imaging with soft tissue matching, the displacement of the CTV is determined from the planned position. Consequently, an appropriate plan of the day is selected from the series of treatment plans.

3 Study design

The chapter deals with the methodology utilized to prepare optimum treatment plans. Treatment planning was done for IMRT and IMPT based upon dose-volume objectives for target volumes and organs at risk. Various evaluation criteria were selected, analyzed and compared between both modalities to quantify the dosimetric differences.

3.1 Patient population

Ten patients with histologically proven locally advanced cervical cancer were included in this comparative treatment planning study. Out of ten patients, five patients received treatment in para-aortic region in addition to pelvic irradiation. Staging was done according to international federation of gynecologic and obstetrics (FIGO).

3.2 Imaging for treatment planning

Computed tomography (CT) imaging was used for treatment planning. Patients were instructed to drink 300ml of water after voiding half an hour prior to the CT scanning. The same drinking protocol was used prior to each treatment fraction in order to standardize bladder volume and, thus, minimize organ motion uncertainties. The CT acquisition was performed using slice thickness of 3mm and pixel size of 1mm. The CT scan was performed in the supine position using a knee and foot positioning device. The patient's bladder was kept full so as to minimize the organ motion uncertainties.

3.3 Volume definitions

Target volumes and organs at risk volumes were delineated on the axial CT images. The GTV was defined as GTV tumour and GTV lymph nodes. The central and regional nodal clinical target volumes (CTV) were outlined separately. The CTV central included the gross tumour volume (GTV) with a 5mm isotropic margin, the cervix, the entire uterus, both parametria and 3cm margin from the GTV down in the vagina (figure 25). CTV elective was created by expanding GTV lymph nodes with 5mm isotropic margin. Pelvic lymph nodes CTV included perivascular fat and connective tissue around vessels of the common iliac, external and

internal iliac, obturator and presacral lymph nodes. Para-aortic lymph node CTV ranges from L4-L5 vertebral body interspace up to the lower border of Th12.

The GTVs, CTVs and OARs used in this thesis were pre-delineated and hence, they are not a part of this study. However, PTV is a geometrical concept so the PTVs were created based upon those pre-delineated CTVs during treatment planning. PTV central was created by adding margins to the CTV central. Two sets of treatment plans were prepared based on different central CTV-PTV margins: anisotropic clinical margin (7 mm L-R, 10 mm S-I, 15 mm A-P) (figure 25) and isotropic reduced margin (7 mm) (figure 28). PTV elective was constituted by CTV elective with 5mm isotropic margin in between (figure 26). The total planning target volume (PTV union) was created by combining both PTVs (PTV central and PTV elective) (figure 27).

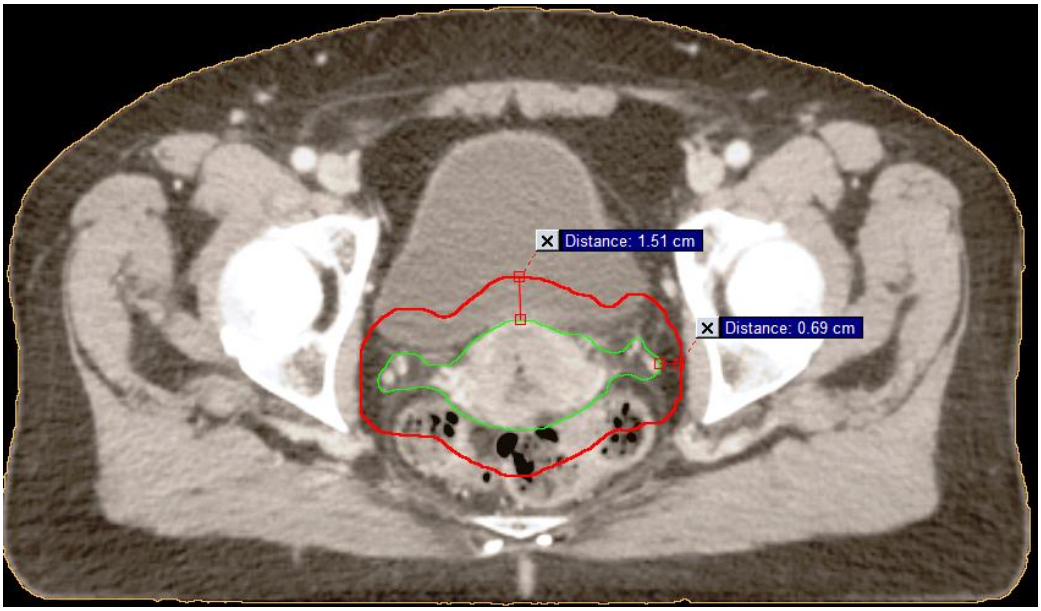

Figure 25: CTV central (light green)-PTV central (dark red) with 1.5cm anterior-posterior margin and 0.7cm left-right margin. Image taken from own work.

Figure 26: CTV (green)-PTV (cyan) elective with 5mm isotropic margin. Image taken from own work.

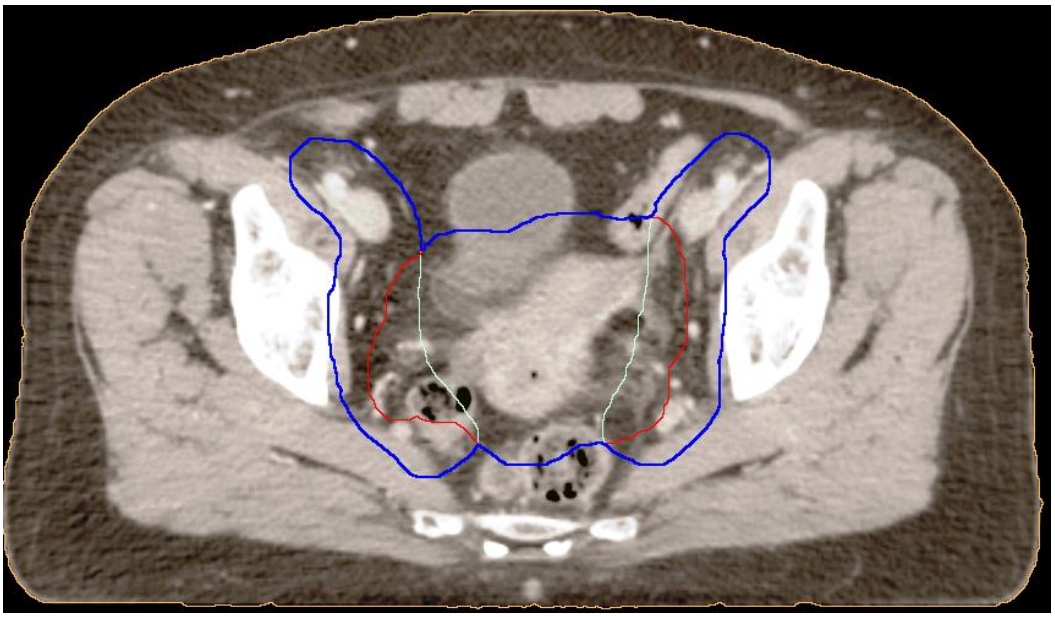

Figure 27: PTV union (blue) = PTV central+ PTV elective with clinical margins (central CTV-PTV margin of 7mm L-R, 10mm S-I, 15mm A-P). Image taken from own work.

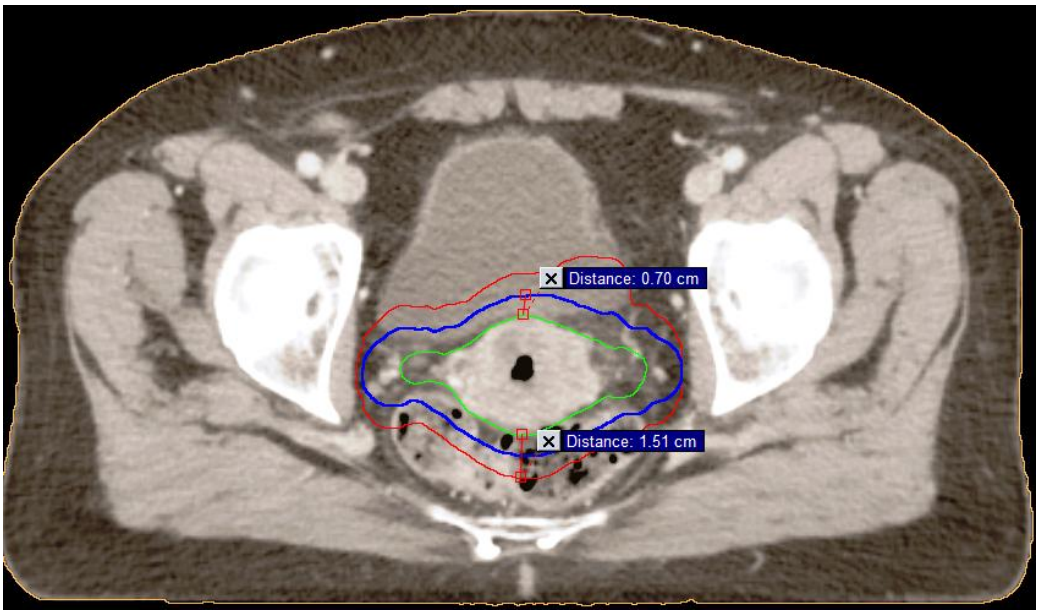

Figure 28: Reduction of Central CTV-PTV to 7mm isotropic. Image taken from own work.

The difference in the two PTV union volumes was due to the difference in CTV-PTV central margin as indicated in figure 29.

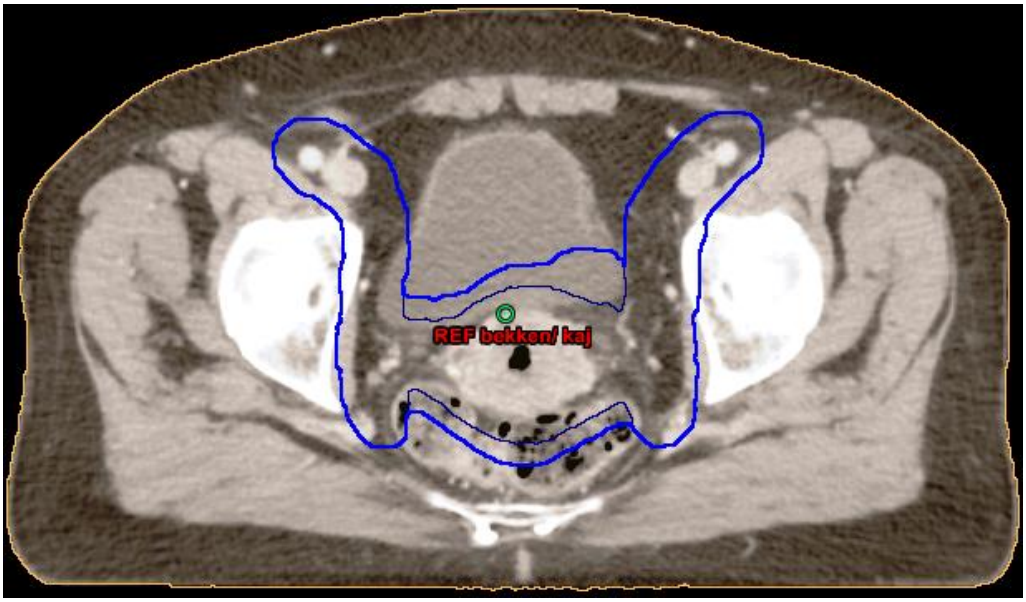

Figure 29: The difference between PTV union (blue) based upon clinical margins and PTV union (dark blue) based upon reduced margins. PTV union (dark blue) = Reduced 7mm central PTV + PTV elective. Reduction of the PTV union (dark blue) volume was due to reduced central CTV-PTV margins (7mm isotropic) from PTV union (blue) (clinical central CTV-PTV margins). Image taken from own work.

Organs at risk (OARs) included body, bowel, bladder, rectum, sigmoideum, pelvic bone, cauda equine, Medulla, left and right kidney. In case OAR is overlapping with PTV, an extra helping structure: OAR-PTV was created to reduce the dose in OARs without affecting dose coverage in PTV.

3.4 Dose prescription

All plans were optimized to deliver 50.4 Gy in 28 fractions (1.8Gy per fraction). All the plans were normalized to the mean of PTV union (PTV union mean=100%).

3.5 Treatment planning

All treatment planning was performed on Eclipse treatment planning system (Varian medical systems, Palo Alto, CA). The PTV dose coverage criteria were set to D98%≥95% (at least 98% of the volume should receive 95% of the prescribed dose). The 3D volume element (voxel) size was isotropic 2.5mm. In case of reduced CTV-PTV margins, extra helping structures were re-defined for OARs due to the possibility of sparing larger volume of the normal organs. Example of the bladder, rectum and bowel sparing from high dose of PTV were shown below in the figures 30(a, b), 31(a, b), 32(a, b).

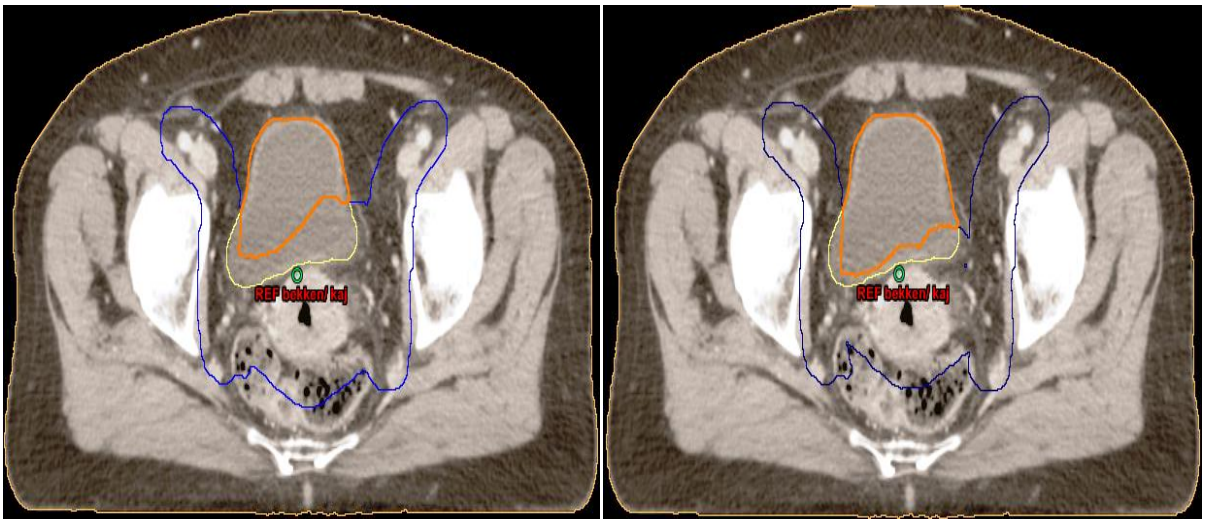

Figure 30a: (Left) The bladder (yellow) using helping structure bladder-PTV (orange) in case of clinical CTV-PTV margins. Figure 30b: (Right) Larger volume of bladder due to the reduced CTV-PTV margins and hence, smaller PTV union volume. Image taken from own work.

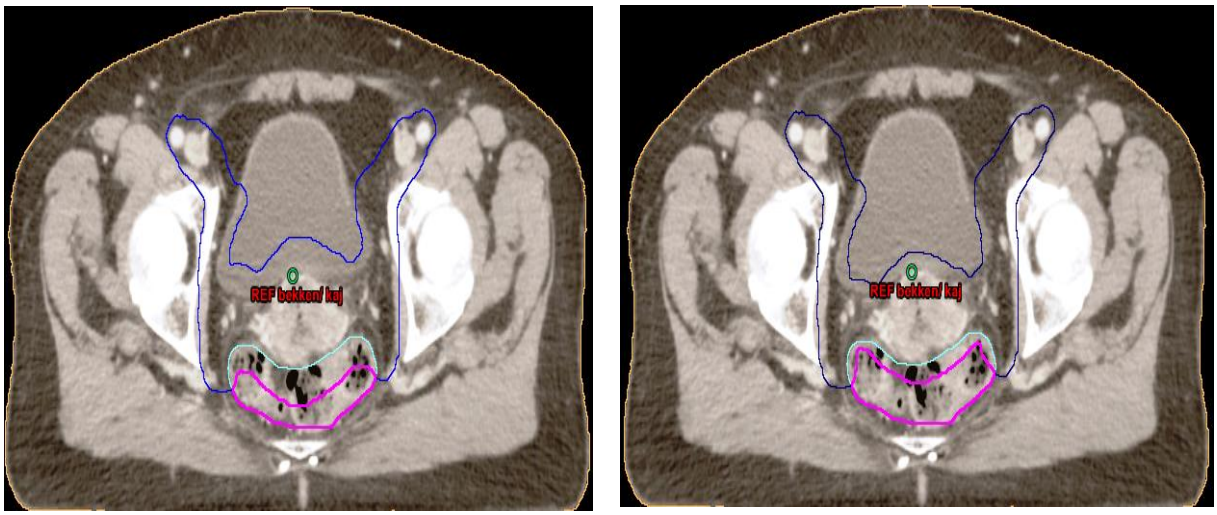

Figure 31a: (Left) Illustration of rectum (cyan) sparing with clinical margins. Rectum-PTV volume with clinical margins is shown in purple color. Figure 31b: (Right) Illustration of rectum (cyan) sparing with reduced margins. Rectum-PTV volume with reduced margins is shown in purple color. Much larger volume of rectum is spared with reduced margins. Image taken from own work.

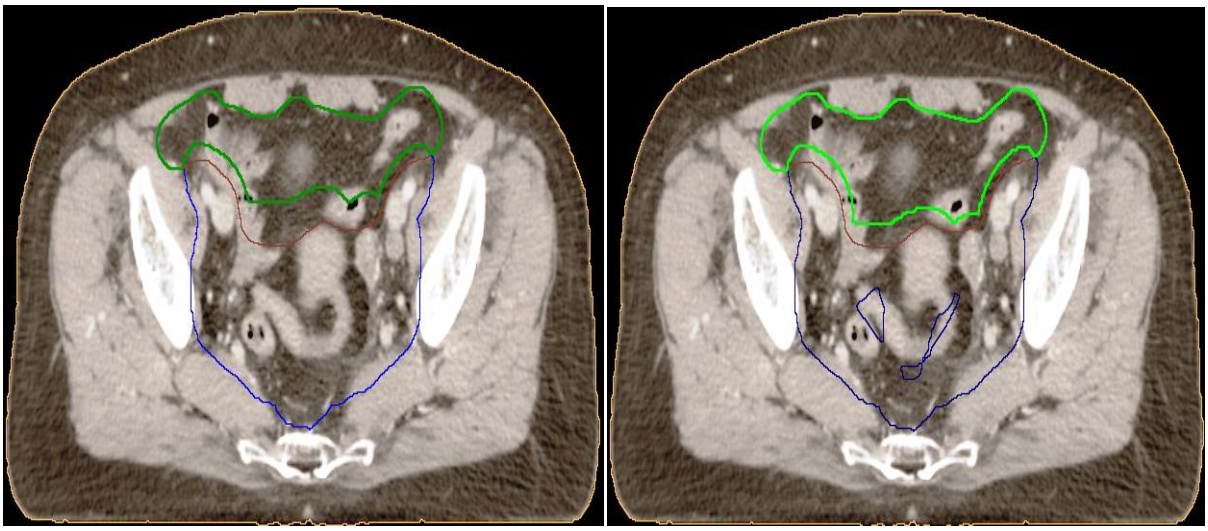

Figure 32a: (Left) Illustration of the bowel (brown) sparing with clinical margins. Bowel-PTV with clinical margins is shown in dark green color. Figure 32b: (Right) Illustration of the bowel (brown) sparing with reduced margins. Bowel-PTV with reduced margins is shown in light green color. Image taken from own work.

Treatment planning was done based upon the procedure from Oslo University Hospital (85). In table 2 the treatment aims used for both IMRT and IMPT planning are listed.

Table 2 Treatment planning aims for IMRT and IMPT

Volumes	**Treatment planning aims**
PTV Union	D98%<95%
Outer body	D2cc<107%
Rectum	As low as possible, but not at the expense of the target volume
Small Bowel	By plotting the entire peritoneal space:volume receiving more than 45Gy should be as small as possible. QUANTEC provide less than 195cc. This may be difficult to achieve, by experience 45Gy is often given to about 300cc
Bladder	As low as possible, but not at the expense of the target volume
Sigmoid	As low as possible, but not at the expense of the target volume
Medulla	50Gy
Cauda equina	60Gy
Kidneys	As low as possible, but not at the expense of target volume. Dose volume requirements for each kidney: V12<55% V20<32% V23<30% V28%<20% Desirable lower dose if possible due to concomitant chemotherapy.

During optimization of IMRT and IMPT, some of the treatment planning dose objectives and constraints were selected and assigned for target volumes and OARs for all the patients. Table 2 shows some of the common dose objectives used during optimization to achieve treatment aims mentioned in table 3. Lower and upper objectives were declared depending upon the required dose distribution over the corresponding volumes. Lower objective for CTV central was defined to cover 100% of the volume with at least 50.4 Gy (100% of prescription dose). To ensure a homogenous dose in PTV union, lower and upper objectives were demanded to cover 100% volume with at least 50Gy and 0% of the volume should not receive dose greater than 51.2 Gy respectively. Lower objective to the target volume determines minimum dose, while upper objectives were subjected to limit the maximum dose to the PTV. Of note was the fact that for PTV union, lower and upper objectives were set at 50 and 51.2 Gy respectively instead of ideal 50.4 Gy because an ideal dose of 50.4 Gy would be difficult to achieve.

For organs at risk, upper objectives were assigned to 0% of the volume should not receive dose greater than 50.4Gy. Therefore, upper objective are considered important to limit the maximum dose in OARs and thus, the side-effects of the treatment. Weighting factors were selected depending upon the priorities assigned to the target volumes and organs at risk during optimization of the treatment plan.

Table 3 Treatment planning dose objectives and organs at risk constraints

Volumes	Volume (%)	Dose (Gy)
CTV Central		
Lower Objective	100	50.4
PTVUnion		
Lower Objective	100	50
Upper Objective	0	51.2
Bladder		
Upper Objective	0	50.4
Bowel		
Upper Objective	0	50.4
Pelvic Bone		
Upper Objective	0	50.4
Rectum		
Upper Objective	0	50.4
Sigmoideum		
Upper Objective	0	50.4

3.5.1 IMRT planning

For each of the patient, IMRT planning was based on seven equally spaced coplanar isocentric 15MV beams (0°, 51°, 103°, 154°, 206°, 257°, 308°) with 3° collimator angle for each field (20). IMRT plans were constructed with the collapsed cone algorithm. Sliding window IMRT delivery technique was used. The IMRT normal tissue constraints included the body, bladder, bowel, rectum, sigmoideum, pelvic bone, cauda equine, Medulla, left and right kidney. PTV was expanded with a margin of 4-5cm.The dose-volume constraints for this volume minus the PTV were assigned to avoid hot spots. An appropriate margin of 4-5mm was laid down around the PTV with the intention that the steep dose gradient caused by dose–volume constraints in PTV expansion minus the PTV will not interfere with the PTV dose coverage. All plans were constructed using normal tissue optimization settings: 0.3cm distance from target border, 105% start dose, 60% end dose and fall off at 0.6cm with priority of 60-70. During optimization process, smoothing factor of 60 was used for both X and Y jaws in all the seven fields. The beam placement and dose-volume constraints were selected, monitored and optimized if needed to maximize the dose uniformity in the PTV while minimizing the dose delivered to the OARs. Quantitatively, all the plans were evaluated by analyzing the dose- volume histograms (DVHs) and qualitatively by inspecting isodose distribution on each CT slice.

3.5.2 IMPT planning

For the proton radiotherapy, IMPT planning was based on modulated pencil beam scanning technique utilizing proton convolution superposition algorithm (version11.0.30). Multi-field optimization was achieved by simultaneously tuning spot energy and spot weights of each pencil beam from all the irradiating fields. The nominal beam energies available were 70-250Mev. IMPT planning was based on three fields: two lateral opposed fields (90° and 270°) and one posterior-anterior (PA 180°) field, to achieve conformal dose distribution in the PTV while sparing normal structures. Therefore, appropriate gantry angles were selected to identify the best geometrical setting for the respective tumour configuration to avoid as much as possible proximal entrance dose through OARs or to minimize the areas of the fields directly abutting against them at the distal edge. For patients receiving para-aortic treatment, the size of the field required was 40cm in S-I direction whereas the available field size of 40X30cm in diameter did not allow treating both PTVs simultaneously. Alternatively, the collimator was

rotated 90° to cover the treatment area but an unexpected machine error appeared. Therefore, split field technique was used because of the technical limitations of the proton modality. Range uncertainties due to HU-stopping power and energy uncertainties were handled by treatment planning system parameter by adding 0.5cm axial proximal/distal margin to cover the target proximally and distally, respectively whereas set-up uncertainties were included in CTV-PTV margins. Spot spacing was set at 5mm and circular lateral target margin of 5 mm. Post processing of all the scanned spots was generated by calculating fluence map of each field and finally the dose calculation was done by combining all the scanning layers.

A total dose of 50.4 cobalt grey equivalent (CGE) with 1.8 CGE per fraction was prescribed and delivered, assuming a generic relative biological effectiveness (RBE) of 1.1 (72). Beam positioning and beam weight optimization was done by inverse planning optimization algorithm to avoid the hot spots at the junction between pelvic and para-aortic fields.

3.6 Evaluation criteria

The evaluation criteria's were the same for IMRT and IMPT treatment modalities. Dose-volume histograms were analyzed for the PTV, Outer body, bowel, bladder, rectum, sigmoideum, pelvic bone, Medulla, left and right kidney. The acceptability of the optimum treatment plan was based on PTV dose coverage criteria $D_{98\%} \geq 95\%$ of the prescribed dose. The ratio of the DVH parameters between IMRT and IMPT were calculated.

Mean organ dose "D_{mean}" was calculated for all organs at risk for each patient. V_{10}, V_{30} and V_{45} were calculated from DVHs for all organs at risk and compared with ideal dose-volume objectives. Additionally, V_{45cc} was calculated for bowel as per QUANTEC recommendation.

For the PTV coverage, $D_{98\%}$ and $D_{2\%}$ were calculated. For the treated volume, $V_{95\%}$ was also calculated.

As per Kataria et al, dose homogeneity index (DHI) is a good indicator of the quality of a treatment plan, but still analysis of DVH parameters and isodose distributions section–by-section in CT image remains as a primary way to evaluate treatment plans. DHI should only be used as a secondary option once the satisfactory treatment plan has been finalized (90). Therefore, isodose distributions of the optimal plans were qualitatively analyzed for PTV and OARs at different dose levels in this study. Additionally, dose conformity index and dose

homogeneity index were calculated to cross verify the finalized treatment plan. The following formulae were used for the respective analysis: DCI = V_{95}/V_{PTV} and DHI = $(D_{2\%}-D_{98\%})/D_{mean}$.

In order to find the hot spots, clinical maximum dose to 2cc of the outer body was calculated for each treatment plan and it should not be more than 107% of the prescribed dose. Student's t-test was done for all statistical comparison between clinical margins and reduced margins for both treatment modalities. P value of <0.05 was considered statistically significant.

4 Results

This chapter presents various clinically important dose-volume parameters to compare two treatment techniques, IMRT and IMPT, both qualitatively and quantitatively. Additionally, the effects of reduced margin on relevant parameters are also mentioned.

4.1 Dose distributions

The isodose distribution for the PTV was qualitatively visualized at 50% and 95% isodose levels. The analysis was apprehended for IMRT and IMPT, both in case of clinical and reduced CTV-PTV margins.

Figure 33 a, b represents the isodose distribution at 95% isodose level for PTV in an IMRT plan for clinical and reduced margins, respectively. In figure 34 a, b represents 95% isodose level for PTV in an IMPT plan for clinical and reduced margins, respectively, are shown. These figures signify the benefit of utilizing smaller CTV-PTV margins in IMRT and IMPT, respectively. Sparing of rectum (orange) and bladder (purple) was achieved for much greater volume utilizing smaller margins. Considering the steeper dose gradient and greater conformity of IMPT around PTV, IMPT effectively surpasses IMRT in sparing greater volume of rectum and bladder.

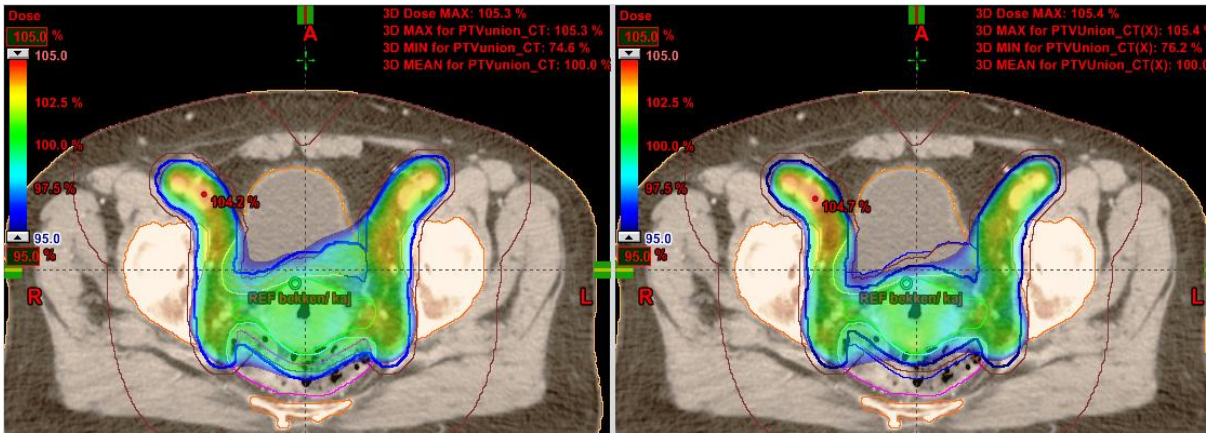

Figure 33: Transverse view of isodose distribution at 95% isodose level for PTV in IMRT. Image on the left (a) represents clinical margins and on the right (b) represents reduced margins.

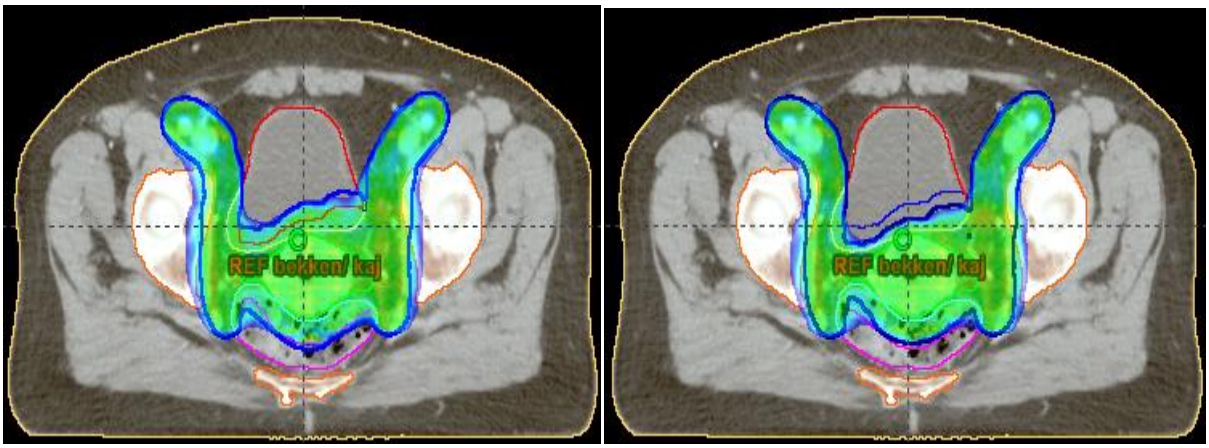

Figure 34: Transverse view of isodose distribution in IMPT at 95% isodose level. Image on the left (a) shows PTV (blue) coverage for clinical margins and on the right (b) shows the PTV (dark blue) coverage for reduced margins.

Dose distribution at 50% isodose level in IMRT and IMPT, respectively can be seen in figure 35 and 36

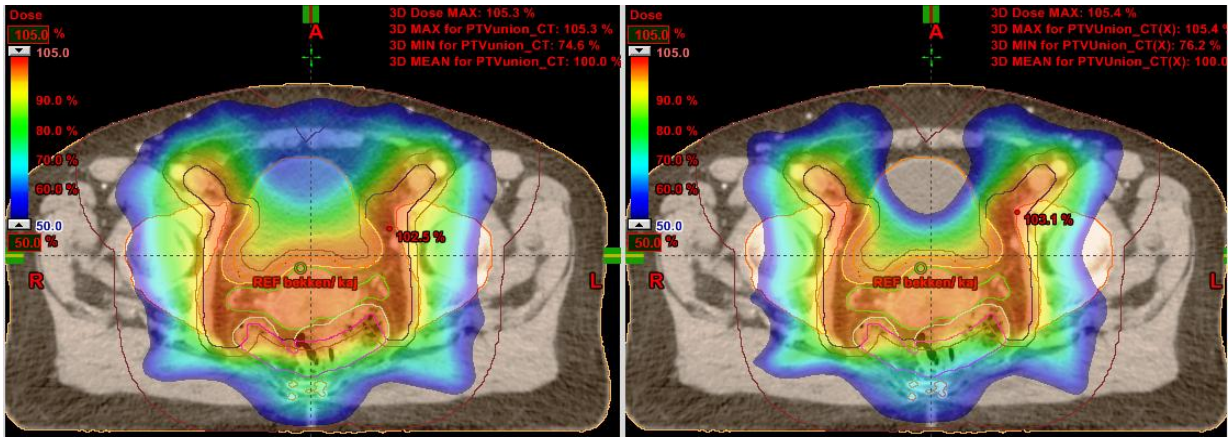

Figure 35: Transverse view of isodose distribution at 50% isodose level in IMRT. Left image (a): 50% dose distribution in IMRT with clinical margins. Right Image (b): 50% dose distribution in IMRT with reduced margins.

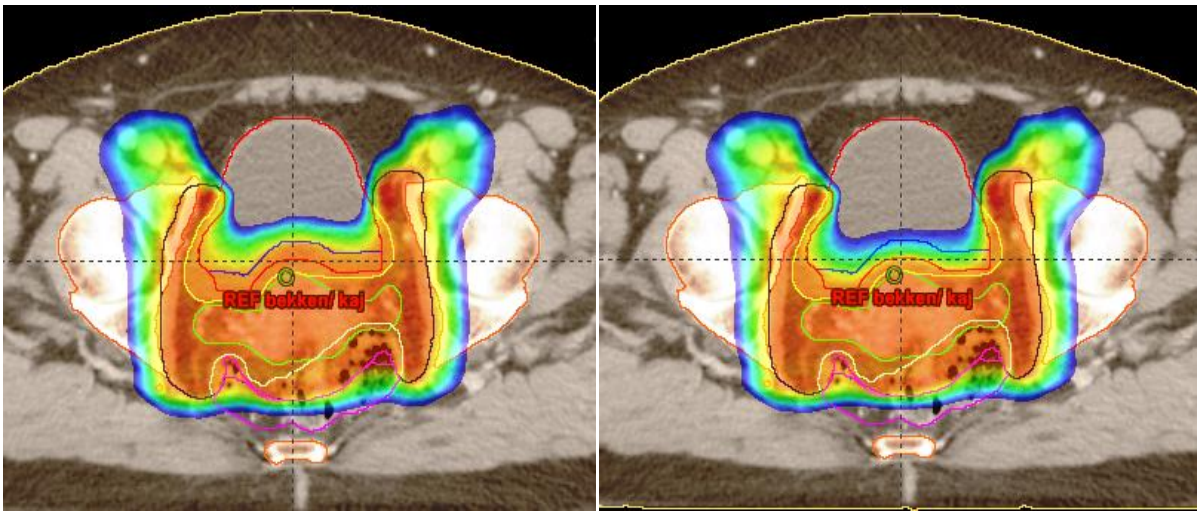

Figure 36: Transverse view of isodose distribution at 50% isodose level in IMPT. Left image (a): 50% dose coverage in IMPT with clinical margins. Right image (b): 50% dose coverage in IMPT with reduced margins.

DVH curves can be seen for IMRT and IMPT, with both clinical and reduced margins, respectively in figure 37 and 38. Substantial sparing of rectum, sigmoid and bladder can be visualized with reduced margins for both modalities.

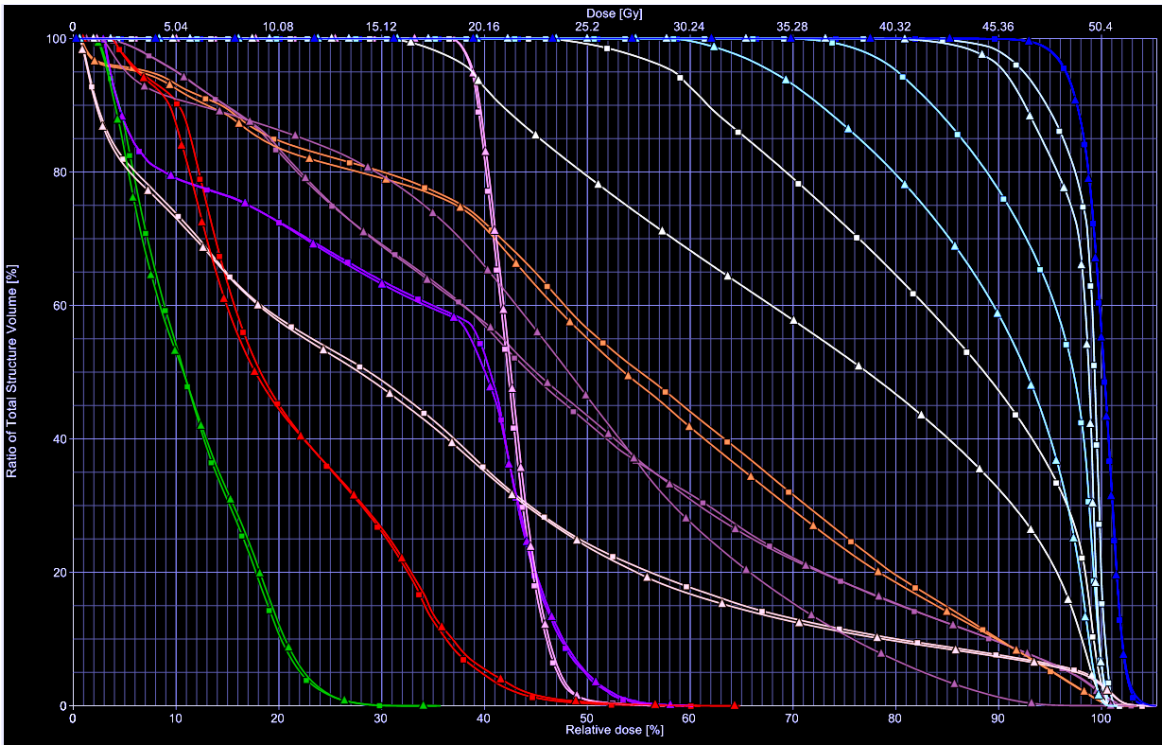

Figure 37: Example of DVH for a para-aortic patient for IMRT plans. Δ represents dose volume parameters for reduced margins whereas □ represents clinical margins. Light green, sky blue, yellow represents sigmoid, rectum and bladder, respectively

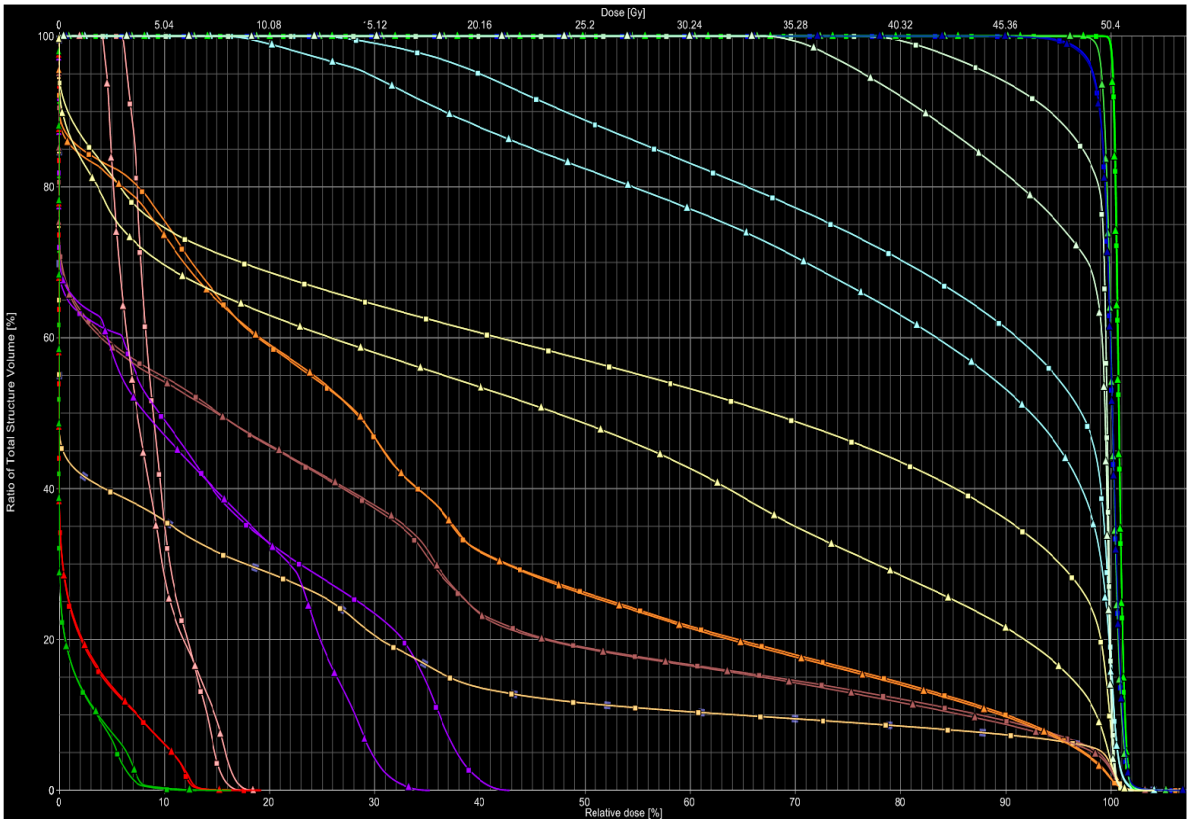

Figure 38: Example of DVH for a para-aortic patient for IMPT plans. Δ represents dose volume parameters for reduced margins whereas □ represents clinical margins. Light green, sky blue, yellow represents sigmoid, rectum and bladder, respectively

4.2 Dose-volume parameters for PTV

Concerning PTV coverage, table 4 quantifies the differences between IMRT and IMPT for clinical and reduced margins.

Table 4 Various parameters to describe dose coverage in PTV are tabulated for IMRT and IMPT, with clinical and reduced margins. All parameters are specified with their mean value ± standard deviation.

	Clinical margins (N=10)				**Reduced margins (N=10)**			
PTV	IMRT		IMPT		IMRT		IMPT	
	Mean±SD	**P-value**	**Mean±SD**	**Ratio**	**Mean±SD**	**P-value**	**Mean±SD**	**Ratio**
D98%	95.5±0.4	<**0.01**	96.8±0.3	0.99	95.3±0.3	<**0.01**	96.5±0.5	0.99
D2%	103.2±0.3	<**0.01**	101.7±0.2	1.01	103.3±0.5	<**0.01**	102.0±0.5	1.01
D2cc (%)	104.4±0.8	<**0.01**	103.7±0.9	1.00	104.9±0.5	<**0.01**	104.0±1.1	1.00
DHI	0.07±0.0	<**0.01**	0.04±0.00	1.58	0.07±0.00	<**0.01**	0.05±0.00	1.46
DCI	0.98±0.0	<**0.01**	0.99±0.0	0.99	0.98±0.0	<**0.01**	0.99±0.0	0.99

Treatment plans from IMRT and IMPT were clinically well accepted with, $D_{98\%} \geq 95\%$ of the prescribed dose. Precisely, $D_{98\%}$ of PTV was 96.8% and 95.5% with IMPT and IMRT, respectively, for clinical margins whereas $D_{98\%}$ of PTV was 96.5% and 95.3% with IMPT and IMRT, respectively for reduced margins. The dosimetric gain achieved by using smaller margins as compare to clinical margins between IMRT and IMPT can be estimated by ratio between IMRT and IMPT. Specifically, the ratio of the $D_{98\%}$ for IMRT and IMPT was found consistent with both clinical and reduced margins. Concisely, the ratio was 0.99 with statistical significance of p-value<0.01. This indicates that the IMPT provides slightly superior dose to 98% of the PTV relative to IMRT. However, this small variation in mean values is not clinically significant, in case of both types of margins (table 4).

$D_{2\%}$, clinical maximum dose to PTV was reported with an average of 103.2% and 101.7% with IMRT and IMPT, respectively for clinical margins. For reduced margins, an average of 103.3% and 102% with IMRT and IMPT respectively was achieved. It can be noticed from table 4 that $D_{2\%}$ with IMPT is relatively less than IMRT for both types of margins but the

average difference between two is minimal with statistically significance of p-value<0.01. Therefore, these small differences will not be considered clinically important. Alike $D_{98\%}$, no dosimetric gain has been seen utilizing smaller margins as compare to clinical margins with a consistent ratio of 1.01.

Referring to table 4, in context of dose homogeneity and conformity, DHI has an average of 0.07 and 0.04 with IMRT and IMPT, respectively for clinical margins. For reduced margins, DHI has an average of 0.07 and 0.05 with IMRT and IMPT, respectively. Therefore, IMPT has proved competency in better homogeneity around PTV as comparative to IMRT, both with clinical and reduced margins. DHI has shown a statistically significance of p-value<0.01. Although, there exists a small variation in their mean values but it is clinically relevant. Likewise, IMPT has evidently provided better dose conformity around PTV as against IMRT with both clinical and reduced margins. The difference between the mean values of IMRT and IMPT is very small but it has shown a statistically significance of p-value <0.01. However, such a small difference between their mean values for IMRT and IMPT is not clinically significant. Similar ratio of 0.99 was achieved resulting in no dosimetric gain between clinical and reduced margins. Overall, IMPT oversteps IMRT with respect to dose homogeneity and conformity around PTV.

For the hot spots, D_{2cc} in the outer body was calculated for IMRT as well as IMPT. Clinical maximum dose (D_{2cc}) to outer body is well under the limit of 107% of the prescribed dose for both clinical and reduced margins. Similar IMRT/IMPT dose-ratio was obtained for both clinical and reduced margins. IMPT was seen comparatively efficient in delivering low hot spots than IMRT (refer to table 4). Precisely, IMPT has kept maximum dose at an average of 103.7% and 104.0% with clinical and reduced margins, respectively.

4.3 Dose-volume parameters for organs at risk

4.3.1 Clinical margins

In case of clinical margins, sparing of various OARs with IMRT and IMPT at different dose levels are reported in table 5 below. The ratio is above 1 for all the parameters, i.e. IMPT demonstrated better sparing of OARs compared to IMRT. However, statistical significant differences are seen for many dose-volume parameters.

Table 5 Various dose-volume parameters are tabulated below to compare sparing of different OARs for IMRT and IMPT with clinical margins. All the parameters are specified as mean value± standard deviation.

OARs		IMRT		IMPT	
	Parameters	**Mean±SD**	**P value**	**Mean±SD**	**Ratio**
Rectum	V30	95.9±4.5	**<0.01**	79.7±14.3	1.20
	V45	77.8±10.2	**<0.01**	63.1±16.3	1.23
	Dmean	92.0±3.5	**<0.01**	81.9±10.3	1.12
Bladder	V30	86.4±11.4	**<0.01**	62.9±17.6	1.37
	V45	60.3±18.2	**<0.01**	50.1±20.6	1.20
	Dmean	85.0±7.9	**<0.01**	66.3±15.3	1.28
Sigmoid	V30	94.6±14.4	**<0.01**	76.6±23.0	1.24
	V45	79.3±17.5	**<0.01**	62.9±26.9	1.26
	Dmean	91.9±8.8	**<0.01**	78.9±19.3	1.17
Bowel	V10	80.1±10.5	**<0.01**	39.5±15.1	2.02
	V30	39.0±8.7	**<0.01**	20.4±8.7	1.91
	V45	17.1±6.8	**<0.01**	12.8±6.2	1.33
	V45 (cc)	404.2±123.70	**<0.01**	298.5±110.50	1.35
	Dmean	50.6±6.2	**<0.05**	34.2±26.8	1.48
Pelvic Bone	V10	79.8±8.3	**<0.01**	65.1±11.1	1.22
	V30	47.8±7.8	**<0.01**	27.3±5.2	1.75
	V45	15.0±3.5	**<0.01**	12.7±3.5	1.18
	Dmean	53.9±6.27	**<0.01**	38.8±5.7	1.39
Left Kidney*	V10	55.5±20.5	**<0.01**	4.9±9.7	11.33
	V30	2.1±4.1	0.15	0.7±1.3	3.24
	Dmean	24.1±7.8	**<0.01**	3.5±4.4	6.81
Right Kidney*	V10	57.7±29.8	**<0.01**	8.0±9.6	7.23
	V30	3.5±6.3	0.24	2.0±2.3	1.78
	Dmean	25.1±10.0	**<0.01**	6.0±5.5	4.16
Medulla*	Dmax	51.7±5.3	**<0.01**	40.3±5.5	1.28
	Dmean	31.4±9.4	**<0.01**	18.3±5.7	1.72
Cauda equina	Dmax	56.9±4.7	**<0.01**	44.3±11.2	1.28
Outer body	V10	44.9±10.0	**<0.01**	24.7±5.6	1.82

***** *Para-aortic Patients (N=5)*

Rectum sparing

For V_{30}, IMPT and IMRT have achieved an average of 79.7% and 95.9%, respectively. The ratio of 1.20 was seen, with a statistical significance level of p-value <0.01. For V_{45}, an average of 77.8% and 63.1% was achieved with IMRT and IMPT, respectively as seen in table 5. The dosimetric differences between IMRT and IMPT are considerably large, with a statistically significant ratio of 1.23. For D_{mean}, IMRT has achieved an average of 92.0% whereas IMPT has obtained an average of 81.9%, respectively. The ratio between IMRT and

IMPT was 1.12, with a statistical significance of p-value <0.01. Therefore, IMPT plans have confirmed superior ability in sparing rectum at V_{30}, V_{45} and D_{mean}.

Bladder sparing

As seen from table 5, IMRT and IMPT have achieved V_{30}, V_{45} with an average of 86.4%, 60.3% and 62.9%, 50.1%, respectively. IMPT has shown consistent pattern in sparing bladder to much greater extent relative to IMRT. IMPT has proven its capability in sparing bladder at both V_{30} and V_{45}. The ratio utilizing IMPT as compared to IMRT at V_{30} and V_{45} was 1.37 and 1.20, respectively with a statistical significance of p-value <0.01.

Also, D_{mean} was well achieved by IMPT with an average of 66.3% whereas IMRT has obtained 85%, respectively. It can be seen from table 5 that the dosimetric gain between IMRT and IMPT was 1.28, with a statistically significance of p-value <0.01. Overall, IMPT has demonstrated better sparing at V_{30}, V_{45} and D_{mean} for bladder.

Sigmoid and Bowel sparing

As seen from table 5, V_{30} was achieved at an average of 94.6% and 76.6% with IMRT and IMPT, respectively. The dosimetric gain of 1.24 was seen between IMRT and IMPT, with a statistical significance of p-value <0.01. Similarly, V_{45} for sigmoid was well spared with an average of 62.9% by IMPT as compare with an average of 79.3% by IMRT. The statistically significant ratio of dosimetric gain was 1.26 for V_{45}. Also, D_{mean} was achieved at 91.9% and 78.9% with IMRT and IMPT, respectively. The ratio obtained was 1.17, with a statistical significance of p-value <0.01. The above mentioned results clearly signify better sparing by IMPT as compare to IMRT at V_{30}, V_{45} and D_{mean} for sigmoid.

On the other hand for bowel, IMRT has achieved 80.1%, 39.0%, 17.1% whereas IMPT has obtained 39.5%, 20.4%, 12.8% at V_{10}, V_{30} and V_{45}, respectively. Evidently, the ratio between IMRT and IMPT was 2.02, 1.91 and 1.33 for V_{10}, V_{30} and V_{45}, with a statistical significance of p-value<0.01 for all dose levels, correspondingly. D_{mean} was achieved at 50.6% and 34.2% with IMRT and IMPT, correspondingly. However, a slightly less significant gain was seen between IMRT and IMPT. The results mentioned above indicate that IMPT has significant spared bowel at all dose levels.

As per QUANTEC recommendation for bowel in section 2.6.3, V_{45} was calculated in cubic centimeters (cc). IMRT and IMPT have achieved an average of 404.3cc and 298.5cc,

respectively. The ratio between IMRT and IMPT was 1.35 which clearly indicates that IMPT provides substantially large sparing at V_{45}, with a statistical significance of p-value <0.01.

Pelvic Bone and Kidney sparing

The dosimetric advantage of IMPT continues for kidneys at V_{10}, V_{30} and pelvic bone sparing at V_{10}, V_{30} and V_{45}, respectively. However, a statistically significant sparing was only seen for V_{10} of kidneys and all dose levels of pelvic bone. As IMRT/IMPT dose-ratio was well above 1 that indicates IMPT is superior in sparing dose to both organs at all above mentioned dose levels. Refer to table 5 for quantitative data.

The same is true at D_{mean} for both organs. For pelvic bone, IMRT and IMPT have shown an average of 53.9% and 38.8%, respectively. The ratio between IMRT and IMPT was 1.39, with a statistical significance of p-value <0.01. Similarly, for left and right kidney, an average of 24.1%, 25.1% was achieved with IMRT whereas IMPT has shown 3.5%, 6.0%, respectively. The ratio between IMRT and IMPT was 6.81 and 4.16 for left and right kidney, respectively. A statistical significance of p-value <0.01 was seen for both kidney.

Medulla and Cauda Equina

IMPT has shown greater sparing at D_{max} for medulla with 40.3% as compare to IMRT with 51.7%. The statistical significance of p-value<0.01 was seen in table 5. Moreover, both IMRT and IMPT have well achieved D_{max} under the limit of D_{max}<50Gy as pointed out in section 2.6.6. D_{mean} was seen at 31.4% by IMRT and 18.3% by IMPT, with a dosimetric gain of 1.72. A statistical significance of p-value <0.01 was also seen.

D_{max} for cauda equina, IMPT has shown better sparing at D_{max} with 44.3% as compare to 56.9% by IMRT. The ratio was 1.28 between IMRT and IMPT, with statistical significance of p-value<0.01. IMPT showcased substantially better sparing at D_{max}. Moreover, IMRT and IMPT both has achieved the D_{max}<60Gy as stated in section 2.6.7.

Outer body, V10 sparing

V_{10} for outer body was calculated. An average of 44.9% and 24.7% was achieved with IMRT and IMPT, respectively. The ratio of 1.82 was calculated between IMRT and IMPT, with a statistical significance of p-value <0.01 as seen in table 5.

4.3.2 Reduced margins

The effects of reduced margin on the sparing of OARs at different parameters between IMRT and IMPT are listed in table 6. The ratio is above 1, i.e. IMPT has shown better sparing for all OARs at different parameters than IMRT. However, statistical significant dosimetric differences are seen for many parameters.

Concerning the reduced margins, table 6 shows the increased differences between IMRT and IMPT at V_{30}, V_{45} of rectum and bladder, V_{10}, V_{30} of bowel, V_{10} of pelvic bone as compare to the results from clinical margins in table 5. For V_{30}, V_{45} of sigmoid and V_{45} of bowel however, less changes in the IMRT to IMPT dose-ratio was found when reducing CTV-PTV margins relative to the results from clinical margins in table 5. Also, the same effects were seen for V_{10} of the both kidney, V_{30}, V_{45} of pelvic bone and D_{max} in medulla, cauda equina. Although, the change in IMRT/IMPT dose-ratio was seen less between clinical and reduced margins but a statistical significance of p-value<0.01 was reported. However, these dosimetric differences are so small that they were not considered clinically significant.

For V_{10} of outer body, a greater dosimetric gain was seen with smaller margins as compared to clinical margins, with statistical significance of p-value <0.01. Refer to table 6.

Table 6 also demonstrates mean dose to OARs achieved with IMRT and IMPT for reduced margins. Larger gain in mean dose to rectum, bladder and bowel was achieved with reduced margins as compared to clinical margins (p-value <0.01). For sigmoid and pelvic bone, smaller difference in the ratio of IMRT/IMPT with reduced margin compared to clinical margin was seen but statistically considerable (p-value <0.01). Such a small variation in D_{mean} for sigmoid and pelvic bone was not clinically relevant. In contrast, dosimetric gain decreased for kidneys with reduced margins as compared to clinical margins. Also, a slight increase in dosimetric gain was seen for medulla with reduced margins as compared to clinical margins.

Table 6 Various dose-volume parameters are tabulated below to compare sparing of different organs at risk for IMRT and IMPT with reduced margins. All the parameters are specified as mean value± standard deviation

OARs		IMRT		IMPT	
	Parameters	**Mean±SD**	**P value**	**Mean±SD**	**Ratio**
Rectum	V30	92.8±7.4	**<0.01**	69.7±16.5	1.33
	V45	63.0±15.4	**<0.01**	48.3±20.0	1.30
	Dmean	87.1±5.6	**<0.01**	73.5±12.6	1.18
Bladder	V30	80.5±12.8	**<0.01**	53.0±19.1	1.52
	V45	49.6±18.1	**<0.01**	37.8±20.6	1.31
	Dmean	80.4±8.4	**<0.01**	57.2±16.7	1.40
Sigmoid	V30	93.6±15.0	**<0.01**	72.8±23.8	1.29
	V45	72.9±18.9	**<0.01**	57.4±26.5	1.26
	Dmean	89.6±9.7	**<0.01**	75.5±19.9	1.19
Bowel	V10	80.5±10.6	**<0.01**	36.7±15.5	2.19
	V30	38.5±8.6	**<0.01**	18.5±8.3	2.08
	V45	15.6±6.1	**<0.01**	11.5±6.1	1.35
	V45 (cc)	369.8±109.01	**<0.01**	269.1±101.8	1.37
	Dmean	50.0±6.3	**<0.01**	25.6±10.1	1.95
Pelvic Bone	V10	79.0±8.4	**<0.01**	60.7±9.1	1.30
	V30	46.3±7.6	**<0.01**	26.6±5.6	1.74
	V45	14.8±3.3	**<0.01**	12.6±3.0	1.17
	Dmean	53.0±6.2	**<0.01**	37.5±5.4	1.41
Left Kidney*	V10	57.3±20.4	**<0.01**	6.5±10.4	8.8
	V30	2.0±3.7	0.15	0.9±1.5	2.26
	Dmean	24.4±7.4	**<0.01**	4.1±4.9	6.00
Right Kidney*	V10	59.6±30.3	**<0.01**	9.9±13.6	6.00
	V30	3.3±5.8	0.22	2.1±3.0	1.59
	Dmean	25.4±9.9	**<0.01**	6.6±6.9	3.83
Medulla*	Dmax	51.8±5.8	0.07	41.5±10.8	1.25
	Dmean	31.1±8.9	**<0.05**	17.2±8.3	1.80
Cauda equina	Dmax	55.1±5.3	**<0.01**	41.7±11.3	1.32
Outer body	V10	44.2±10.1	**<0.01**	23.0±4.5	1.92

** Para-aortic Patients (N=5)*

4.4 Dose-volume parameters between clinical and reduced margins for IMRT

4.4.1 Dose-volume parameters for PTV

It can be seen from table 7 that the ratio is 1 or nearly 1 for all the parameters between clinical and reduced margins, i.e. no dosimetric gain has been achieved utilizing reduced margins as

compare to clinical margins for IMRT. However, statistical significance is seen for many dose-volume parameters.

Table 7 Various dose-volume parameters for PTV are included for clinical and reduced margins. All parameters are specified as mean± standard deviation.

PTV	**Clinical margins**	**Reduced margins**		
Parameters	**IMRT**	**IMRT**	**Ratio**	**P-value**
D98%	95.5±0.4	95.3±0.3	0.99	<0.01
D2%	103.2±0.3	103.3±0.5	1.00	0.2
D2cc	104.4±0.8	104.9±0.5	1.00	<0.05
DHI	0.07±0.0	0.07±0.0	1	0.01
DCI	0.98±0.0	0.98±0.0	1	<0.1

Referring to table 7, IMRT has achieved $D_{98\%} \geq 95\%$ for both clinical and reduced margins. Similarly, $D_{2\%}$ was also found well under the limit of 107%, for both clinical and reduced margins. In terms of dose homogeneity and dose conformity, DHI and DCI have an average of 0.07 and 0.98, for both clinical and reduce margins, respectively. Clinical maximum dose, D_{2cc} was found to be 104.4% and 104.9% for clinical and reduced margins, respectively. $D_{98\%}$, D_{2cc}, DHI and DCI have shown statistical significance level of p-value <0.05 whereas $D_{2\%}$ has shown statistically non-significant p-value of 0.2. Although, there exists statistical significance for most of the parameters between clinical and reduced margins but the mean differences are so small, hence they are clinically insignificant.

4.4.2 Dose-volume parameters for organs at risk

Sparing of various OARs at different dose levels with IMRT between clinical and reduced margins are reported in table 8. The ratio is above 1 for most of the parameters, i.e. reduced margins have demonstrated better OARs sparing as compare to clinical margins with IMRT. However, statistical significance is seen for many dose-volume parameters.

Table 8 Several dose-volume parameters are tabulated below for OARs sparing with IMRT between clinical and reduced margins. All the parameters are specified as mean± standard deviation.

OARs		Clinical margins	Reduced margins		
	Parameters	**IMRT**	**IMRT**	**Ratio**	**P-value**
Rectum	V30	95.9±4.5	92.8±7.4	1.03	**<0.01**
	V45	77.8±10.2	63.0±15.4	1.23	**<0.01**
	Dmean	92.0±3.5	87.1±5.6	1.05	**0.00**
Bladder	V30	86.4±11.4	80.5±12.8	1.07	**<0.05**
	V45	60.3±18.2	49.6±18.1	1.21	**<0.01**
	Dmean	85±7.9	80.4±8.4	1.05	**0.00**
Sigmoid	V30	94.6±14.4	93.6±15.0	1.01	<**0.05**
	V45	79.3±7.5	72.9±18.9	1.08	**<0.01**
	Dmean	91.9±8.8	89.6±9.7	1.02	**<0.01**
Bowel	V10	80.1±10.5	80.5±10.6	0.99	0.3
	V30	39.0±8.7	38.5±8.6	1.01	0.1
	V45	17.1±6.8	15.6±6.1	1.09	**<0.01**
	V45 (cc)	404.2±123.70	369.8±109.01	1.09	**<0.01**
	Dmean	50.6±6.2	50.0±6.3	1.01	0.1
Pelvic Bone	V10	79.8±8.3	79.0±8.4	1.01	**<0.05**
	V30	47.8±7.8	46.3±7.6	1.03	**<0.01**
	V45	15.0±3.5	14.8±3.3	1.01	0.2
	Dmean	53.9±6.27	53.0±6.2	1.01	**0.00**
Left kidney*	V10	55.5±20.5	57.3±20.4	0.96	0.07
	V30	2.1±4.1	2.0±3.7	1.05	0.3
	Dmean	24.1±7.8	24.4±7.4	0.98	0.2
Right Kidney*	V10	57.7±29.8	59.6±30.3	0.96	**<0.05**
	V30	3.5±6.3	3.3±5.8	1.06	0.2
	Dmean	25.1±10	25.4±9.9	0.98	0.2
Medulla*	Dmax	51.7±5.3	51.8±5.8	0.99	0.4
	Dmean	31.4±9.4	31.1±8.9	1.00	0.2
Cauda equina	Dmax	56.9±4.7	55.1±5.3	1.03	**<0.05**
Outer body	V10	44.9±10.0	44.2±10.1	1.01	**<0.01**

***** *Para-aortic Patients (N=5)*

In table 8, for rectum, V_{30} was achieved with 92.8% for reduced margins as compared to 95.9% for clinical margins. The dosimetric gain of 1.03 was seen, with a statistically significant p-value of <0.01. For V_{45}, an average of 77.8% and 63.0% was achieved for clinical and reduced margins, respectively. The dosimetric gain of 1.23 was seen, with a statistical significance level of p-value <0.01. Correspondingly, D_{mean} was obtained with 92.0% and 87.1% for clinical and reduced margins, correspondingly. The ratio between clinical and reduced margins was 1.05, with a p-value of 0. Similarly for bladder, V_{30}, V_{45} with 86.4%, 60.3% and 80.5%, 49.6% were achieved for clinical and reduced margins,

respectively. The dosimetric gain between clinical and reduced margins was 1.07 and 1.21 for V_{30} and V_{45}, respectively with a statistical significant p-value of <0.05 and <0.01, respectively. For D_{mean}, an average of 85% and 80.4% was obtained for clinical and reduced margins, with a ratio of 1.05, respectively. The statistical significance of p-value 0 was seen. Although, V_{30} and D_{mean} for rectum and bladder have shown statistical significance but such a small variation in mean values was not clinically significant. However, V_{45} for rectum and bladder have shown much greater dosimetric gain utilizing reduced margins compared to clinical margins and hence, they are considered clinically significant.

For sigmoid, V_{30} was achieved with an average of 94.6% and 93.6% for clinical and reduced margins, respectively. The ratio of 1.01 between clinical and reduced margins was seen, with a statistical significance of p-value <0.05. For V_{45} and D_{mean}, an average of 79.3%, 91.9% and 72.9%, 89.6% were achieved for clinical and reduced margins, respectively. The dosimetric gain was 1.08 and 1.02, with a statistical significance of p-value <0.01, correspondingly. Although, V_{30} and D_{mean} for sigmoid have ratio above 1 with a statistical significance but this small difference in mean values was not clinically significant. However, the dosimetric gain at V_{45} is considered clinically significant. Refer to table 8 for quantitative data.

For bowel, V_{10} was achieved with 80.1% and 80.5% whereas for V_{30}, an average of 39% and 38.5% was obtained for clinical and reduced margins, respectively. The dosimetric gain was 0.99 and 1.01, with a non-statistical significance. For V_{45}, an average of 17.1% and 15.6% was achieved for clinical and reduced margins. The dosimetric gain was 1.09, with a statistical significant p-value of <0.01. However, V_{45} was also calculated in cubic centimeters. Correspondingly, an average of 404.2cc and 369.8cc was achieved for clinical and reduced margins. The dosimetric gain was 1.09, with a statistical p-value of <0.01. Also, D_{mean} was achieved with 50.6% and 50% for clinical and reduced margins, correspondingly. The ratio was 1.01, with a non-statistical significance. Overall, the dosimetric gain at V_{45} and V_{45cc} are considered clinically significant.

Pelvic bone, V_{10}, V_{30} was achieved with 79.8%, 47.8% and 79%, 46.3% for clinical and reduced margins, respectively. The ratio was found to be 1.01 and 1.03 between clinical and reduced margins at V_{10} and V_{30}, respectively. The statistical significance was seen for both parameters with p-value of <0.05 and <0.01. Furthermore, for V_{45}, D_{mean} were found to be at an average of 15%, 53.9% and 14.8%, 53.0% for clinical and reduced margins, respectively. The ratio was 1.01 and 1 for V_{45} and D_{mean}, correspondingly. However, the statistical

significance of p-value 0 was only seen for D_{mean}. Overall, the results shown above for pelvic bone were not clinically significant due to very small average differences between clinical and reduced margins, as it can be seen from the ratios mentioned above.

Referring to table 8 for left and right kidney, V_{10}, D_{mean} have shown decrease in dosimetric gain between clinical and reduced margins. V_{10} for right kidney has shown a statistical significance of p-value <0.05. However, V_{30} for left and right kidney have achieved a dosimetric gain of 1.05 and 1.06, respectively with a statistically non-significance.

For medulla, D_{max}, D_{mean} have achieved an average of 51.7%, 3.4% and 51.8%, 31.1% for clinical and reduced margins, respectively. The statistically non-significant dosimetric gain of 0.99 and 1 was seen. However for cauda equina, D_{max} was achieved with 56.9% and 55.1% for clinical and reduced margins, correspondingly. The dosimetric gain of 1.03 was seen, with a statistical significance of p-value <0.05. It can be seen from the ratios mentioned above that the differences between their mean values were very small and hence, they are not clinically significant. Similarly, V_{10} to outer body was obtained with 44.9% and 44.2% for clinical and reduced margins, respectively. The ratio was found to be 1.01, with a statistically significant p-value of <0.01. Likewise, V_{10} to outer body is not clinically significant.

5 Discussion

The aim of this study is to quantify the dosimetric differences between IMRT and IMPT in terms of target dose coverage and sparing of OARs. A second aim is to investigate the effects of reduced margins as compared to clinically recommended population-based margins on target dose coverage and OARs sparing, which supports personalized strategies in adaptive radiotherapy.

There exists a paucity of scientific data for comparison between IMRT and IMPT in cervical cancer and the impact of using smaller margins for dosimetric benefits in patients with smaller cervix-uterus motion. Therefore, this study will contribute in the development of patient-specific adaptive radiotherapy.

The results in the present study are compared with Georg et al study (20). Their study is the only relevant study available in cervical cancer till date for dosimetric comparison as they have only used IMPT. However, there exist few differences between two studies. Their study involved 1cm isotropic margins and different IMPT field set-up, with one each in A-P and P-A direction. Also, they have only included para-aortic patients. Moreover, the differences specific to each organ will be discussed later in the respective sub-chapter. Therefore, results in their study are not directly comparable with our results.

5.1 PTV

The clinical acceptability of treatment plans is fulfilled with IMRT and IMPT, for both clinical and reduced margins (table 4). For clinical margins, the dosimetric differences between IMRT and IMPT have shown no clinical significance. The same is true for reduced margins. Similar results were stated by Georg et al for PTV coverage (20). Apparently, it indicates that PTV was adequately covered with 95% isodose distribution. Evidently, there is no gain obtained with tighter margins as compare to clinical margins since the ratio between two was similar. Likewise $D_{98\%}$, there exists no gain in $D_{2\%}$ with reduced margins as compared to clinical margins.

Clinical maximum dose, D_{2cc} to outer body was well restricted under the limit of 107% of the prescribed dose in all 10 patients (table 4). The same ratio has been found for normal and reduced margins which basically mean the gain of IMPT as compared to IMRT for both kinds

of margin is the same. In terms of hot spots, IMRT plans result in slightly higher dose in outer body than IMPT. It can be explained by the dose deposition properties of photon beams in IMRT technique where substantially high dose is deposited in the entrance channel proximal to the target volume.

PTV dose homogeneity was consistently superior with IMPT plans compared to corresponding IMRT plans, with clinical and reduced margins. There exists a dosimetric gain of utilizing smaller margins compared to clinical margins for DHI. The reason for better homogeneity by IMPT can be understood from the $D_{2\%}$ of PTV in table 4. As the average PTV DVH of IMPT falls sharply past 50.4Gy with IMPT due to sharper dose gradient, therefore it results in more homogenous dose to PTV. However, IMRT has a longer tail beyond 50.4Gy due to relatively slower dose gradient. Hence, it results in comparatively less homogenous dose to PTV. On the other hand, PTV dose conformity was found superior with both IMRT and IMPT, with no clinical relevance between two, for both clinical and reduced margins (table 4). Reasonably, superior conformity around PTV by IMPT is due to sharp distal dose fall-off and finite range of proton beams. Georg et al have also stated in their study that IMPT has achieved better dose homogeneity with 6 whereas IMRT has obtained 12 (20). In contrast to our study, they stated better dose conformity with 1.24 and 1.38 by IMPT and IMRT, respectively (20).

5.2 Bowel

Bowel is a major site for absorption of nutrients and quite susceptible to gastro-intestinal infection (GI). Often during radiotherapy, small bowel is irradiated incidentally. Majority of symptoms appears within 3 years post RT. Mal absorption is one of the significant late effects of RT but the dose-volume limits are not yet well specified (84). It has been seen from the results in table 5 and 6 that V_{45} is statistical significantly reduced by IMPT as compare to IMRT for both clinical and reduced margins. The ratio between IMRT and IMPT was 1.33 and 1.35 for clinical and reduced margins, respectively. As the ratios 1.33 and 1.35 are more or less equal, therefore, no clinically significant dosimetric gain was achieved utilizing reduced margins instead of clinical margins at V_{45}. Reduction in CTV-PTV margins has caused less impact on bowel sparing at V_{45} due to less overlapping of bowel with PTV and hence, smaller margins has brought no increase in bowel-PTV volume to be spared. The result at V_{45} clearly indicates that IMPT has quite well restricted high dose irradiation to bowel due

to its steep distal dose-fall in P-A field. Again it can be seen from table 5 that IMPT has demonstrated better sparing of the bowel as compare to IMRT at V_{10} and, V_{30}, for clinical margins. However, with reduced margins much greater sparing was seen by IMPT as compare to IMRT at V_{10}, V_{30} as seen in table 6. The above stated results at V_{10} and V_{30} show that the sparing of large volume of bowel at V_{10} and V_{30} by IMPT owes to the low entrance dose characteristics of IMPT. Moreover, the use of P-A field in IMPT has no direct contribution of the dose in bowel. The difference in dosimetric gain has been substantially large with reduced margins than clinical margins for both V_{10} and V_{30}.

The study by Georg D et al and the present study can be compared in terms of bowel sparing at the V_{30}, V_{45} and D_{mean} dose levels (20). Georg et al obtained 41% and 19% at V_{30} for the small bowel with IMRT and IMPT, respectively. Thus, the ratio obtained was 2.15. Comparatively, for the same dose level, our study has shown 39% vs 20.4% and 38.5% vs 18.5% with IMRT and IMPT for clinical and reduced margins, respectively, with a corresponding ratio of 1.91 and 2.08 (table 5 and 6). It can be seen from above that the ratios 2.15 and 2.08 are not very different and hence, the dosimetric gain at V_{30} between two studies are more or less comparable. However at V_{45}, Georg et al have achieved sparing of bowel volume from 13.1% to 2.7% with IMRT and IMPT, respectively. The ratio between IMRT and IMPT was 4.85. Comparatively at V_{45}, the present study achieved 17.1%, 15.6% and 12.8%, 11.5% with IMRT and IMPT for clinical and reduced margins, correspondingly. This means a ratio of 1.33 and 1.35. Clearly, Georg et al have achieved far greater extent of sparing in their study compare to the results obtained in this study for both clinical and reduced margins. Further in this study, D_{mean} for IMRT was 50.6% (25.5Gy) and 50.0% (25.2Gy) for clinical and reduced margins, respectively whereas Georg et al study found D_{mean} for IMRT of 27.2Gy. On the other hand for IMPT, this study achieved 34.2% (17.2Gy) and 25.6% (12.9Gy) for clinical and reduced margins respectively as compare to 13.4Gy in their study. In this study, the ratio between IMRT and IMPT was 1.48 and 1.95 for clinical and reduced margins, respectively whereas it was 2.02 in their study. It can be seen from above that the ratio 1.95 and 2.02 are not very different and hence, dosimetric gain at D_{mean} between two studies are clinically comparable.

Overall, much greater clinically significant sparing of the bowel can be seen at V_{45} in Georg et al study as compared to the results achieved in the present study. This difference at V_{45} sparing between two studies is primarily due to the different method of delineating bowel

volumes as follows: In Georg et al study, the small bowel was formed by delineating individual loops (20) whereas in this study, the entire peritoneal cavity was delineated as bowel. Secondly, they delineated and analyzed small bowel and colon separately (20) whereas this study has analyzed the combination of small bowel and colon as one volume "bowel". For the sake of verification, the volume of bowel in the present study was calculated and compared with the volume of small bowel stated in their study. The average volume of small bowel was 1127cc in their study whereas an average of 2795cc was found for the bowel in the present study. The differences in the delineation of the bowel between two studies can also be seen in figure 39 (a, b). These differences between two studies mentioned above are certainly expected to influence DVH parameters. Moreover, their study has only involved para-aortic irradiation whereas this study has involved half of the patients with only pelvic irradiation.

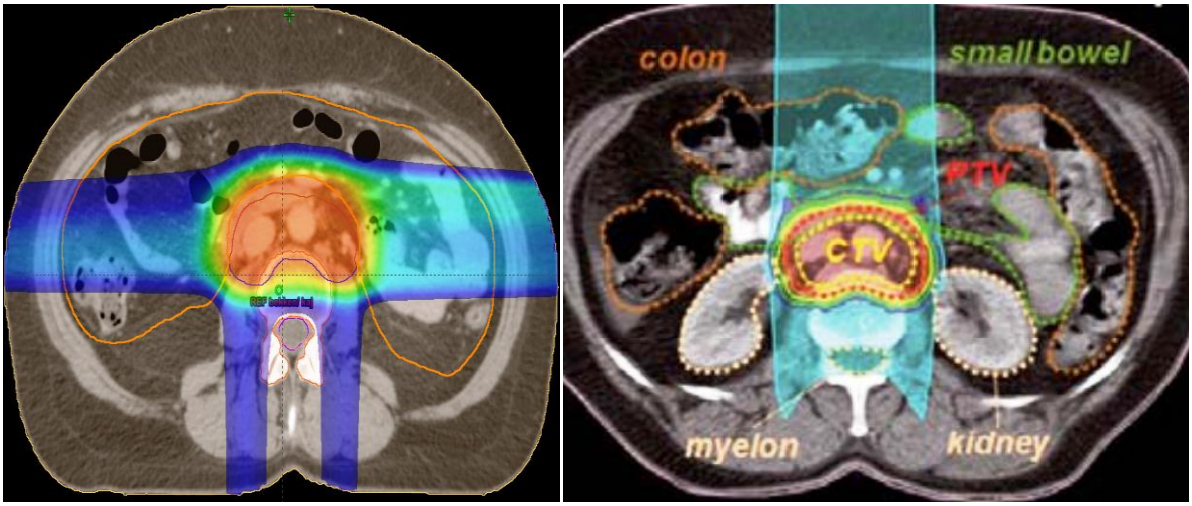

Figure 39: Differences in the delineation of bowel. a) Contouring of the bowel (orange color) as whole peritoneal cavity in the present study. Also, small bowel and colon are combined together in one volume as bowel. b) Contouring of the bowel (green color) as individual loops. Also, small bowel and colon are delineated and analyzed separately in Georg et al study (20).

QUANTEC recommends V_{45}<195cc as this dose limit is associated to acute toxicities (84). However, according to dose planning in cervix cancer at Oslo University Hospital, V_{45}<195cc may be difficult to achieve and the local procedure recommended V_{45}<300cc and V_{45}<450-600cc in case of pelvic and pelvic plus para-aortic LN irradiation, respectively. In table 5 and 6 it is evident that we were able to achieve V_{45} with 404.2cc, 369.87cc and 298.5cc, 269.1cc by IMRT and IMPT for clinical and reduced margins, respectively. In these tables the V_{45} for

all the 10 patients are averaged, i.e. including both pelvic (N=5) and para-aortic (N=5) patients. Since the sparing of bowel by using IMPT most probably will be influenced by whether or not the para-aortic region is included, figures for these two groups are found separately. For pelvic irradiation, the average V_{45} achieved by IMRT was 343.5cc and 306.1cc for clinical and reduced margins, respectively. Whereas the corresponding results achieved by IMPT were 249.3 and 221.5. This clearly indicates the benefit of using IMPT as compared to IMRT for this group of patients. However, the dosimetric ratio was 1.37 and 1.38 for clinical and reduced margins, respectively. It indicates no dosimetric gain achieved utilizing smaller margins instead of clinical margins.

Similarly, for pelvic plus para-aortic irradiation, V_{45} achieved by IMRT was 464.9cc and 433.5cc with clinical and reduced margins, respectively. On the other hand, the results obtained by IMPT were 347.7cc and 316.6cc with clinical and reduced margins, correspondingly. A clear-cut difference in V_{45} was seen with IMPT as compared to IMRT, with both types of margin. The ratio was 1.33 and 1.36 between IMRT and IMPT, with clinical and reduced margins. Precisely, these ratios are more or less similar as that for pelvic patients. Therefore, alike pelvic patients, there exists no dosimetric gain between clinical and reduced margins in para-aortic patients. Para-aortic LN irradiation was carried out by extended-field IMRT and hence, larger volume of bowel has to be included to adequately irradiate the para-aortic LN. For that reason, V_{45} in para-aortic irradiation is relatively larger than the pelvic irradiation alone. As per the dose/volume recommendations stated before, V_{45} for bowel in this study are well acceptable.

5.3 Bladder

Radiotherapy with or without chemotherapy for pelvic malignancies is associated with genitourinary complications. Overall, the incidence of severe late GU toxicities is less than 10% with cervical cancer patients (91). In this study a reduction in V_{30} and V_{45} was achieved with IMPT compared to IMRT at a statistical significance level with p-value<0.01(table 5 and 6), both with clinical and reduced margins. The dosimetric gain, though, was largest for reduced margins both for V_{30} and V_{45}. One reason worth mentioning for the better sparing by IMPT is the selection of beam orientation and number of treatment fields during treatment planning. In this study, three IMPT fields have been used: two laterally opposed and one posterior-anterior whereas for IMRT, seven fields were used to cover the complex and

irregular shape of cervical cancer. It is the differences in the dose deposition pattern of photons and protons due to their different physical characteristics as already discussed before in the sub-chapter for bowel. Therefore, the above mentioned differences justify the reason for large volume of bladder receiving low dose for IMRT and greater extent of bladder dose sparing by IMPT.

Another reason for dosimetric gain with reduced margins as compared to clinical margins is due to the influence of reduction in CTV-PTV margins centrally on the bladder volume. As the bladder is overlapping with the PTV centrally, a decrease in PTV volume will result in the increase of bladder-PTV volume. This structure was used in plan optimization and upper objectives were assigned to push the dose down to spare maximum of this volume without compromising with PTV coverage.

Results obtained for bladder V_{30}, V_{45} and D_{mean} in the present study can be compared to the results in the study by Georg et al (20). In our study, V_{30} for IMRT was shown to be 86.4% and 80.5% for clinical and smaller margins, respectively, while the correspondingly figure in Georg et al was 76.6%. V_{30} for IMPT achieved was 62.9% and 53.0% for clinical and reduced margins respectively as compare to 58.0% in their study. The dosimetric gain by IMPT compared to IMRT was 1.32 in their study while it was 1.37 and 1.52 for clinical and reduced margins in our study. Therefore at V_{30}, the present study has showed a slightly higher gain as compared to Georg et al. It can be seen from above that for smaller margins, IMPT has reduced V_{30} to 53% compared to 58% in Georg et al study. It can be explained by the difference in beam arrangement between the two studies during treatment planning. IMPT beam in anterior-posterior direction passes through the bladder to reach the target volume and hence, relatively larger volume of bladder was exposed to V_{30}. On the other hand, no IMPT beam was used in anterior-posterior direction in the present study and therefore, much larger volume of bladder was spared at V_{30}. However at V_{45}, IMRT has shown 60.3% and 49.6% for clinical and reduced margins respectively as compared to 33.8% in their study whereas, for IMPT the V_{45} were 50.1% and 37.8% with clinical and reduced margins, correspondingly as compared to 27.6% in their study. The ratio of dosimetric gain in their study was 1.22. Comparatively, the ratio was 1.20 and 1.31 with clinical and reduced margins in our study. Therefore, greater gain was demonstrated with smaller margins in our study. It is to be noted that for clinical margins the ratio 1.20 is not very different than 1.22 in their study and hence, they are clinically comparable. However, a much greater dosimetric gain was seen with ratio

of 1.31 for reduced margins. This difference in dosimetric gain between the two studies can be explained by the difference in CTV-PTV margins. The impact of smaller margins on the bladder sparing at V_{45} was already explained in the preceding paragraph. Similarly, D_{mean} was also compared between the two studies. In their study for bladder, D_{mean} was achieved with 38.7Gy and 33.6Gy with IMRT and IMPT, respectively and hence, only small improvement in D_{mean} was obtained with IMPT. Referring to table 5 and 6, this study has shown greater dosimetric gain for D_{mean} with both types of margin as compare to the results showed in their study.

It is important to mention that we have used a drinking protocol in our study to minimize the inter-fraction and intra-fraction cervix-uterus motion and with increasing bladder filling also keeps the bladder outside the treated volume (23, 92). Since the bladder is a highly distensible organ a constant volume of bladder is difficult to maintain due to variation in filling, bowel filling and respiration (83). Bladder volume is known to have impact on the position of cervix and uterus. As already stated before in section 2.6.2, EBRT is often combined with chemotherapy and followed by intra-cavitary brachytherapy boost to tumour however, the success of this treatment protocol often comes with the risk of small bowel and bladder complications. A constant bladder filling will limit the inter-fraction and intra-fraction bladder variation which in turn will limit the variation in cervix-uterus position. Additionally, full bladder will push the large volume of bowel outside treatment field (93) and with the increasing bladder filling, part of the bladder also moves out of treatment volume (23, 92). However, a review study by Jadon et al revealed that no studies have investigated to standardize bladder volumes in cervical cancer (22). Moreover, studies on prostate and bladder cancer show that constant bladder volume is difficult to maintain due to reduction in bladder capacity with treatment course and radiation cystitis (22). A study by Ahmed R et al in cervical cancer with 500ml of water intake with the intent to have comfortably full bladder verifies the same trend in bladder volume variation with time as in prostate cancer patients (94). The study also concluded that the bladder filling affects change in internal target volume due to pelvic rotation in prone position. Overall, variation in bladder volume influences the cervix and uterine motion. In this study, we have used 300ml of comfortably full bladder protocol with the intent to maximize bowel sparing within the treatment field. Constant bladder volume limits the variation in cervix-uterus motion and hence, it allows the usage of smaller margins as generously larger margin negates the benefit of using conformal radiation therapy. Therefore, smaller margins with online image guided CBCT with soft tissue

matching will support adaptive radiotherapy to avoid treatment related morbidity and avoiding the under dosing of target volume.

5.4 Rectum and sigmoid

As seen in table 5 for clinical margins, IMPT managed to minimize the radiation burden on rectum at V_{30} and V_{45} significantly with p-value<0.01. This is achieved by utilizing rectum-PTV helping structure during plan optimization. With the effect of reduced CTV-PTV margin on rectum sparing, much greater dosimetric differences were seen at V_{30} and V_{45} (table 6). It can be explained by the increase in the Rectum-PTV help structure volume due to the reduction in central CTV-PTV margins (figure 31a, b). It made possible to push the dose down to much larger volume of the rectum. Therefore, a larger volume of rectum can be spared with IMPT.

The selection of two opposed lateral fields allows the potential of IMPT in reducing the radiation load largely to all OARs. The geometrical placement of posterior-anterior field primarily went both through the rectum and sigmoid to reach the PTV. Therefore, reduction in CTV-PTV margins centrally has considerable influence on the volume of rectum to be spared. The major advantages of reduced margins are seen for rectum and bladder sparing.

It is important to mention here that protons are highly dependent upon the stopping power of different material; proton range is more in air than tissues. Consequently, the presence of air in rectum can have an adverse effect on the range of proton beams. As P-A field used in this study traverses through the air in rectum and therefore, changes in the rectal air volume may affect the proton range. For these reason, it may results either in under dosing of the target volume or over dosing of the normal tissues such as bladder. The presence of air in the rectum can be seen as black cavity in figure 40a.

Also seen in table 5 and 6 for sigmoid, IMPT has shown greater sparing than IMRT at V_{30} and V_{45} for both clinical and reduced margins, with statistically significance of p-value <0.01. Over and all, the dosimetric difference between clinical and reduced margins were seen the same at all dose levels. Therefore, no dosimetric gain was seen with reduced margins compared to clinical margins. The impact of reducing CTV-PTV central margin seems less on sigmoid. Primarily, majority of sigmoid resides inside the PTV and therefore, pushing the dose down will spare sigmoid but at the cost of losing adequate coverage to PTV and hence, a

trade-off was made to maximize local tumour control at the planning stage. For that reason, the dosimetric gain was not evidently demonstrable with reduced margin relative to clinical margins.

V_{30}, V_{45} and D_{mean} for rectum in this study can be compared to the results in the study by Georg et al (20). In their study, IMRT and IMPT have achieved V_{30} of 90% and 82.8%, respectively, while the corresponding figures for V_{45} were 64.1% and 47.3%. The ratio of dosimetric gain was 1.08 and 1.35 between IMRT and IMPT at V_{30} and V_{45}, respectively. These results can be compared with the results obtained in this study shown in table 5 and 6. It can be well seen that the gain for clinical and reduced margins at V_{30} in this study is greater than the gain obtained in Georg et al study. Oppositely, gain at V_{45} was higher in their study than the present study. Also, the dosimetric gain was 1.11 at D_{mean} in their study. Comparing with results from table 5 and 6 in the present study, no gain was seen in D_{mean} at clinical margins whereas a little higher dosimetric gain was seen at smaller margins.

The differences in dosimetric gain at the above mentioned dose levels between two studies can be explained by the fact that Georg et al has delineated rectal wall (20) whereas in this study, whole rectum was delineated. These differences in the delineation of the rectum can be seen below in figure 40(a, b). It is important to mention that the contouring of the rectal wall is more useful as it is more prone to toxicities rather than the inside volume of rectum as it mostly contains air or feces. However, delineation of rectal wall is a complex task and requires a lot of time and efforts. Therefore, the whole rectum was used as a substitute in the present study. Precisely, the average volume of rectum was 91cc in this study whereas an average of 146cc was mentioned for rectal wall in their study. The above mentioned differences in the rectal volumes between two studies are expected to influence DVH parameters.

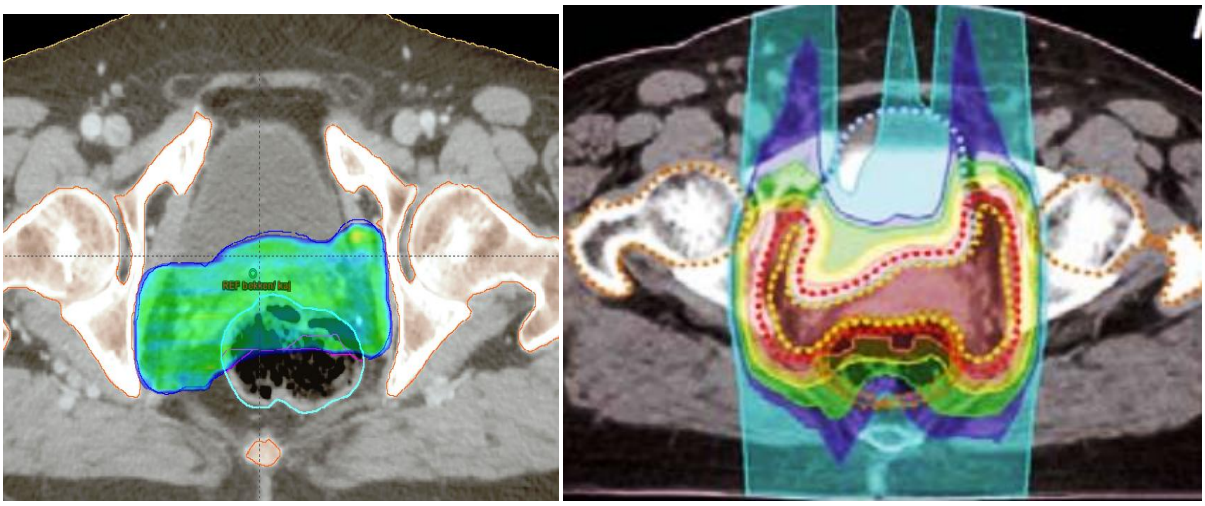

Figure 40: Differences in the delineation of the rectum. a) Contouring of the whole rectum (sky blue color) in the present study. b) Contouring of the rectum wall (two parallel dotted orange lines) in Georg et al study (20).

5.5 Pelvic bone

Most of the total body bone marrow reserve is located in pelvic bones. With the recent analysis, this approach has been known to effectively increase the local tumour control with subsequent increase in acute hematologic toxicities. Low dose irradiation (V_{10} and V_{20}) of pelvic bone has been found to be the significant factor associated with HT toxicity (8, 13). Therefore, IMPT seems a logical substitute due to its physical characteristics. In this study, V_{10}, V_{30} and V_{45} for pelvic bone sparing with IMRT and IMPT, for clinical and reduced margins are tabulated in table 5 and 6.

For IMRT, V_{10} was 79.8% and 79% for clinical and reduced margins, respectively. Whereas for IMPT, V_{10} was at 65.1% and 60.7% for clinical and reduced margins, correspondingly. It is clear from the results that IMPT has significantly spared larger volume of pelvic bone as compared to IMRT with p-value <0.01. Possibly, it is the low entrance dose of two opposed lateral IMPT fields which resulted in better sparing of pelvic bone at V_{10}. Furthermore, a decent dosimetric gain was achieved with reduction in CTV-PTV margins compared to clinical margins. Conclusively, it can be said that with the use of IMPT the incidence of acute hematologic toxicity can be potentially minimized due to reduction in volume of pelvic bone receiving low dose irradiation (V_{10}).

IMPT also demonstrated superior sparing at V_{30} and V_{45} compared to IMRT, with both clinical and reduced margins, as can be seen in table 5 and 6. However, dosimetric gain was observed consistently same between clinical and reduced margins.

It is important to mention that few study have stated to include pelvic bone marrow in the optimization process (14, 95). However, a study by Umesh Mahantshetty has reported the use to pelvic bone as a surrogate to active bone marrow as it is much easier to delineate pelvic bone than pelvic bone marrow cavities (96). Therefore, based upon the above mentioned reference, the present study has contoured pelvic bone and used in the optimization of the treatment plans.

5.6 Kidneys

Referring to table 5 and 6, IMPT has significantly spared V_{10} for the left and right kidneys as compared to IMRT. For normal and reduced margins, IMPT has proved its potential in sparing low dose irradiation to kidneys, with statistical significance of p-value<0.01. However, a non significant sparing of kidneys was seen at V_{30} and V_{45} with IMPT compared to IMRT. The dosimetric gain was seen to decrease with reduced margins compared to normal margins at all dose ranges.

Mean kidney dose (D_{mean}) was found <15Gy and V28Gy<10%, with both normal and reduced margins for both modalities. As per dose/volume limits for kidneys mentioned in section 2.6.6, IMRT and IMPT has performed tremendously well in sparing dose to kidneys.

D_{mean} for left and right kidneys can be compared to the results in the study by Georg et al (20). In their study for left kidneys, IMRT and IMPT have achieved a D_{mean} of 17.3Gy and 2.2Gy, respectively. The dosimetric gain of 7.86 was seen. Similarly for right kidney, IMRT and IMPT have shown a D_{mean} of 16.9Gy and 1.4Gy, correspondingly, with a dosimetric gain of 12.07. In the present study for clinical margins, IMRT and IMPT have achieved a D_{mean} of 12.1Gy, 12.6Gy and 1.7Gy, 3Gy for left and right kidneys, respectively. The dosimetric gain of 7.11 and 4.2 was seen for left and right kidney, correspondingly. It can be seen that the ratios of 7.11 and 7.86 for left kidney between the present study and Georg et al study are not very different and hence, the respective dosimetric gain are clinically non-significant. However for right kidney, a clinically significant dosimetric gain was seen in their study as compared to this study.

5.7 Medulla and cauda equina

For clinical margins, D_{mean} for medulla was found to be 31.4% and 18.3% with IMRT and IMPT, respectively. For the reduced margins, the corresponding figures were 31.1% and 17.2%. Therefore, a non-significant and almost consistent dosimetric gain was observed between reduced and clinical margins.

Moreover, maximum dose (D_{max}) for medulla was reported at <30Gy with both clinical and reduced margins for both modalities. Therefore, dose-volume recommendations mentioned in section 2.6.6 are well satisfied. No significant dosimetric gain was seen at D_{max} between clinical and reduced margins. The results for D_{max} in medulla are shown in table 5 and 6.

From the table 5 and 6, the results for cauda equina at D_{max} indicates that both IMRT and IMPT have sufficiently achieved the criteria of D_{max}<60Gy as mentioned in section 2.6.7.

5.8 Outer body

V_{10} was seen to be higher for IMRT compared to IMPT with both clinical and reduced margins in table 5 and 6, respectively. The result indicates that much larger volume of normal tissues received 10Gy i.e. low dose irradiation, from IMRT than IMPT. The use of many treatment fields in IMRT to spread the low-dose region around the target volume, results in over-spilling of low doses to larger volume of surrounding normal tissues. In contrast, proton beams in IMPT deposit relatively lesser dose proximally to target volume.

V_{10} of outer body signifies integral dose to normal tissues. Therefore, an increase in V_{10} to outer body means a consequent increase in integral dose to normal tissues. This can be seen as a drawback of IMRT. A study by Hall and Wuu has speculated if this lower dose to large volume of normal tissues could be prime reason for radiation induced secondary cancer in the future (97). The reason entails from the fact that more number of monitoring units needs to be delivered in IMRT field delivery and hence, more total body dose due to leakage radiation. Secondarily, IMRT employs greater number of fields which irradiates bigger volume of normal tissues with low dose irradiation. Both these factors tend to increase the risk of secondary radiation induced cancer. IMRT is likely to increase the risk of secondary malignancies by 1.75% (97). The introduction of IMPT spot scanning technique has provided as an alternative to substantially reduce the risk of second cancers (17). Reasonably, it is due

to the less production of neutrons in spot scanning technique which results in less scattered dose to patient by a factor of 10 times less than IMRT. A study by Lomax et al also confirmed that integral dose to normal tissues can be substantially reduced with protons due to low entrance dose channel proximal to target volume (62).

5.9 Benefits of smaller margins for IMRT

As already stated before, that the intention of using smaller margins is to keep the normal tissue from being irradiated by high dose of radiation. The results shown in the table 8 quantifies the dosimetric gain obtained with reduced margins as compared to clinical margins for IMRT. Generally, OARs can be substantially spared with the reduction in margins.

In case of IMRT, major dosimetric gain was evidently visible at high dose level (V_{45}) of rectum, bladder, sigmoid and bowel with respective ratios of 1.23, 1.21, 1.08 and 1.09. All the four OARs have shown statistical significance of p-value<0.01. The dosimetric benefit of such a magnitude is of highly clinical significance. The justification for the dosimetric gain at V_{45} with smaller margins for rectum, bladder and sigmoid is explained as follows. It can also be seen from $D_{2\%}$ in the table 7 that IMRT demonstrated slower dose gradient past prescription dose. Therefore, hot spots occurs much deeper in PTV whereas cold spots occurs around the periphery of PTV. This explains the fact that dose distribution around the periphery of PTV is lower than dose inside the PTV and there exists a much slower dose gradient far from the edges of PTV. It concludes that the immediately abutting structures can be spared with high dose irradiation with IMRT treatment plans. Since rectum and bladder are immediately abutting structures they can be spared at high dose level (V_{45}) due to relatively low dose around the edges of PTV. Moreover, the reduction of CTV-PTV margins results in the increase of rectum-PTV and bladder-PTV volume to be spared from high dose irradiation. Sigmoid falls mostly inside the PTV but reduction in CTV-PTV margins results in the slight decrease of sigmoid overlapping with PTV and hence, it could be spared at V_{45} with gain of only 1.08 relative to clinical margins. Bowel falls mostly outside the PTV with only a small volume overlapped with PTV and hence, reduction in CTV-PTV margins hardly shown any significant increase in bowel-PTV volume to be spared. Therefore, smaller margins has only resulted in the dosimetric gain of 1.09 compared to clinical margins.

5.10 Adaptive radiotherapy in cervical cancer

The potential of IMRT and IMPT treatment for the cervical cancer enables highly conformal dose distribution around target volume (8, 18). In cervix cancer, target shape and position is highly influenced by pelvic organ volume and position changes over time. As a result, matching of pelvic anatomy during patient positioning at treatment unit may vary from planned pelvic anatomy. Therefore, appropriate CTV-PTV safety margins are employed to avoid the risk of target volume under dosing and unnecessary inclusion of normal tissues in high dose irradiation. However, highly conformal treatments are more prone to large inter-fraction organ motion than intra-fraction motion (22). Various studies have confirmed the influence of variation in bladder filling, rectum filling and tumour regression are the major contributors of change in cervix and uterus shape and position (23, 28). Intra-fraction motion of pelvic organs was found less pronounced with a mean of 0.1-3.0 mm but there is no predominant direction of intra-fraction movement (24). Uterus moves more than cervix with maximum displacement of upto 48mm anterior-posterior in uterine fundus. However, the displacement of such a magnitude in uterine fundus was shown in only one study (25). Bladder filling was co-related largely with uterine motion with majorly at uterine fundus whereas rectal filling has more impact on cervix and vaginal displacement (23, 25). The influence of variation in bladder filling on cervix-uterus motion can be seen in figure 1. Cervix cancer is known to regress over the treatment course resulting in the shrinkage of tumour volume (28) and hence, online image guidance and advanced online treatment planning should be utilized to reduce the radiation exposure to normal tissues (98).

One way to solve the above discussed inter-fraction and intra-fraction cervix-uterine motion is to employ generous population based CTV-PTV margins which reduces the risk of target under dosing but unnecessarily causes high doses to normal tissues and hence, normal tissue toxicity (23-25, 99). This strategy is promising in terms of target dose coverage but negates the benefit of using highly conformal treatment strategies. Additionally, it has been demonstrated by various studies that impact of bladder filling on inter-fraction cervix-uterine deformation and displacement is patient-specific (26, 27). Hence, it varies from patient to patient. Figure 2 shows the inter-patient variability in cervix-uterus motion. Therefore, inter-patient variability of bladder filling limits the benefit of using standard population based margins (29).

One section of this study involves clinical CTV-PTV margins of 7 mm (L-I), 10 mm (S-I) and 15 mm (A-P) properly encompass the inter-fraction and intra-fraction internal cervix-uterus motion. It has been known from studies that cervix has greater movement in A-P and S-I than laterally. Moreover, bladder filling has more impact on movement of uterine fundus in A-P and S-I direction with a displacement of 5-40mm in S-I and 0-65mm in A-P direction (26). Clearly, the intra-fraction motion of cervix-uterus is larger in A-P and S-I than laterally. Tyagi et al has assessed that impact of inter-fraction cervix-uterus motion and confirmed that 15mm margins in A-P are not sufficient to cover CTV in 32% of fractions (89). However, the missed CTV volume is minimal (4cc) with a maximum missing in uterine fundus. It is important to notice that although uterine fundus has shown maximum displacement, this region has minimum evidence of any microscopic disease and its inclusion in CTV is a topic of research debate at present (22). Thus, the choice of 15mm in A-P, 10mm in S-I and 7mm in L-R is well accepted clinically. Moreover, large movements in uterine fundus due to variation in bladder filling were seen only among a small percentage of patients. Therefore, it seems illogical to use larger margins to accomodate the variation in cervix-uterus for a small percentage of patients. Instead, it makes more sense to use smaller margins to benefit larger percentage of patients. Few studies have also confirmed that constant bladder filling limits the variation in uterine fundus motion (24, 25) and hence, drinking protocol of 300ml of water was employed in this study with the intent of comfortably full bladder achievement.

Alternatively, smaller CTV-PTV margins can be employed to potentially reduce the chances of irradiating normal tissue to high doses. But, for patient with large target motion this strategy can cause inadequate target dose coverage (100) as seen in figure 41. Therfore, a prior knowledge of a pre-treatment established correlation of impact of bladder filling on variation in cervix-uterine motion is mandatory. Smaller CTV-PTV margins of 7mm is an approach valid only for smaller target motion. Through the optimum utilization of online image guiding CBCT with soft tissue matching, smaller CTV-PTV margins can prove as a potential strategy in adaptive radiotherapy. Smaller margins can reduce the normal tissues involvement while achieving excellent target dose coverage. Keeping all this in mind, in this quantitative study all the 10 patients were replanned with smaller (7mm) CTV-PTV central margins with the intent to maximize the OARs sparing without compromising dose to the CTV. Also, the study has evidently shown the potential differences achieved using smaller margins over clinically recommended population based margins for IMRT and IMPT. The

dosimetric gain with smaller margins can be seen as a support to adaptive strategies in radiotherapy of cervical cancer with the aim to reduce the dose to normal OARs.

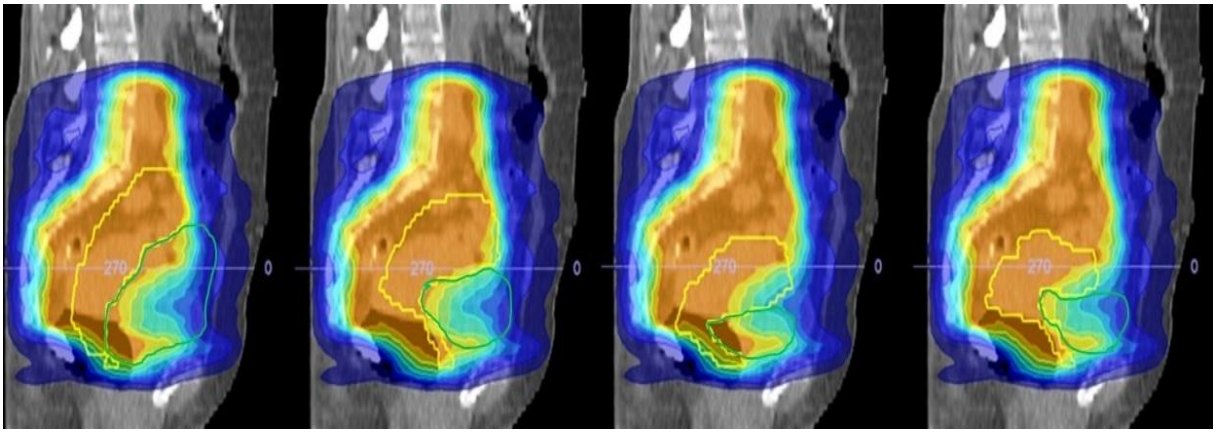

Figure 41 : Impact of using smaller CTV-PTV margins in case of patients with large target motion results in target underdosing as seen above with these planned dose distribution. The bladder and cervix-uterus are shown in green and yellow color, respectively. Image source: (31)

6 Conclusions

The goal of this study was to explore if IMPT is potentially better than IMRT in terms of target dose coverage and OARs sparing, for clinical margins. Further, the effects of smaller margins were investigated as against standard population based margins to quantify the dosimetric gain for clinically relevant dose-volume parameters. Moreover, the benefits of using smaller margin for IMRT were studied. It is evident from the results of two modalities that IMPT has dosimetric advantages in limiting dose to all the OARs over IMRT, for both clinical and smaller margins while maintaining excellent target coverage. Low dose to outer body was also considerably reduced with IMPT which signifies less integral dose and hence, less chances of resulting in radiation induced secondary cancer.

With the effect of smaller margins, a clinically significant dosimetric gain was seen for the volumes of rectum and bladder. The same is true for bowel but only at low and medium dose levels. Sigmoid was seen to be less clinically benefited utilizing smaller margins since it mostly resides inside the PTV for larger pelvic malignancies, such as for patients with cervical cancer. Importantly, a decent dosimetric gain was also apparent in low dose to outer body. A clinically non-significant dosimetric variation was seen for pelvic bone, medulla and cauda equina. The dosimetric gain was however reduced for kidneys.

Considering the fact that IMRT is currently the most available radiotherapy technique worldwide, the impact of smaller margins as compare to clinical margins were separately investigated for IMRT. The use of smaller margins has brought clinically significant reduction, most notably to rectum and bladder, at high dose level. Whereas at the same level, a decent dosimetric gain was seen for sigmoid and bowel. These dosimetric benefits of employing smaller margins around PTV can prove clinically advantageous to patients with smaller organ motion.

Briefly, it can be concluded that IMPT is significantly superior over IMRT in limiting dose to the OARs in the treatment of locally advanced cervical cancer. IMPT can be considered as a potential substitute for IMRT in improving treatment related side-effects. The use of smaller margins have also proved substantially large reduction in dose to rectum and bladder, which can contribute in the development of personalized adaptive radiotherapy for cervical cancer patients.

7 Future scope in research

One limitation of the present study was the use of smaller number of cervical cancer patients. Hence, this study can be taken further with large patient population to identify the dosimetric benefits of IMPT compared to IMRT. More studies should involve active spot scanning beam delivery technique (IMPT) and explore different field set-ups to add more degree of freedom in comparative studies.

Importantly, the present study has been a dosimetric analyses and not a clinical evaluation. While, IMPT does appears to limit the radiation exposure to normal tissues to a greater extend but there exists no clear evidence whether this reduction will lead to differences in acute and late toxicity. Therefore, more studies should aim towards dose effect based mathematical modeling between IMRT and IMPT to estimate TCP and NTCP for the verification of their biological impact. Furthermore, long-term clinical follow-up is required to evaluate late toxicity in the cervical cancer patients treated with IMPT. Hence, the research community should consider it as a topic of future study.

Additionally, in order to facilitate the clinical implementation of personalized adaptive radiotherapy it is crucial to standardize the bladder and rectum filling protocols to minimize the variation in cervix-uterus motion. Hence, more research work should be carried out in this direction.

Moreover, the wide spread employment of online image guidance such as 4D CBCT with soft tissues matching will anticipate the clinical practice of adaptive radiotherapy.

Lastly, research initiatives should be taken in determining the impact of air pockets in rectum on range uncertainties in IMPT.

Bibliography

1. Eifel PJ, Winter K, Morris M, Levenback C, Grigsby PW, Cooper J, et al. Pelvic irradiation with concurrent chemotherapy versus pelvic and para-aortic irradiation for high-risk cervical cancer: an update of radiation therapy oncology group trial (RTOG) 90-01. J Clin Oncol. 2004;22(5):872-80.

2. Morris M, Eifel PJ, Lu J, Grigsby PW, Levenback C, Stevens RE, et al. Pelvic radiation with concurrent chemotherapy compared with pelvic and para-aortic radiation for high-risk cervical cancer. N Engl J Med. 1999;340(15):1137-43.

3. UK CR. Cervical cancer statistics and outlook: Cancer Research UK; 2014 [cited 2015 27 July]. Available from: http://www.cancerresearchuk.org/about-cancer/type/cervical-cancer/treatment/cervical-cancer-statistics-and-outlook.

4. Peters WA, 3rd, Liu PY, Barrett RJ, 2nd, Stock RJ, Monk BJ, Berek JS, et al. Concurrent chemotherapy and pelvic radiation therapy compared with pelvic radiation therapy alone as adjuvant therapy after radical surgery in high-risk early-stage cancer of the cervix. J Clin Oncol. 2000;18(8):1606-13.

5. Kirwan JM, Symonds P, Green JA, Tierney J, Collingwood M, Williams CJ. A systematic review of acute and late toxicity of concomitant chemoradiation for cervical cancer. Radiother Oncol. 2003;68(3):217-26.

6. Chatani M, Matayoshi Y, Masaki N, Narumi Y, Teshima T, Inoue T. Prophylactic irradiation of para-aortic lymph nodes in carcinoma of the uterine cervix. A prospective randomized study. Strahlenther Onkol. 1995;171(11):655-60.

7. Grigsby PW, Lu JD, Mutch DG, Kim RY, Eifel PJ. Twice-daily fractionation of external irradiation with brachytherapy and chemotherapy in carcinoma of the cervix with positive para-aortic lymph nodes: Phase II study of the Radiation Therapy Oncology Group 92-10. Int J Radiat Oncol Biol Phys. 1998;41(4):817-22.

8. Brixey CJ, Roeske JC, Lujan AE, Yamada SD, Rotmensch J, Mundt AJ. Impact of intensity-modulated radiotherapy on acute hematologic toxicity in women with gynecologic malignancies. Int J Radiat Oncol Biol Phys. 2002;54(5):1388-96.

9. Portelance L, Chao KC, Grigsby PW, Bennet H, Low D. Intensity-modulated radiation therapy (IMRT) reduces small bowel, rectum, and bladder doses in patients with cervical cancer receiving pelvic and para-aortic irradiation. International Journal of Radiation Oncology* Biology* Physics. 2001;51(1):261-6.

10. Mundt AJ, Lujan AE, Rotmensch J, Waggoner SE, Yamada SD, Fleming G, et al. Intensity-modulated whole pelvic radiotherapy in women with gynecologic malignancies. Int J Radiat Oncol Biol Phys. 2002;52(5):1330-7.

11. Roeske JC, Lujan A, Rotmensch J, Waggoner SE, Yamada D, Mundt AJ. Intensity-modulated whole pelvic radiation therapy in patients with gynecologic malignancies. International Journal of Radiation Oncology* Biology* Physics. 2000;48(5):1613-21.

12. Mundt AJ, Mell LK, Roeske JC. Preliminary analysis of chronic gastrointestinal toxicity in gynecology patients treated with intensity-modulated whole pelvic radiation therapy. Int J Radiat Oncol Biol Phys. 2003;56(5):1354-60.

13. Mell LK, Kochanski JD, Roeske JC, Haslam JJ, Mehta N, Yamada SD, et al. Dosimetric predictors of acute hematologic toxicity in cervical cancer patients treated with concurrent cisplatin and intensity-modulated pelvic radiotherapy. Int J Radiat Oncol Biol Phys. 2006;66(5):1356-65.

14. Lujan AE, Mundt AJ, Yamada SD, Rotmensch J, Roeske JC. Intensity-modulated radiotherapy as a means of reducing dose to bone marrow in gynecologic patients receiving whole pelvic radiotherapy. Int J Radiat Oncol Biol Phys. 2003;57(2):516-21.

15. Beriwal S, Gan GN, Heron DE, Selvaraj RN, Kim H, Lalonde R, et al. Early clinical outcome with concurrent chemotherapy and extended-field, intensity-modulated radiotherapy for cervical cancer. International Journal of Radiation Oncology* Biology* Physics. 2007;68(1):166-71.

16. Salama JK, Mundt AJ, Roeske J, Mehta N. Preliminary outcome and toxicity report of extended-field, intensity-modulated radiation therapy for gynecologic malignancies. Int J Radiat Oncol Biol Phys. 2006;65(4):1170-6.

17. Hall EJ. Intensity-modulated radiation therapy, protons, and the risk of second cancers. Int J Radiat Oncol Biol Phys. 2006;65(1):1-7.

18. Slater JD, Slater JM, Wahlen S. The potential for proton beam therapy in locally advanced carcinoma of the cervix. Int J Radiat Oncol Biol Phys. 1992;22(2):343-7.

19. Smith AR. Vision 20/20: proton therapy. Med Phys. 2009;36(2):556-68.

20. Georg D, Georg P, Hillbrand M, Potter R, Mock U. Assessment of improved organ at risk sparing for advanced cervix carcinoma utilizing precision radiotherapy techniques. Strahlenther Onkol. 2008;184(11):586-91.

21. Georg D, Kirisits C, Hillbrand M, Dimopoulos J, Potter R. Image-guided radiotherapy for cervix cancer: high-tech external beam therapy versus high-tech brachytherapy. Int J Radiat Oncol Biol Phys. 2008;71(4):1272-8.

22. Jadon R, Pembroke CA, Hanna CL, Palaniappan N, Evans M, Cleves AE, et al. A systematic review of organ motion and image-guided strategies in external beam radiotherapy for cervical cancer. Clin Oncol (R Coll Radiol). 2014;26(4):185-96.

23. Buchali A, Koswig S, Dinges S, Rosenthal P, Salk J, Lackner G, et al. Impact of the filling status of the bladder and rectum on their integral dose distribution and the movement of the uterus in the treatment planning of gynaecological cancer. Radiother Oncol. 1999;52(1):29-34.

24. Chan P, Dinniwell R, Haider MA, Cho YB, Jaffray D, Lockwood G, et al. Inter- and intrafractional tumor and organ movement in patients with cervical cancer undergoing

radiotherapy: a cinematic-MRI point-of-interest study. Int J Radiat Oncol Biol Phys. 2008;70(5):1507-15.

25. Taylor A, Powell ME. An assessment of interfractional uterine and cervical motion: implications for radiotherapy target volume definition in gynaecological cancer. Radiother Oncol. 2008;88(2):250-7.

26. Ahmad R, Hoogeman MS, Bondar M, Dhawtal V, Quint S, De Pree I, et al. Increasing treatment accuracy for cervical cancer patients using correlations between bladder-filling change and cervix-uterus displacements: proof of principle. Radiother Oncol. 2011;98(3):340-6.

27. Bondar L, Hoogeman M, Mens JW, Dhawtal G, de Pree I, Ahmad R, et al. Toward an individualized target motion management for IMRT of cervical cancer based on model-predicted cervix–uterus shape and position. Radiotherapy and Oncology. 2011;99(2):240-5.

28. Beadle BM, Jhingran A, Salehpour M, Sam M, Iyer RB, Eifel PJ. Cervix regression and motion during the course of external beam chemoradiation for cervical cancer. International Journal of Radiation Oncology* Biology* Physics. 2009;73(1):235-41.

29. Bondar M, Hoogeman M, Mens J, Quint S, Ahmad R, Dhawtal G, et al. Individualized nonadaptive and online-adaptive intensity-modulated radiotherapy treatment strategies for cervical cancer patients based on pretreatment acquired variable bladder filling computed tomography scans. International Journal of Radiation Oncology* Biology* Physics. 2012;83(5):1617-23.

30. van de Bunt L, van der Heide UA, Ketelaars M, de Kort GA, Jurgenliemk-Schulz IM. Conventional, conformal, and intensity-modulated radiation therapy treatment planning of external beam radiotherapy for cervical cancer: The impact of tumor regression. Int J Radiat Oncol Biol Phys. 2006;64(1):189-96.

31. Oncology CDLfMRRfr. Workpackage 2 - Image Guided Adaptive Radiation Therapy (IGART): http://www.meduniwien.ac.at/radonc; [cited 2015 07 August]. Available from: http://www.meduniwien.ac.at/hp/radonc/workpackages/workpackage-2-image-guided-adaptive-radiation-therapy-igart/.

32. Ahmad R. Personalized management of complex anatomy variations in cervical cancer IMRT [Phd]. Rotterdam, The Netherlands: Erasmus University Rotterdam; 2014.

33. institute Nc. What is Cancer? : National Cancer Institute at the National Institutes of Health; 2014 [cited 2014 07 November]. Available from: http://www.cancer.gov/cancertopics/cancerlibrary/what-is-cancer.

34. Ltd MI. What is cancer? What causes cancer? : Medicalnewstoday; 2004 [cited 2014 07 November]. Available from: http://www.medicalnewstoday.com/info/cancer-oncology/.

35. Larsen IK. Cancer in Norway 2013-Cancer incidence,mortality,survival and prevalence in Norway Oslo: Cancer Registry of Norway; 2015. Available from: http://www.kreftregisteret.no/Global/Cancer%20in%20Norway/2013/CIN_2013.pdf.

36. Association Nccc-ApoASH. Cervical cancer overview: National cervical cancer coalition; 2015 [cited 2014 07 November]. Available from: http://www.nccc-online.org/index.php/cervicalcancer.

37. Wiebe E, Denny L, Thomas G. Cancer of the cervix uteri. Int J Gynaecol Obstet. 2012;119 Suppl 2:S100-9.

38. UK CR. Cervical cancer staging: Cancer Research UK; 2014 [cited 2014 09 November]. Available from: http://www.cancerresearchuk.org/about-cancer/type/cervical-cancer/treatment/cervical-cancer-stages.

39. Goldman LW. Principles of CT and CT technology. Journal of nuclear medicine technology. 2007;35(3):115-28.

40. Dowsett D, Kenny PA, Johnston RE. The Physics of Diagnostic Imaging Second Edition: CRC Press; 2006.

41. Saksouk FA. Cervical cancer imaging: Medscape; 1994-2015 [cited 2015 03 November]. Available from: http://emedicine.medscape.com/article/402329-overview.

42. Halperin EC, Brady LW, Wazer DE, Perez CA. Perez & Brady's Principles and Practice of Radiation Oncology: Lippincott Williams & Wilkins; 2013.

43. Njeh CF. Tumor delineation: The weakest link in the search for accuracy in radiotherapy. J Med Phys. 2008;33(4):136-40.

44. Stubbs B. The management of tumour localization for radiotherapy. Proc R Soc Med. 1973;66(12):1234.

45. Dobbs H, Webb S. Clinical applications of x-ray computed tomography in radiotherapy planning. Webb's Physics of Medical Imaging2012. p. 153.

46. Ajaz M. Biological Imaging-Guided Intensity-Modulated Radiation Therapy of Uterine Cervical Cancer [Masters]. Oslo, Norway: Unievrsity of Oslo; 2007.

47. Khan FM, Gerbi BJ. Treatment planning in radiation oncology: Lippincott Williams & Wilkins Philadelphia; 2007.

48. Mayles P, Nahum A, Rosenwald J-C. Handbook of radiotherapy physics: theory and practice: CRC Press; 2007.

49. Hellebust TP, Mirza MR. Radiotherapy for Cervical Cancer. In: Ayhan A, Reed N, Gultekin M, Dursun P, editors. Textbook of Gynaecological Oncology. Turkey: Güneş Publishing; 2012.

50. Schlegel W, Bortfeld T, Grosu A-L. New technologies in radiation oncology: Springer; 2006.

51. Bethesda. Prescribing, recording and reporting photon beam therapy (Report 50). USA: 1978.

52. Bethesda. Prescribing, recording and reporting photon beam therapy (Supplement to ICRU report 50). USA: 1993.

53. Levernes S. Volumes and doses for external radiotherapy-Definitions and recommendations. Statens Straalevern, Oesteraas (Norway), 2012.

54. The Royal college of Radiologists SacoR, Institute of Physics and Engineering in Medicine. On target ensuring geometric accuracy in radiotherapy. London: 2008.

55. America RSoN. Intensity-Modulated radiation therapy(IMRT): radiologyinfo.org; 2013 [cited 2015 30 January]. Available from: http://www.radiologyinfo.org/en/info.cfm?pg=imrt.

56. Online E. Radiation oncology, physics, Intensity modulated raiation therapy (IMRT): acpsem; 2012 [cited 2015 15 February]. Available from: http://www.acpsem.org.nz/index.php/rosigdocuments/cat_view/176-career.

57. Podgorsak EB. Radiation oncology physics2005.

58. Oldham M, Neal A, Webb S. A comparison of conventional 'forward planning' with inverse planning for 3D conformal radiotherapy of the prostate. Radiother Oncol. 1995;35(3):248-62.

59. Paganetti H, Bortfeld T. Proton Beam Radiatherapy-The state of Art. 2005 15 Jaunary 2015. Report No.

60. De Laney TF, Kooy HM. Proton and charged particle radiotherapy: Lippincott Williams & Wilkins; 2008.

61. Niemierko A, Urie M, Goitein M. Optimization of 3D radiation therapy with both physical and biological end points and constraints. Int J Radiat Oncol Biol Phys. 1992;23(1):99-108.

62. Lomax AJ, Bortfeld T, Goitein G, Debus J, Dykstra C, Tercier PA, et al. A treatment planning inter-comparison of proton and intensity modulated photon radiotherapy. Radiother Oncol. 1999;51(3):257-71.

63. Koehler AM, Schneider RJ, Sisterson JM. Flattening of proton dose distributions for large-field radiotherapy. Med Phys. 1977;4(4):297-301.

64. Grusell E, Montelius A, Brahme A, Rikner G, Russell K. A general solution to charged particle beam flattening using an optimized dual-scattering-foil technique, with application to proton therapy beams. Phys Med Biol. 1994;39(12):2201-16.

65. Pedroni E, editor Latest developments in proton therapy. Proceedings of EPAC; 2000.

66. Linz U. Ion Beam Therapy: Fundamentals, Technology, Clinical Applications: Springer Science & Business Media; 2011.

67. Quan EM, Liu W, Wu R, Li Y, Frank SJ, Zhang X, et al. Preliminary evaluation of multifield and single-field optimization for the treatment planning of spot-scanning proton therapy of head and neck cancer. Med Phys. 2013;40(8):081709.

68. Kanai T, Kawachi K, Kumamoto Y, Ogawa H, Yamada T, Matsuzawa H, et al. Spot scanning system for proton radiotherapy. Med Phys. 1980;7(4):365-9.

69. Phillips MH, Pedroni E, Blattmann H, Boehringer T, Coray A, Scheib S. Effects of respiratory motion on dose uniformity with a charged particle scanning method. Phys Med Biol. 1992;37(1):223-34.

70. Bortfeld T, Jokivarsi K, Goitein M, Kung J, Jiang SB. Effects of intra-fraction motion on IMRT dose delivery: statistical analysis and simulation. Phys Med Biol. 2002;47(13):2203-20.

71. Engelsman M, Mazal A, Jaffray D. Patient positioning and set-up verification for planning and treatment. Proton and Charged Particle Radiotherapy2008. p. 57-69.

72. Bethesda. Prescribing, recording and reporting proton beam-therapy. USA: 2007.

73. Bourhaleb F, Marchetto F, Attili A, Pitta G, Cirio R, Donetti M, et al. A treatment planning code for inverse planning and 3D optimization in hadrontherapy. Comput Biol Med. 2008;38(9):990-9.

74. Oelfke U, Bortfeld T. Inverse planning for photon and proton beams. Med Dosim. 2001;26(2):113-24.

75. Deasy JO, Shepard DM, Mackie TR, editors. Distal edge tracking: A pro-posed delivery method for conformal proton therapy using intensity-nodula-tion. XIIth International Confer-ence on the Use of Computers in Radiation Therapy; 1997; Madison: Medical Physics Publishing.

76. Gerweck L, Paganetti H, DeLaney T, Kooy H. Radiobiology of charged particles. Proton and charged particle radiotherapy2008. p. 8-18.

77. Linz U. Physical and biological rationale for using ions in therapy. Ion Beam Therapy: Springer; 2012. p. 45-59.

78. Gueulette J, Gahbauer R, Jones DT, Slabbert J, Wambersie A. The Impact of Radiation Quality on Cure Rate. Ion Beam Therapy: Springer; 2012. p. 81-93.

79. Schulte R, Ling T. Early and late responses to ion irradiation. Ion Beam Therapy: Springer; 2012. p. 61-79.

80. Michalski JM, Gay H, Jackson A, Tucker SL, Deasy JO. Radiation dose-volume effects in radiation-induced rectal injury. Int J Radiat Oncol Biol Phys. 2010;76(3 Suppl):S123-9.

81. Marks LB, Yorke ED, Jackson A, Ten Haken RK, Constine LS, Eisbruch A, et al. Use of normal tissue complication probability models in the clinic. Int J Radiat Oncol Biol Phys. 2010;76(3 Suppl):S10-9.

82. Logsdon MD, Eifel PJ. Figo IIIB squamous cell carcinoma of the cervix: an analysis of prognostic factors emphasizing the balance between external beam and intracavitary radiation therapy. Int J Radiat Oncol Biol Phys. 1999;43(4):763-75.

83. Viswanathan AN, Yorke ED, Marks LB, Eifel PJ, Shipley WU. Radiation dose-volume effects of the urinary bladder. Int J Radiat Oncol Biol Phys. 2010;76(3 Suppl):S116-22.

84. Kavanagh BD, Pan CC, Dawson LA, Das SK, Li XA, Ten Haken RK, et al. Radiation dose-volume effects in the stomach and small bowel. Int J Radiat Oncol Biol Phys. 2010;76(3 Suppl):S101-7.

85. Djupvik LH, al e. Doseplanlegging cervix cancer. Oslo: 2014.

86. Waldenstrom AC, Olsson C, Wilderang U, Dunberger G, Lind H, Alevronta E, et al. Relative importance of hip and sacral pain among long-term gynecological cancer survivors treated with pelvic radiotherapy and their relationships to mean absorbed doses. Int J Radiat Oncol Biol Phys. 2012;84(2):428-36.

87. Dawson LA, Kavanagh BD, Paulino AC, Das SK, Miften M, Li XA, et al. Radiation-associated kidney injury. Int J Radiat Oncol Biol Phys. 2010;76(3 Suppl):S108-15.

88. Kirkpatrick JP, van der Kogel AJ, Schultheiss TE. Radiation dose-volume effects in the spinal cord. Int J Radiat Oncol Biol Phys. 2010;76(3 Suppl):S42-9.

89. Tyagi N, Lewis JH, Yashar CM, Vo D, Jiang SB, Mundt AJ, et al. Daily online cone beam computed tomography to assess interfractional motion in patients with intact cervical cancer. Int J Radiat Oncol Biol Phys. 2011;80(1):273-80.

90. Kataria T, Sharma K, Subramani V, Karrthick KP, Bisht SS. Homogeneity Index: An objective tool for assessment of conformal radiation treatments. J Med Phys. 2012;37(4):207-13.

91. Marks LB, Carroll PR, Dugan TC, Anscher MS. The response of the urinary bladder, urethra, and ureter to radiation and chemotherapy. Int J Radiat Oncol Biol Phys. 1995;31(5):1257-80.

92. Mundt AJ, Roeske JC, Lujan AE, Yamada SD, Waggoner SE, Fleming G, et al. Initial clinical experience with intensity-modulated whole-pelvis radiation therapy in women with gynecologic malignancies. Gynecol Oncol. 2001;82(3):456-63.

93. Kim TH, Chie EK, Kim DY, Park SY, Cho KH, Jung KH, et al. Comparison of the belly board device method and the distended bladder method for reducing irradiated small bowel volumes in preoperative radiotherapy of rectal cancer patients. Int J Radiat Oncol Biol Phys. 2005;62(3):769-75.

94. Ahmad R, Hoogeman MS, Quint S, Mens JW, de Pree I, Heijmen BJ. Inter-fraction bladder filling variations and time trends for cervical cancer patients assessed with a portable 3-dimensional ultrasound bladder scanner. Radiotherapy and oncology. 2008;89(2):172-9.

95. Mell LK, Tiryaki H, Ahn KH, Mundt AJ, Roeske JC, Aydogan B. Dosimetric comparison of bone marrow-sparing intensity-modulated radiotherapy versus conventional techniques for treatment of cervical cancer. Int J Radiat Oncol Biol Phys. 2008;71(5):1504-10.

96. Mahantshetty U, Krishnatry R, Chaudhari S, Kanaujia A, Engineer R, Chopra S, et al. Comparison of 2 contouring methods of bone marrow on CT and correlation with hematological toxicities in non-bone marrow-sparing pelvic intensity-modulated radiotherapy with concurrent cisplatin for cervical cancer. Int J Gynecol Cancer. 2012;22(8):1427-34.

97. Hall EJ, Wuu CS. Radiation-induced second cancers: the impact of 3D-CRT and IMRT. Int J Radiat Oncol Biol Phys. 2003;56(1):83-8.

98. Kerkhof EM, Raaymakers BW, van der Heide UA, van de Bunt L, Jurgenliemk-Schulz IM, Lagendijk JJ. Online MRI guidance for healthy tissue sparing in patients with cervical cancer: an IMRT planning study. Radiother Oncol. 2008;88(2):241-9.

99. van de Bunt L, Jurgenliemk-Schulz IM, de Kort GA, Roesink JM, Tersteeg RJ, van der Heide UA. Motion and deformation of the target volumes during IMRT for cervical cancer: what margins do we need? Radiother Oncol. 2008;88(2):233-40.

100. Lim K, Kelly V, Stewart J, Xie J, Cho YB, Moseley J, et al. Pelvic radiotherapy for cancer of the cervix: is what you plan actually what you deliver? Int J Radiat Oncol Biol Phys. 2009;74(1):304-12.

Appendix

Raw data

OAR	IMRT	IMPT	IMRT(X)	IMPT(X)
Rectum(V10)				
Patient 1	100	93.59	100	91.52
Patient 2	100	95.74	100	88.12
Patient 3	78.18	96.01	64.58	93.13
patient 4	100	98.06	97.06	87.72
Patient 5	100	99.99	100	100
Patient 6	100	100	100	99.01
Patient 7	99.89	91.42	98.38	84.34
Patient 8	99.93	98.79	99.15	97.21
Patient 9	100	99.68	100	96.74
Patient 10	99.74	97.38	98.62	96.92
Mean	97.774	97.066	95.779	93.471
SD	6.885138908	2.884503423	11.00657829	5.363202712
Ttest	0.379964479		0.277650684	
Ratio	1.007294006		1.024692151	

OAR	IMRT	IMPT	IMRT(X)	IMPT(X)
Rectum(V30)				
Patient 1	100	77.32	100	69.74
Patient 2	88.44	76.73	80.36	65.39
Patient 3	93.88	85.56	89.58	77.72
Patient 4	89.36	69.99	84.01	60.64
Patient 5	99.91	88.33	99.28	74.2
Patient 6	100	83.37	99.77	77.32
Patient 7	93.18	45.9	85.4	32.03
Patient 8	98.86	97.21	97.72	94.94
Patient 9	100	80.9	98.47	63.88
Patient 10	95.73	92.13	93.4	80.72
Mean	95.936	79.744	92.799	69.658
SD	4.536146676	14.28294	7.425726227	16.5149
Ttest	0.001638837		0.000301978	
Ratio	1.203049759		1.332208792	

OAR	IMRT	IMPT	IMRT(X)	IMPT(X)
Rectum(V45)				
patient 1	84.1	64.69	73.2	52.96
patient 2	65.64	62.64	51.39	47.47
patient 3	78.19	71.39	64.56	59.38
patient 4	75.34	54.46	53.57	32.47
patient 5	79.8	71.09	63.59	44.79
Patient 6	78.95	62.04	60.58	53.99
Patient 7	59.85	30.45	39.76	15.14
Patient 8	97.41	95.65	95.51	92.72
Patient 9	75.95	56.03	54.19	40.34
Patient 10	82.37	62.71	73.52	43.91
Mean	77.76	63.115	62.987	48.317
SD	10.166	16.28475	15.3538906	19.98835
ttest	0.000313		0.000455899	
Ratio	1.232037		1.303619844	

OAR	IMRT	IMPT	IMRT(X)	IMPT(X)
Bladder(V10)				
patient 1	100	74.81	100	66.56
patient 2	100	71.6	100	63.06
patient 3	100	71.54	100	58.24
patient 4	100	80.59	100	67.79
patient 5	100	55	100	51.72
Patient 6	100	68.75	100	63.07
Patient 7	100	100	100	100
Patient 8	100	94.27	100	93.16
Patient 9	100	80.17	100	74.32
Patient 10	100	79.63	100	71.43
Mean	100	77.636	100	70.935
SD	0	12.77537579	0	15.03223518
Ttest	0.000181518		8.80818E-05	
Ratio	1.288062239		1.409741312	

OAR	IMRT	IMPT	IMRT(X)	IMPT(X)
Bladder(V30)				
Patient 1	76.93	52.67	74.29	42.32
Patient 2	86.52	60.02	77.42	51.43
Patient 3	81.97	59.92	79.26	44.14
Patient 4	66.59	50.83	61.82	42.46
Patient 5	74.05	40.34	70.8	33.84
Patient 6	93.46	53.42	68.74	42.98
Patient 7	100	100	100	98.57
Patient 8	98.96	84.46	97.61	69.56
Patient 9	87.86	69.34	81.27	60.64
Patient 10	97.54	57.6	93.78	43.57
Mean	86.388	62.86	80.499	52.951
SD	11.41668253	17.56615	12.82736437	19.06641
Ttest	9.95908E-05		4.00303E-05	
Ratio	1.374292078		1.520254575	

OAR	IMRT	IMPT	IMRT(X)	IMPT(X)
Bladder(V45)				
Patient 1	47.89	35.03	40.2	26.53
Patient 2	59.05	49.58	47.82	40.21
Patient 3	59.55	50.24	48.38	32.79
Patient 4	40.59	33.44	34.35	22.58
Patient 5	41.94	29.01	32.9	20.31
Patient 6	48.65	36.62	33.71	22.14
Patient 7	99.21	94.5	92.14	86.98
Patient 8	81.46	73.94	65.04	52.58
Patient 9	62.18	57.77	54.79	48.05
Patient 10	62.06	40.96	46.91	26.28
Mean	60.258	50.109	49.624	37.845
SD	18.21409	20.58457	18.0713802	20.59012
Ttest	5.45E-05		8.78606E-06	
Ratio	1.202538		1.311243229	

OAR	IMRT	IMPT	IMRT(X)	IMPT(X)
Sigmoideum(V10)				
Patient 1	100	100	100	100
Patient 2	100	100	100	99.27
Patient 3	100	98.26	100	97.25
Patient 4	100	99.97	100	98.79
Patient 5	100	94.11	100	93.11
Patient 6	100	100	100	100
Patient 7	100	88.55	100	81.76
Patient 8	100	100	100	100
Patient 9	100	89.63	100	73.92
Patient 10	100	47.71	99.9	47.08
Mean	100	91.823	99.99	89.118
SD	0	16.13130431	0.031622777	17.27632536
Ttest	0.071702786		0.038701924	
Ratio	1.089051763		1.121995556	

OAR	IMRT	IMPT	IMRT(X)	IMPT(X)
Sigmoideum(V30)				
Patient 1	100	100	100	100
Patient 2	100	84.5	98.99	78.3
Patient 3	98.11	92.9	95.31	86.05
Patient 4	94.36	76.11	91.25	70.47
Patient 5	100	74.14	100	67.26
Patient 6	100	100	100	100
Patient 7	100	45.72	99.29	39.51
Patient 8	100	98.9	100	97.73
Patient 9	100	53.53	99.44	49.27
Patient 10	53.97	40.1	51.58	39.5
Mean	94.644	76.59	93.586	72.809
SD	14.40399343	22.96096	15.03144423	23.83716
Ttest	0.007757199		0.005971596	
Ratio	1.235722679		1.285363073	

OAR	IMRT	IMPT	IMRT(X)	IMPT(X)
Sigmoideum(V45)				
Patient 1	100	96.48	98.39	96.11
Patient 2	76.58	62.27	58.35	52.94
Patient 3	83.8	78.55	73.65	70.09
Patient 4	73.07	45.56	67.6	42.37
Patient 5	68.19	56.83	63.01	45.1
Patient 6	98.65	94.36	96.84	82.5
Patient 7	77.68	25.38	62.78	20.45
Patient 8	98.5	95.14	97.53	93.82
Patient 9	74.54	37.85	67.85	35.75
Patient 10	42.09	36.17	42.79	35.35
Mean	79.31	62.859	72.879	57.448
SD	17.54775	26.85214	18.86263882	26.52716
Ttest	0.006588		0.003209466	
Ratio	1.261713		1.268608133	

OAR	IMRT	IMPT	IMRT(X)	IMPT(X)
Bowel(V10)				
Patient 1	55.77	38.81	56.59	38.08
Patient 2	76.71	65.27	80.87	59.78
patient 3	76.13	46.05	70.84	44.35
patient 4	84.45	29.63	87.72	20.9
Patient 5	85.45	57.42	84.18	55.83
Patient 6	83.28	45.75	83.85	45.9
Patient 7	73.71	15.21	73.41	12.35
Patient 8	84.03	41.58	87.38	35.28
Patient 9	94.46	24.39	89.98	20.76
Patient 10	87.3	31.18	89.64	33.41
Mean	80.129	39.529	80.446	36.664
SD	10.49432381	15.11781102	10.60931059	15.46747067
Ttest	4.51872E-05		2.84308E-05	
Ratio	2.027094032		2.194141392	

OAR	IMRT	IMPT	IMRT(X)	IMPT(X)
Bowel(V30)				
Patient 1	32.6	16.3	31.02	14.94
patient 2	45.64	33.28	47.17	30.4
patient 3	45.5	28.12	44.04	24.29
patient 4	43.47	13.91	41.18	11.34
Patient 5	52.23	31.91	51.73	31.02
Patient 6	32.18	16.75	31.48	16.6
Patient 7	24.33	7.47	25.02	6.53
Patient 8	45.53	26.46	45.11	23.24
Patient 9	36.62	14.88	37.03	12.43
Patient 10	31.81	15.03	31.57	14.62
Mean	38.991	20.411	38.535	18.541
SD	8.718022775	8.77775	8.620921902	8.280262
Ttest	2.51375E-07		1.0766E-07	
Ratio	1.910293469		2.078366863	

OAR	IMRT	IMPT	IMRT(X)	IMPT(X)
Bowel(V45)				
Patient 1	16.51	11.79	13.26	10.34
Patient 2	20.87	18.27	20.53	15.91
Patient 3	21.24	18.13	19.67	16.18
Patient 4	18.72	7.45	15.21	6.22
Patient 5	28.68	22.63	26.61	20.86
Patient 6	9.99	9.45	9.97	8.96
Patient 7	7.98	4.2	6.95	3.64
Patient 8	24.01	18.88	20.78	16.78
Patient 9	12.02	8.68	12.08	7.64
Patient 10	10.73	8.64	10.59	8.53
Mean	17.075	12.812	15.565	11.506
SD	6.800924	6.155655	6.133221466	5.557916
Ttest	0.000638		0.000119679	
Ratio	1.332735		1.352772467	

OAR	IMRT	IMPT	IMRT(X)	IMPT(X)
Pelvic bone(V10)				
Patient 1	73.88	65.17	74.38	66.09
patient 2	70.44	53.35	70.14	49.01
Patient 3	72.02	65.27	69.06	61.75
Patient 4	71.3	51.27	71.23	48.18
patient 5	74.41	59.65	72.97	55.77
Patient 6	84.81	59.03	83.71	59.28
Patient 7	86.15	80.14	85.59	76.64
Patient 8	90.15	84.99	89.7	65.59
Patient 9	82.85	72.83	81.62	69.95
Patient 10	92.04	59.5	91.33	55.16
Mean	79.805	65.12	78.973	60.742
SD	8.274132717	11.09972572	8.395565033	9.0928211
Ttest	0.000347708		7.81422E-05	
Ratio	1.225506757		1.30013829	

OAR	IMRT	IMPT	IMRT(X)	IMPT(X)
Pelvic bone(V30)				
Patient 1	45.29	23.26	44.14	23.48
patient 2	40.64	23.41	39.41	23.16
patient 3	40.74	23.78	40.36	23.02
Patient 4	40.37	24.06	38.3	21.26
patient 5	44.95	28.05	42.82	27.11
Patient 6	44.68	21.95	42.35	21.69
Patient 7	52.32	31.26	51.87	31.93
Patient 8	64.77	39.24	61.66	36.51
Patient 9	47.49	29.67	47.46	34.04
Patient 10	56.22	28	54.56	23.66
Mean	47.747	27.268	46.293	26.586
SD	7.887027394	5.247947	7.569393121	5.556582
Ttest	3.82739E-08		3.47415E-07	
Ratio	1.751026845		1.741254796	

OAR	IMRT	IMPT	IMRT(X)	IMPT(X)
Pelvic bone(V45)				
Patient 1	14.6	11.01	12.43	11.4
Patient 2	13.32	11	13.32	11.03
Patient 3	13.24	11.75	12.64	10.78
Patient 4	11.72	10.27	14.44	8.17
Patient 5	16.01	13.98	14.58	13.78
Patient 6	10.7	10.37	10.44	10.11
Patient 7	16.56	13.96	17.08	13.77
Patient 8	23.47	18.99	22.21	18.26
Patient 9	14.28	12.36	13.93	16.06
Patient 10	16.44	13.38	16.61	13.05
Mean	15.034	12.707	14.768	12.641
SD	3.545003	2.610875	3.262408109	2.981359
Ttest	7.66E-05		0.008771547	
Ratio	1.183127		1.168262005	

Target volume	IMRT	IMPT	IMRT(X)	IMPT(X)
PTVUnion_CT(D98%)				
Patient 1	96.54	97.38	96.09	97.55
Patient 2	95.47	96.88	95.47	96.44
patient 3	95.41	96.18	95.41	96.18
Patient 4	95.2	96.69	95.19	95.89
Patient 5	95.3	96.75	95.07	96.43
Patient 6	95.19	97.14	95.07	96.89
Patient 7	95.59	96.55	95.24	96.29
Patient 8	95.58	96.76	95.27	96.6
Patient 9	95.17	97.01	95.08	96.83
Patient 10	95.24	96.89	95.16	96.3
Mean	95.469	96.823	95.305	96.54
SD	0.40798829	0.328026083	0.308265758	0.462433178
Ttest	1.20384E-06		1.41971E-06	
Ratio	0.986015719		0.987207375	

PTVUnion_CT(D2%)	IMRT	IMPT	IMRT(X)	IMPT(X)
Patient 1	102.83	101.46	102.6	101.17
Patient 2	103.46	101.66	103.14	101.75
Patient 3	103.35	101.87	103.56	101.85
Patient 4	103.58	101.69	104.21	102.24
Patient 5	103.326	101.6	103.65	101.76
Patient 6	102.91	101.6	103.13	101.68
Patient 7	102.65	101.84	102.94	102.11
Patient 8	103.18	101.56	102.8	101.72
Patient 9	103.54	101.65	103.5	103.2
Patient 10	103	101.95	103.06	102.39
Mean	103.1826	101.688	103.259	101.987
SD	0.320909887	0.153101	0.474117894	0.544917
Ttest	1.95393E-07		2.08746E-05	
Ratio	1.014697899		1.012472178	

DHI	IMRT	IMPT	IMRT(X)	IMPT(X)
Patient 1	-0.0629	-0.0408	-0.0651	-0.0362
Patient 2	-0.0799	-0.0478	-0.0767	-0.0531
Patient 3	-0.0794	-0.0569	-0.0815	-0.0567
Patient 4	-0.0838	-0.05	-0.0902	-0.0635
Patient 5	-0.08026	-0.0485	-0.0858	-0.0533
Patient 6	-0.0772	-0.0446	-0.0806	-0.0479
Patient 7	-0.0706	-0.0529	-0.077	-0.0582
Patient 8	-0.076	-0.048	-0.0753	-0.0512
Patient 9	-0.0837	-0.0464	-0.0842	-0.0637
Patient 10	-0.0776	-0.0506	-0.079	-0.0609
Mean	-0.07714	-0.04865	-0.07954	-0.05447
SD	0.006297	0.004422	0.006837836	0.008286
Ttest	7.08E-08		4.84004E-08	
Ratio	1.585529		1.46025335	

Bowel	IMRT	IMPT	IMRT(X)	IMPT(X)
V45(cc)				
Patient 1	324.18	231.72	260.72	203.08
Patient 2	292.89	256.64	288.24	223.65
Patient 3	330.1	281.49	305.81	251.09
Patient 4	330.08	131.07	267.21	109.6
Patient 5	440.73	345.93	408.65	320.39
Patient 6	429.19	406.15	429.44	385.33
Patient 7	519.37	273.49	453.6	237.41
Patient 8	673.7	529.69	583.5	470.71
Patient 9	436.44	315.48	438.13	277.59
Patient 10	266.16	213.8	263.17	212.25
Mean	404.284	298.546	369.847	269.11
SD	123.7045806	110.5083	109.0184561	101.808
Ttest	0.000670334		0.000218716	
Ratio	1.354176576		1.374333915	

Outer body	IMRT	IMPT	IMRT(X)	IMPT(X)
V10				
Patient 1	39.06	23.98	38.98	23.75
Patient 2	39.57	25.97	39.21	24.51
Patient 3	32.7	19.93	31.71	18.57
Patient 4	31.84	16.82	31.53	15.33
Patient 5	39.95	23.43	38.29	22.64
Patient 6	58.26	28.88	57.82	28.54
Patient 7	46.43	23.09	45.8	21.15
Patient 8	59.99	37.34	59.92	31.03
Patient 9	53.99	26.22	52.51	23.99
Patient 10	46.85	21.3	46.45	20.7
Mean	44.864	24.696	44.222	23.021
SD	10.00764619	5.600554	10.0714236	4.549563
Ttest	1.50875E-06		1.87782E-06	
Ratio	1.81665047		1.920941749	

Outer body	IMRT	IMPT	IMRT(X)	IMPT(X)
D2cm3				
Patient 1	104.34	103.02	104.14	102.27
Patient 2	105.12	102.97	104.83	103.01
patient 3	104.41	104.01	104.81	103.4
Patient 4	105.35	102.91	105.5	104.4
Patient 5	105.05	102.95	105.37	103
Patient 6	104.27	103.57	104.7	104
Patient 7	103.65	103.77	105.38	104.3
Patient 8	102.53	104.59	104.3	104
Patient 9	104.97	103.24	104.74	105.6
Patient 10	104.61	105.7	105.13	105.47
Mean	104.43	103.673	104.89	103.945
SD	0.835557033	0.900383252	0.456970702	1.068417833
Ttest	0.071770132		0.008237396	
Ratio	1.007301805		1.009091346	

OAR	IMRT	IMPT	IMRT(X)	IMPT(X)
Left Kidney (V10)				
Patient 6	45.48	0	44.76	0
Patient 7	38.36	0	42.26	0
Patient 8	76.97	22.09	81.24	23.83
Patient 9	78.33	2.39	77.97	8.76
Patient 10	38.11	0	40.41	0
Mean	55.45	4.896	57.328	6.518
SD	20.48627223	9.667291761	20.4272727	10.39452837
Ttest	0.000998243		0.000375516	
Ratio	11.3255719		8.795335993	
OAR	IMRT	IMPT	IMRT(X)	IMPT(X)

OAR	IMRT	IMPT	IMRT(X)	IMPT(X)
Left Kidney (V30)				
Patient 6	0	0	0.04	0
Patient 7	0	0	0	0
Patient 8	9.42	2.97	8.54	3.49
Patient 9	0.84	0.33	1.09	1
Patient 10	0.43	0	0.47	0
Mean	2.138	0.66	2.028	0.898
SD	4.085697003	1.299211	3.666683788	1.51229
Ttest	0.150845737		0.157319552	
Ratio	3.239393939		2.258351893	

OAR	IMRT	IMPT	IMRT(X)	IMPT(X)
Left Kidney (V45)				
Patient 6	0	0	0	0
Patient 7	0	0	0	0
Patient 8	1.49	0.86	1.35	0.96
Patient 9	0	0	0	0.13
Patient 10	0	0	0	0
Mean	0.298	0.172	0.27	0.218
SD	0.666348	0.384604	0.603738354	0.418593
ttest	0.18695		0.29352482	
Ratio	1.732558		1.23853211	

OAR	IMRT	IMPT	IMRT(X)	IMPT(X)
Cauda Equina(V10)				
patient 1	56.7	15.64	57.14	14.45
patient 2	53.95	31.56	52.31	22.74
patient 3	37.83	48.32	44.84	14.06
Patient 4	44.22	21.58	51.64	21.88
patient 5	50.73	22.95	52.9	25.58
Patient 6	100	0	100	0
Patient 7	100	100	100	100
Patient 8	100	100	100	99.73
Patient 9	100	100	100	100
Patient 10	100	88.84	100	61.89
Mean	74.343	52.889	75.883	46.033
SD	27.52115592	40.12196252	25.59241209	40.33572804
Ttest	0.030850668		0.005393011	
Ratio	1.405642005		1.648447853	

OAR	IMRT	IMPT	IMRT(X)	IMPT(X)
Right Kidney (V10)				
Patient 6	11.24	0	12.77	0
Patient 7	76.53	8.21	80.6	6.62
Patient 8	89.86	23.78	91.41	33.85
Patient 9	54.64	0.51	55.81	4.45
Patient 10	56.37	7.4	57.55	4.77
Mean	57.728	7.98	59.628	9.938
SD	29.82655981	9.611329253	30.26750601	13.58660259
Ttest	0.004204823		0.003921391	
Ratio	7.234085213		6	

OAR	IMRT	IMPT	IMRT(X)	IMPT(X)
Right Kidney (V30)				
Patient 6	0	0	0	0
Patient 7	0	2.82	0	2.41
Patient 8	14.57	5.43	13.36	7.11
Patient 9	0.13	0	0.23	0
Patient 10	2.79	1.57	2.78	0.77
Mean	3.498	1.964	3.274	2.058
SD	6.30289378	2.270227	5.759243006	2.990664
Ttest	0.244480666		0.223232519	
Ratio	1.781059063		1.590864917	

OAR	IMRT	IMPT	IMRT(X)	IMPT(X)
Right Kidney (V45)				
Patient 6	0	0	0	0
Patient 7	0	1.05	0	0.87
Patient 8	4.59	1.72	3.76	1.95
Patient 9	0	0	0	0
Patient 10	0.18	0.38	0.17	0
Mean	0.954	0.63	0.786	0.564
SD	2.03408	0.745117	1.664145426	0.861528
Ttest	0.325889		0.31900679	
Ratio	1.514286		1.393617021	

OAR	IMRT	IMPT	IMRT(X)	IMPT(X)
Medulla Dmax (%)				
Patient 6	59.5	42.8	60.4	35.3
Patient 7	52.5	47.6	54.5	53.3
Patient 8	52	36.6	50	29
Patient 9	45	41	45.8	52.3
Patient 10	49.3	33.6	48.4	37.4
Mean	51.66	40.32	51.82	41.46
SD	5.296508284	5.445365002	5.745607018	10.80939406
ttest	0.007967362		0.077295979	
Ratio	1.28125		1.249879402	

V95%	IMRT	IMPT	IMRT(X)	IMPT(X)
Patient 1	1780	1774.09	1641.11	1648.29
Patient 2	1373.36	1381.35	1264.29	1282.2
Patient 3	1215.25	1218.41	1100	1103.82
Patient 4	1368.97	1388.8	1250.91	1259.09
Patient 5	1290	1297.37	1169.33	1181.36
Patient 6	1700	1736.13	1583	1641.44
Patient 7	1928.48	1935.39	1814.52	1826.32
Patient 8	1883.6	1892.4	1763.12	1775.76
Patient 9	1625.9	1644.09	1541.31	1562.97
Patient 10	2230	2257.7	2100	2121.44

VPTV cm3	IMRT	IMPT	IMRT(X)	IMPT(X)
Patient 1	1791	1785.5	1655.2	1655.1
Patient 2	1393.1	1391.9	1282.2	1269.76
Patient 3	1234.7	1233.8	1117.5	1117.6
Patient 4	1393.8	1375.82	1273.6	1273.7
Patient 5	1311.6	1307.1	1191.8	1191.8
Patient 6	1730.9	1745.3	1613.2	1652.7
Patient 7	1954.7	1955.7	1846.5	1847.4
Patient 8	1910.5	1910	1793.7	1793.7
Patient 9	1655.4	1655.4	1571.6	1571.7
Patient 10	2268.5	2273.8	2139.6	2145.4

DCI	IMRT	IMPT	IMRT(X)	IMPT(X)
Patient 1	0.993858	0.99361	0.991487434	0.995885
Patient 2	0.98583	0.99242	0.98603182	1.009797
Patient 3	0.984247	0.987526	0.984340045	0.98767
Patient 4	0.982185	1.009434	0.982184359	0.988529
Patient 5	0.983532	0.992556	0.981146165	0.99124
Patient 6	0.982148	0.994746	0.981279445	0.993187
Patient 7	0.986586	0.989615	0.982680747	0.988589
Patient 8	0.98592	0.990785	0.982951441	0.989998
Patient 9	0.98218	0.993168	0.980726648	0.994446
Patient 10	0.983028	0.992919	0.981491868	0.988832
Mean	0.984951	0.993678	0.983431997	0.992817
SD	0.003545	0.005924	0.003262023	0.006579
Ttest	0.002843		0.000401492	
Ratio	0.991218		0.990546675	

D_{mean}

Bladder	Volume Cm3	IMRT %	IMPT %	IMRT(X) %	IMPT(X) %
Patient 1	430.2	79	58.7	76.4	49.4
Patient 2	226.8	85.6	62.8	79.4	53.9
Patient 3	162.4	83.8	63.1	79.9	48.2
Patient 4	489.2	72.7	59.1	68.5	48.9
Patient 5	363.3	76.2	44.8	72.9	39.3
Patient 6	220	84.3	56.3	73.3	46.8
Patient 7	65.8	98.8	97.9	96.9	95.6
Patient 8	68.7	94.2	85.6	89.7	74.5
Patient 9	70	86	71.1	82.5	63.7
Patient 10	336.3	89	63.4	84.1	51.8
Mean	243.27	84.96	66.28	80.36	57.21
SD		7.881652393	15.26374062	8.448168769	16.65148976
Ttest		6.61869E-05		1.95242E-05	
Ratio		1.281834641		1.404649537	

Bowel	Volume Cm3	IMRT	IMPT	IMRT(X)	IMPT(X)
Patient 1	1964.2	40.4	23	38.8	21.4
Patient 2	1404.7	52.9	42.5	55	39.6
Patient 3	1552.8	53.2	34.7	51.2	32.4
Patient 4	1759.6	53.6	20	53.8	16.6
Patient 5	1535.8	59.9	106.3	58.4	40.6
Patient 6	4296.7	47.7	26.8	47.8	26.6
Patient 7	6517.2	41.6	10.9	41	9.3
Patient 8	2807.8	55.9	33.1	55.4	29
Patient 9	3631.7	53.2	21	51.2	17.4
Patient 10	2480.5	47.2	23.6	47.4	23.5
Mean	2795.1	50.56	34.19	50	25.64
SD		6.212746753	26.833	6.32525801	10.08719761
Ttest		0.026332476		1.66443E-06	
Ratio		1.478794969		1.950078003	

Rectum	Volume Cm3	IMRT	IMPT	IMRT(X)	IMPT(X)
Patient 1	121.1	95	80.6	92.1	74.2
Patient 2	75.6	87.3	79.9	80.9	70.2
Patient 3	150.2	91.6	86	86.8	79.3
Patient 4	26.8	89	75.6	81	65.3
Patient 5	110.7	93.3	87.8	89.2	76.3
Patient 6	145	94.2	84.8	89	79.6
Patient 7	80.7	86.6	57.6	78.7	45.8
Patient 8	35.5	98	97.5	97	95.2
Patient 9	102.6	92.9	82.6	87.3	70.6
Patient 10	61.2	92.5	86.7	88.8	78.6
Mean	90.94	92.04	81.91	87.08	73.51
SD		3.54313107	10.34294714	5.580282749	12.60471252
test		0.001316471		0.000292761	
Ratio		1.123672323		1.184600735	

Sigmoideum	Volume Cm3	IMRT	IMPT	IMRT(X)	IMPT(X)
Patient 1	17.6	97.5	98.6	98.1	98.5
Patient 2	104.9	93.4	84.6	87.8	79.3
Patient 3	41.5	94.6	91.5	91.6	86.6
Patient 4	69.4	90.4	78.3	88.2	74.5
Patient 5	30.9	91.7	76.6	90	71.7
Patient 6	35.3	98.4	98.3	97.5	95.5
Patient 7	84	92.8	56.9	88.5	51.6
Patient 8	20.8	99.2	98.2	99	97.3
Patient 9	97.9	93.1	63.2	90.9	57.5
Patient 10	71.2	68.3	42.8	64.7	42.2
Mean	57.35	91.94	78.9	89.63	75.47
SD		8.806083756	19.34350307	9.748395879	19.89254746
test		0.006399872		0.004242516	
Ratio		1.165272497		1.187624222	

Cauda Equina	Volume Cm3	IMRT	IMPT	IMRT(X)	IMPT(X)
Patient 1	18.5	24.5	9.4	24.1	7.6
Patient 2	18.8	21.6	13.1	20.8	11.5
Patient 3	14.9	15.7	13.2	17.3	10.7
Patient 4	13	19.3	9.8	20.8	9.6
Patient 5	25.1	20.5	8.5	19.4	10.5
Patient 6	22.1	42.5	9.6	42.8	8.5
Patient 7	27.7	49.9	37.8	47.9	36.4
Patient 8	10.6	44.6	43.8	43.5	40.7
Patient 9	14.4	41	40.5	41.6	51.6
Patient 10	9.9	43.5	32.1	43.2	29.6
Mean	17.5	32.31	21.78	32.14	21.67
SD		13.0185722	14.79082298	12.504417	16.34163395
Ttest		0.003105454		0.007746804	
Ratio		1.483471074		1.483156437	

Left Kidney	Volume Cm3	IMRT	IMPT	IMRT(X)	IMPT(X)
Patient 1					
Patient 2					
Patient 3					
Patient 4					
Patient 5					
Patient 6	129.6	21.3	1.6	21.1	1.6
Patient 7	287.4	16.4	1.4	17.7	1.2
Patient 8	146.4	34.7	11.1	34.7	12.1
Patient 9	141.6	29.7	3.3	29.5	5.1
Patient 10	191.6	18.5	0.3	18.9	0.3
Mean	179.32	24.12	3.54	24.38	4.06
SD		7.781516562	4.360389891	7.384578526	4.850051546
Ttest		0.00025501		6.83979E-05	
Ratio		6.813559322		6.004926108	

Right Kidney	Volume Cm3	IMRT	IMPT	IMRT(X)	IMPT(X)
Patient 1					
Patient 2					
Patient 3					
Patient 4					
Patient 5					
Patient 6	127.3	11.7	0.8	11.6	0.8
Patient 7	349.8	27.5	9.4	28.7	8.5
Patient 8	113.9	39.5	13.6	38.9	17.8
Patient 9	155.6	24.2	1	24.5	2.5
Patient 10	185.2	22.7	5.4	23.1	3.5
Mean	186.36	25.12	6.04	25.36	6.62
SD		9.990595578	5.516158083	9.870055724	6.875827223
test		0.000909254		0.000379913	
Ratio		4.158940397		3.83081571	

Medulla	Volume Cm3	IMRT	IMPT	IMRT(X)	IMPT(X)
Patient 1					
Patient 2					
Patient 3					
Patient 4					
Patient 5					
Patient 6	22.4	31.8	14	31.7	11.8
Patient 7	16.8	16.5	10.9	16.5	12.1
Patient 8	9.3	41.1	24	39.4	12.7
Patient 9	14.4	30.5	22.9	31.2	31.2
Patient 10	7.4	37.2	19.6	36.8	18.2
Mean	14.06	31.42	18.28	31.12	17.2
SD		9.363599735	5.669832449	8.872823677	8.252575356
Ttest		0.004071778		0.025188199	
Ratio		1.718818381		1.809302326	

Pelvic Bone	Volume Cm3	IMRT	IMPT	IMRT(X)	IMPT(X)
Patient 1	1828.8	51.1	35.5	50.5	35.8
Patient 2	1740.7	47.6	33.1	46.9	32.2
Patient 3	1262.3	47.9	36.2	46.7	35.4
Patient 4	1434.4	47.1	33.6	47.1	30.7
Patient 5	1404.9	50.6	37.7	48.4	36.2
Patient 6	1753.8	54.3	34.8	53.1	34.5
Patient 7	2181.4	58.4	45	58	44.6
Patient 8	1135.9	65.2	51	63.8	45.8
Patient 9	1708.3	54.9	42.2	54.1	44.4
Patient 10	1551.7	61.9	39	61.2	35.7
Mean	1600.22	53.9	38.81	52.98	37.53
SD		6.269502904	5.70836618	6.229107302	5.400216045
Ttest		1.23822E-07		9.46416E-07	
Ratio		1.388817315		1.411670663	

Doseplanlegging cervix cancer

Oslo universitetssykehus	Retningslinje **Doseplanlegging cervix cancer** Kreft, kirurgi og transplantasjon / Avd. medisinsk fysikk		
Dokument-ID: 39408 **Versjon:** 0 **Status:** Under arbeid.	**Dokumentansvarlig:** Linda Holth Djupvik **Utarbeidet av:** Taran Paulsen Hellebust, Irene Berntsen, Kjersti Bruheim og Linda Holth Djupvik	**Godkjent av:** Ikke godkjent	**Godkjent fra:**

1. Endringer siden forrige versjon
Dette er 1. versjon

2. Hensikt og omfang
Retningslinjen beskriver metode for doseplanlegging av cervix cancer, herunder kort beskrivelse av inntegning av målvolum og risikovolum, utgangspunkt for feltoppsett, og dosebegrensninger for målvolum og risikovolum. Prosedyre for å produsere bildegrunnlaget for doseplanlegging av cervix cancer, er beskrevet i "CT for doseplanlegging - Gjennomføring generelt" og "CT bekken for doseplanlegging".

Retningslinjen omfatter pasienter som skal ha strålebehandling med følgende fraksjonering:

- 1.8Gy x 28 mot bekkenet som primær behandling
- 1.8Gy x 28 mot paraortal-regionen (hvis indikasjon)
- 2.0Gy x 7 som en boost til patologiske lymfeknuter (hvis indikasjon)

Vulva cancer, corpus cancer og bestråling av paraortalområdet etter tidligere gitt bekkenbestråling omtales i eget dokument.
Retningslinjen er til hjelp for stråleterapeuter, fysikere og leger som er involvert i doseplanlegging av kurativ gynekologisk cancer.

3. Ansvar
Diagnoseansvarlig fysiker har ansvaret for oppdatering av prosedyren.
Høringsinstanser: Prosedyreutvalget, styringsgruppa, diagnosegruppa, enhetsledere apparat, fagansvarlige stråleterapeuter, diagnoseansvarlig onkolog og diagnoseansvarlig fysiker.

4. Fremgangsmåte
4.1 Inntegning av volumer
4.1.1 Inntegning av risikoorgan

Tabell 1: Risikoorgan (OAR) som skal tegnes inn ved IMRT

Volum	Beskrivelse	Type	Tegnes av	Farge
Rectum	Hele rectum tegnes inn. Fra linea dentata til overgangen til kolon sigmoideum	OAR	Stråleterapeut/Lege	Rosa
SmallBowel	Hele det peritonale rom skal tegnes inn. Craniell begrensning: Til og med L1 ved paraortal bestråling, L4 ved bekkenbestråling	OAR	Stråleterapeut/Lege	Lys grønn
Femoral head	Tegner inn hoftekulene til troch minors øvre kant	OAR	Stråleterapeut	Mørk grønn
Bladder	Hele blæren tegnes inn	OAR	Stråleterapeut/Lege	Gul
Sigmoideum	Kan tegnes hvis ønskelig	OAR	Lege	Brun
Medulla	Tegner inn medulla fra toppen av nyrene og til cauda equina (mellom L2 og L3) Tegnes inn ved bestråling av paraortal region.	OAR	Stråleterapeut	Grønn
Cauda equina	Kan tegnes hvis ønskelig.	OAR	Stråleterapeut	Lys lilla
Kidney	Nyrene tegnes inn som separate volum. Tegnes inn ved bestråling av paraortal region.	OAR	Stråleterapeut	Mørk lilla

4.1.2 Inntegning av målvolumer ved bekkenbestråling

Tabell 2: Målvolumer som skal tegnes inn ved primær bekkenbestråling av cervix cancer.

Volum	Beskrivelse	Type	Tegnes av	Farge
GTV_T	Primærtumor	Målvolum	Lege	Oransje
GTV_Nx	Patologiske forstørrede lymfeknuter, ved inntegning av flere GTV_N skal de nummereres. Lokalisering av de ulike volumene angis på rekvisisjonen	Målvolum	Lege	Oransje
GTV_P	Del av GTV_T i parametrie eller på bekkenveggen som ikke vil motta tilstrekkelig dose fra brachybehandlingen, og som derfor må boostes med ekstern strålebehandling	Målvolum	Lege	Oransje
CTV_T	GTV_T + 5mm	Målvolum	Lege	Rød
CTV_centr_50.4Gy	CTV_T + parametriet bilateralt + hele uterus + ovariene + øvre halvdel av vagina, men minst 3 cm fra tumor	Målvolum	Lege	Rød
CTV_Nx_64Gy	GTV_Nx + 5 mm (respekter sikre anatomiske barrierer)	Målvolum	Lege	Rød
CTV_P_xGy	GTV_P + 5-10 mm margin	Målvolum	Lege	Rød
CTV_E_pel_50.4Gy	Lymfeknutestasjoner illiaca externa + iliaca interna + iliaca communis. Ikke inn i naturlig barrierer (bein/musklatur)	Målvolum	Lege	Rød
CTV_E_par_50.4Gy	Dette volumet tegnes inn istedenfor CTV_E_pel_50.4Gy hvis paraortal regionen skal behandles. Lymfeknutestasjoner illiaca externa + iliaca interna + iliaca communis + paraortale lymfeknuter. Ikke inn i naturlig barrierer (bein/musklatur)	Målvolum	Lege	Rød
CTV_E_gro_50.4Gy	Lymfeknutestasjoner i lyske	Målvolum	Lege	Rød
PTV_centr_50.4Gy	CTV_centr_50.4Gy + CTV-PTV margin i henhold til bildeprotokoll	Målvolum	Stråleterapeut	Blå
PTV_Nx_64Gy	CTV_Nx_64Gy + CTV-PTV margin i henhold til bildeprotokoll	Målvolum	Stråleterapeut	Blå
PTV_P_xGy	CTV_P_xGy + individuelt vurderte marginer	Målvolum	Lege	Blå
PTV_E_50.4Gy	CTV_Nx_64Gy + CTV_E_pelv_50.4Gy/CTV_E_par_50.4Gy + CTV_E_gro50.4Gy + CTV-PTV margin i henhold til bildeprotokoll	Målvolum	Stråleterapeut	Blå

CTV_E_par_50.4Gy tenges kun inn dersom paraortale lymfeknuter skal behandles.
CTV_E_gro_50.4Gy tegnes kun inn dersom lyskene skal behandles.

4.1.3 Inntegning av målvolumer ved postoperativ bestråling av cervix cancer

Tabell 3: Målvolumer som skal tegnes inn ved postoperativ bestråling av cervix cancer.

Volum	Beskrivelse	Type	Tegnes av	Farge
GTV_Nx	Patologiske forstørrede lymfeknuter, ved inntegning av flere GTV_N skal de nummereres. Lokalisering av de ulike volumene angis på rekvisisjonen	Målvolum	Lege	Oransje
CTV_Nx_64Gy	GTV_Nx + 5 mm (respekter sikre anatomiske barrierer)	Målvolum	Lege	Rød
CTV_E_pel_50.4Gy	Lymfeknutestasjoner iliaca externa + iliaca interna + iliaca communis. Ikke inn i naturlig barrierer (bein/musklatur)	Målvolum	Lege	Rød
CTV_E_par_50.4Gy	Paraortale lymfeknuter	Målvolum	Lege	Rød
CTV_E_gro_50.4Gy	Lymfeknutestasjoner i lyske	Målvolum	Lege	Rød
CTV_cenpo_50.4Gy	Vagina og eventuelt tumorseng (dersom det er ufri rand som ikke dekkes ved brachy som skal strålebehandles eksternt).	Målvolum	Lege	Rød
PTV_E_50.4Gy	CTV_E_pel_50.4Gy + CTV_E_par_50.4Gy + CTV_E_gro_50.4Gy + CTV_Nx_50.4Gy + CTV-PTV-margin i henhold til bildeprotokoll	Målvolum	Stråleterapeut	Blå
PTV_Nx_64Gy	CTV_Nx_64Gy + CTV-PTV-margin i henhold til bildeprotokoll	Målvolum	Stråleterapeut	Blå
PTV_cenpo_50.4Gy	CTV_tumors_50.4Gy+ CTV-PTV-margin i henhold til bildeprotokoll	Målvolum	Stråleterapeut	Blå

CTV_E_gro_50.4Gy tegnes kun inn dersom lyskene skal behandles.

4.1.4 CTV-PTV margin

Tabell 4: CTV-PTV margin for ulike protokoller

Volum	Bildeprotokoll	L/R (mm)	C/C (mm)	A/P (mm)
PTV_E_50.4Gy	Daglig online match på bein	5	5	5
PTV_centr_50.4Gy	Daglig online match på bein	7	10	15
PTV_Nx_64Gy	Daglig online match på bein	5	5	5
PTV_cenpo_50.4Gy	Daglig online match på bein	7	7	7
PTV_E_50.4Gy	Systematisk protokoll, match på bein	7	7	7
PTV_centr_50.4Gy	Systematisk protokoll, match på bein	7	10	15
PTV_Nx_64Gy	Systematisk protokoll, match på bein	7	7	7
PTV_cenpo_50.4Gy	Systematisk protokoll, match på bein	7	7	7

4.2 Feltoppsett

4.2.1 Forutsetninger

En halv time før CT opptak og hver behandling skal pasienten tømme blæren og deretter drikke to glass vann (300 ml).

Sjekk at følgende kriterier er tilfredsstilt:

- Adekvat CT (handling dersom dette ikke er tilfelle)
- Fiksering og leie etter retningslinjer gitt i Fiksering og leie for strålebehandling i bekkenregion
- Hvis det er metall i behandlingsområdet må dette tas hensyn til ved planlegging.

4.2.2 Planoppsett

Det skal lages én hovedplan. Dersom det foreligger patologiske lymfeknuter skal det lages en eller flere boostplaner avhengig hva som er rekvirert.
Dersom det er mulig plasseres isosenter i referansepunktet fra CT-opptaket.

4.2.3 Behandlingsfelt for hovedplan

Ved konvensjonell behandling dekkes alle PTV som ikke skal ha boost-dose av fire felt. Det angis ingen fast margin fra PTV til feltgrense i antall millimeter. Feltgrensen legges slik at dosedekningen til PTV blir akseptabel. Det er ønskelig at marginen er så liten som mulig for å redusere dosen til friskvevet rundt. I praksis anbefales det å bruke marginer angitt i tabell 4. Da oppfylles i de fleste tilfellene dosekravene. Dersom så ikke er tilfelle, endres denne marginen.

Tabell 5: Utgangspunkt for feltoppsett for hovedplan ved konvensjonell behandling av bekken.

Felt nr.	Feltnavn	Energi [MV]	Gantryvinkel [grader]	Kollimatorvinkel [grader]	Vekt [%]	Kile	Feltforming margin PTV-MLC (MLC i middelposisjon)
1	1	15 etv. 10	0	0	100	nei	Lateralt: 5mm Craniocaudalt: 7 mm
2	2	15 etv. 10	90	0	100	nei	Frontdors: 3 mm Craniocaudalt: 7 mm
3	3 BF	15 evt. 10	180	0	100	nei	Lateralt: 5mm Craniocaudalt: 7 mm
4	4	15 evt. 10	270	0	100	nei	Frontdors: 3 mm Craniocaudalt: 7 mm

Segmenter må benyttes dersom man ikke oppnår tilfredstillende dosefordeling.
Bordfaktor blir lagt til på aktuelle felt ved å legge til BF i feltnavnet. Dette for å ta hensyn til absorbsjon i behandlingsbordet. Dette gjelder ikke for IMRT planer.

Tabell 6: Utgangspunkt for feltoppsett for hovedplan ved konvensjonell behandling av bekken og paraortalregion.

Felt nr.	Feltnavn	Energi [MV]	Gantryvinkel [grader]	Kollimatorvinkel [grader]	Område	Vekt [%]	Kile	Feltforming margin PTV-MLC (MLC i middelposisjon)
1	1	15 evt. 10	0	0	stort	100	nei	Lateralt: 5mm Craniocaudalt: 7 mm
2	2	15 evt. 10	0	0	cran	50	nei	
3	3	15 evt. 10	0	0	seg cran	18	nei	
4	4	15 evt. 10	90	0	stort	50	nei	Frontdors: 3 mm Craniocaudalt: 7 mm
5	5	15 evt. 10	90	0	caud	60	nei	
6	6	15 evt. 10	180	0	stort	130	nei	Lateralt: 5mm Craniocaudalt: 7 mm
7	7	15 evt. 10	180	0	cran	50	nei	
8	8	15 evt. 10	180	0	seg cran	33	nei	
9	9	15 evt. 10	180	0	seg caud	18	nei	
10	10	15 evt. 10	270	0	stort	50	nei	Frontdors: 3 mm Craniocaudalt: 7 mm
11	11	15 evt. 10	270	0	caud	60	nei	

Tabell 7: Utgangspunkt for feltoppsett for hovedplan ved IMRT

Felt nr.	Feltnavn	Energi [MV]	Gantryvinkel	Kollimatorvinkel
1	1	15 etv. 10	0	3
2	2	15 evt. 10	51	3
3	3	15 evt. 10	103	3
4	4	15 evt. 10	154	3
5	5	15 evt. 10	206	3
6	6	15 evt. 10	257	3
7	7	15 evt. 10	308	3

Tips ved optimalisering: Ved planlegging av gyn-planer har dekning til PTV høyest prioritet. Målet med IMRT teknikken er å oppnå konform dosefordeling rundt PTV. På denne måten kan risikoorganer spares i størst mulig grad. Tynntarmsparing har høy prioritet. Bruk "surrounding dose fall off" aktivt, og vis varsomhet med å sette strenge "maksdose objectives" siden deler av risikoorganet ofte er inkludert i PTV. Bruk derfor heller "max average objective" (med unntak av medulla og cauda equina hvor "max dose objective" med fordel kan brukes). Deler av PTV eller risikorganer kan generes for bruk som optimeringsvolumer (eks område av PTV som ikke dekkes eller del av risikoorgan som ikke er inkludert i PTV)

4.2.4 Behandlingsfelt for boostplan

Feltarrangementet velges individuelt ut i fra hvor boost-området er lokalisert.
Dersom boostvolumet er lokalisert til en side, bør det generelt ikke benyttes feltinngang fra motsatt side.
Ved mange lymfeknuter bør IMRT/VMAT vurderes.

4.2.5 Forberedelse for IGRT

Det skal laget ISO-felt som inkluderer representative, stabile skjelettstrukturer for matching på behandlingsapparat.

4.3 Krav til dosering og toleransedoser

Alle dosevolumkrav er veiledende og må alltid vurderes individuelt.

Normering: Middel i CTV/CTV union
Ved dosering til flere enkeltvolumer må man påse at middelverdien i hvert enkelt målvolum ikke varierer med mer enn +/- 2%.

Tabell 8: Klinisk maksimumsdose, D2 (D2: dosen til 2ccm av ytterkonturen)

Teknikk	*D2*
IMRT	*107%*
Konvensjonell	*105%*

Tabell 9: Dosegrenser til målvolum (D98: Minimumsdosen til 98% av volumet)

Målvolum	D98
CTV	95%
PTV	95%

Tabell 10: Dosegrenser til inntegnede risikoorganer

Risikovolum	Dosebegrensning 1
Rektum	Så lavt som mulig, men ikke på bekostning av målvolumet.
Small Bowel	Ved inntegning av hele det peritonale rom: Volumet som får mer enn 45 Gy skal være så lite som mulig. Quantec oppgir mindre enn 195 cm^3 . Dette kan være vanskelig å oppnå, og erfaringsmessig gis ofte 45 Gy til ca 300 cm^3.
Femoral head	Max 50% kan få 50Gy eller mer
Bladder	Så lavt som mulig, men ikke på bekostning av målvolumet. Merk at dersom blæren har stort volum, vil dosesparing til blære kunne gi redusert dose til tynntarm ved mindre blære ved behandling.
Sigmoideum	Så lavt som mulig, men ikke på bekostning av målvolumet.
Medulla	50Gy
Cauda equina	60Gy
Kidney	Så lavt som mulig, men ikke på bekostning av målvolumet. V12<55% V20<32% V23<30% V28<20% Ønskelig med lavere dose dersom mulig på grunn av samtidig kjemoterapi.

4.4 Klargjøring for behandling som utføres på doseplan

1. Systemspesifikk klargjøring .
2. Inntegning av matchestrukturer på iso-felt, alt. BF og side-felt, se Matchestrukturer.
3. Valg av bildeprotokoll, se Avbildning ved strålebehandling.
4. Estimering av dosebidrag fra iso-felt/behandlingsfelt brukt i bildeverifiseringen, se Dosebidrag fra isofelt.
5. Doseplanen godkjennes av stråleterapeut, lege og fysiker.

5. Definisjoner

For definisjon av max og min-doser, vekting, kiler, osv. se generelle retningslinjer ved doseplanlegging.

Andre eHåndboksdokumenter

- Eclipse/ARIA - Nivåstruktur og navning